ULTRAFINE GRINDING FOR IMPROVED MINERAL LIBERATION IN FLOTATION CONCENTRATES

by

JENNIFER MARIE PARRY

B.A.Sc., The University of British Columbia, 2004

A THESIS SUBMITTED IN PARTIAL FULFILMENT OF THE
REQUIREMENTS FOR THE DEGREE OF

MASTER OF APPLIED SCIENCE

In

THE FACULTY OF GRADUATE STUDIES

(Mining Engineering)

THE UNIVERSITY OF BRITISH COLUMBIA

August 2006

Abstract

As the minerals industry is required to process increasingly complex, finely-grained ores, stirred mills are replacing ball mills for regrind applications in flotation circuits. Stirred mills are able to produce fine grind sizes in an energy efficient manner and without additional size classification. Laboratory grinding trials were conducted using two high-speed stirred mills; one vertical and one horizontal, to treat three lead-zinc concentrator flotation streams which are currently reground using tower mills. The effect of stirred milling, in particular mill type, stress intensity and grind size, on downstream processing was investigated in terms of energy requirements, particle size distributions, mineral liberation and mineral breakage rates.

It was shown that the breakage rates of hard and soft minerals converge at high stress intensities. The high stress intensity and open circuit configuration of high-speed stirred mills allow them to remedy the effects of density and hardness in streams ground in primary ball mills with classifying cyclones. By varying the stress intensity in a mill via the impeller speed it is possible to target either hard or soft minerals for liberation depending on the requirements of a particular flotation stream. A lower impeller speed would be used in order to improve liberation of softer minerals without needlessly grinding harder minerals, while a higher impeller speed would be necessary if liberation of hard minerals were important. The difference in impeller speed requirements reflects the difference in optimal stress intensity for grinding hard and soft minerals.

The two high-speed stirred mills had similar energy requirements, and both mills had lower specific energy requirements than full-scale tower mills treating the same flotation streams. The vertical stirred mill products contained a greater proportion of fines compared to the horizontal mill products when compared using the Rosin-Rammler distribution, although this result was not consistent across different means of size distribution characterization. Mineral liberation behavior was similar for the horizontal and vertical high-speed stirred mills. The greatest benefit of regrinding using high-speed stirred mills was improved quartz liberation.

Table of Contents

List of Tables

List of Figures

List of Symbols

a   Rosin-Rammler distribution size coefficient (particle size at which 36.8% of particles retained)

b   Rosin-Rammler distribution width coefficient

P_{80} particle size at which 80% of particles pass in product

F_{80} particle size at which 80% of particles pass in feed

SI   stress intensity

R^2 coefficient of determination

W_p Weight % passing

W_r Weight % retained

x   particle size

ρ media density

$\hat{\beta}_0$ intercept of the fitted regression line

$\hat{\beta}_1$ slope of the fitted regression line

X_i values of the corresponding point X_i

Y_i values of the corresponding point Y_i

$\overline{Y}$ sample mean of the observations on Y

$\hat{Y}$ estimated response at X_i based on the fitted regression line

Acknowledgements

CHAPTER 1 Introduction

1.1 Background

As high-grade, mineralogically simple ore deposits become rarer, it has become necessary to process increasingly complex, fine-grained ores. The energy costs for grinding to the mineral liberation size of such ores are often prohibitive when using conventional grinding technologies such as ball mills. Even if the mineral liberation size can be achieved, over-grinding often takes place and valuable minerals are lost as slimes (Lofthouse et al, 1999). Stirred mills have been applied to such industries as cosmetics and industrial minerals for decades; however, as of the early 1990s, the only stirred mill technology used in metalliferous concentrators was the tower mill which is used primarily for producing P_{80}s between 20 and 40 µm. High-speed stirred mill technologies, capable of efficiently grinding to P_{80}s below 20 µm, were adapted to meet the needs of these high-tonnage operations. Both horizontal and vertical stirred mills are now employed in metalliferous concentrators, including the tower mill, the IsaMill and the stirred media detritor. Stirred mills are increasingly replacing balls mills in regrind applications for flotation circuits. Stirred mills are believed to behave differently from conventional mills in terms of energy requirements, breakage mechanisms and particle size distributions. An understanding of these differences, particularly those affecting downstream processing, would allow improvements to be made in the operation of these technologies in regrind circuits. Stirred mills differ amongst themselves in terms of stress intensity, power intensity, open or closed circuit operation, impeller design, and horizontal or vertical configuration. A comparison of different stirred mills would help operations to select the most appropriate one for a given regrind circuit.

The Red Dog Mine in Alaska currently uses tower mills in their three regrind circuits. Two high-speed stirred mills, one vertical and one horizontal, were compared in terms of energy requirements, particle size distributions and mineral liberation in order to evaluate their suitability for replacing the tower mills in this application.

1.2 Objectives

The research objectives are:

- To assess the effect of stress intensity on breakage rates for minerals of different hardness
- To investigate the effect of mill type on grinding energy requirements
- To assess the effect of stirred milling on downstream processing in terms of particle size distributions and mineral liberation

1.3 Methodology

Grinding trials were conducted to determine the effect of stirred milling on grinding energy requirements, product particle size distributions and mineral liberation. Intermediate lead flotation concentrate and two intermediate zinc flotation concentrates from Teck Cominco's Red Dog Mine were reground using two high-speed stirred mills, one horizontal and one vertical. The regrind circuits currently used to treat these concentrates were also characterized in terms of particle size distributions and mineral liberation. Procedures for running the grinding trials and analyzing the products are outlined in Chapter 3.

CHAPTER 2 Literature Review

2.1 Introduction

Stirred mills are increasingly being used for regrind applications in flotation circuits. Research on stirred milling has focused on the effect of mill type and operating conditions on grinding energy requirements and product particle size distributions. The effect of operating conditions and mill stress intensity on particle breakage rates has also been investigated (Kwade et al, 2002; Yue et al, 2003; Ma et al, 1998). The present study includes work in both of these areas; however, a greater emphasis is put on the relationship between mill stress intensity and mineral liberation. This literature review will describe the commonly used types of ultrafine grinding technologies. The effect of stirred milling on downstream processes, primarily in flotation regrind applications, will be discussed. Differences in mill design and operation affecting grinding energy requirements, breakage rates, particle size distributions and mineral liberation in stirred milling will be presented.

2.2 Stirred Mills for Regrind Circuits

It is often advantageous to regrind a flotation stream rather than producing a finer overall feed to the flotation circuit. This reduces overall energy consumption as only the finely-grained portion of the ore body is ground to a finer liberation size. Ball mills have traditionally been used for these regrind applications. In ball mills, motion is imparted to the media by rotation of the mill shell. The speed of rotation is limited by the critical speed at which the media would centrifuge. Ball mills use steel media of between 20 and 50mm for finer grind sizes (Andreatidis, 1995). Ball mills have the disadvantages of poor energy efficiency, high sliming, large footprint and contamination of the product with steel media when compared to stirred mills (Lichter et al, 2002); therefore, stirred mills are becoming the preferred technology for regrind circuits. Stirred mills impart motion to the media through an impeller while the shell remains stationary.

There are two fundamentally different classes of stirred mills that can be referred to as slow speed or high speed. The first class includes the tower mill or Vertimill and conventional

pin mills where a relatively slow impeller speed and coarse media size result in the fluid having a limited effect on the interaction of the media with itself. The second class includes the Netzsch/IsaMill and the Stirred Media Detritor. In these mills the impeller speed is high enough to effectively fluidize the media such that it takes on the flow pattern of a viscous fluid. The first class of stirred mill is most efficient at grinding coarse, hard feeds, while the second class of mill is more efficient for ultrafine milling (down to <15μm) using fine feeds (Lichter et al, 2002). Both types of stirred mill technologies were originally used for grinding industrial minerals, such as kaolin, and were later adapted to the needs of the metalliferous industries. The jet mill and centrifugal mill are also used to grind to ultrafine sizes; however, they are not currently used to improve mineral liberation in flotation circuits.

The tower mill was the first technology adapted for use in metalliferous concentrators. Slurry is fed to the bottom of the mill and is discharged at the top. Motion is imparted to the media through a screw which rotates at 80-150 rpm (Andreatidis, 1995). A settling zone at the top of the mill is used to separate media from the ground product. The need for a settling zone limits the tip speed to below ~3m/s and the media to sizes greater than ~3mm. The media size is typically between 9 and 20mm (Weller et al, 1999). These limitations on tip speed and media size make the tower mill less suited for ultrafine grinding (top sizes < 10μm). The tower mill has an advantage of simple design compared to the horizontal stirred mill as there is no need for a mechanical seal on the stirrer shaft and cooling water is unnecessary (Weller et al, 1999). Figure 1 shows a diagram of a tower mill.
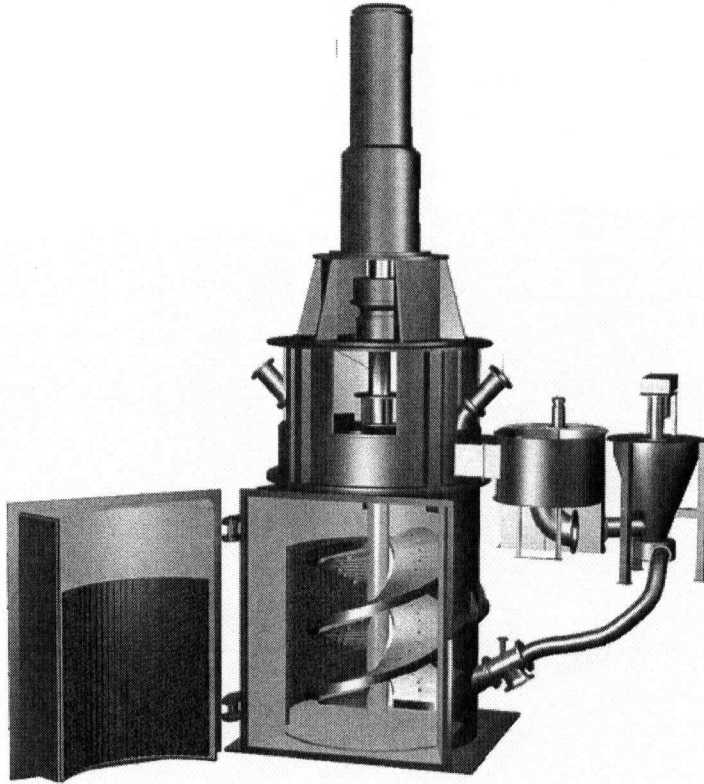
Figure 1. Schematic of a tower mill (Svedala, 2006)

The stirred media detritor (SMD) is a vertical stirred mill that was developed by English China Clay for grinding kaolin. It has an octagonal body which supports an internal multi-armed impeller. Slurry is fed through an inlet nozzle in the upper part of the chamber. A vortex is formed in the grinding chamber which is open to the atmosphere. Media is retained using a series of wedge profile polyurethane screens, and milled product is allowed to discharge through these screens into a launder (Davey, 2002). Figure 1 shows a schematic of a full-scale SMD.
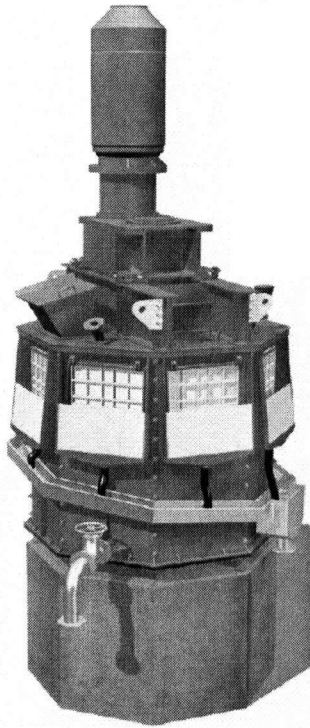
Figure 2. Schematic of a Metso Minerals stirred media detritor (Metso Minerals, 2006)

The IsaMill is a horizontal stirred mill with a fixed cylindrical shell. It is a scaled-up version of the Netzsch mill which is used for grinding pigments and fillers. Inside this shell are internal rotating grinding discs on a shaft. This impeller is able to operate at very high speed due to its horizontal orientation and unique method of retaining media in the chamber. At the discharge end of the mill, an extension of the shaft rotates around the media screen such that media is accelerated away from the screen. This reduces clogging of the screen thus making higher throughputs and impeller speeds possible. A certain amount of pressure (100 to 200kPa) is maintained in the IsaMill chamber to keep the mill charge suspended while achieving the necessary residence time for grinding to the target size (Weller et al, 1999; Gao et al, 2002). The high impeller speed creates heat in the mill; therefore, temperature is maintained by surrounding the mill with a water-cooled jacket. The IsaMill's throughput is often limited by hydraulic packing (Jankovic, 2003). Figure 3 shows a schematic of an IsaMill.
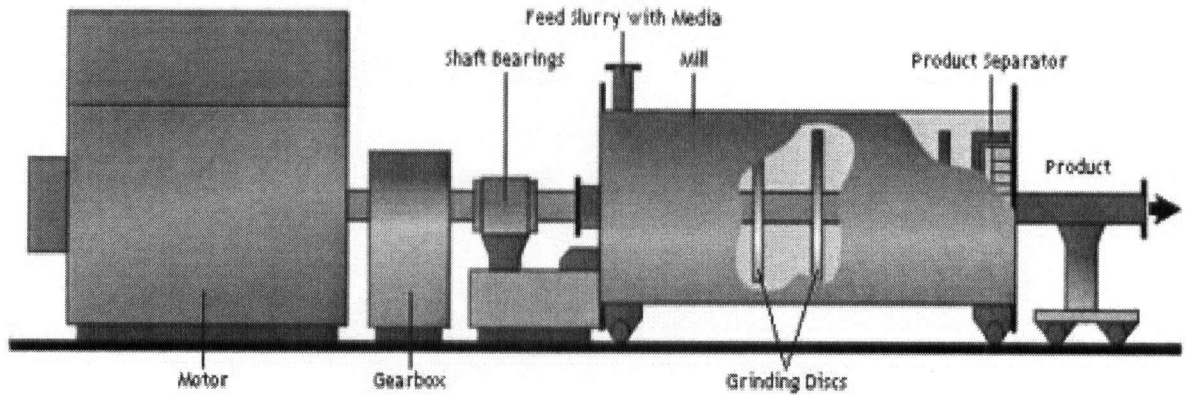
Figure 3. Schematic of an IsaMill (Xstrata, 2006)

Both the SMD and the IsaMill are typically run in open circuit, while the tower mill is run in closed circuit. Classifying cyclones sort particles by both size and density. Dense minerals, such as galena, are more likely to be recirculated than light minerals, such as quartz. This potentially results in over-grinding of dense minerals and under-grinding of light minerals. As circulating loads create classification issues, an open circuit configuration is preferable. Table 1 compares important characteristics of the three common types of stirred mill.

Table 1. Characteristics of different stirred mills

Type of Mill	Tower Mill	IsaMill	Stirred Media Detritor
Orientation	Vertical	Horizontal	Vertical
Circuit configuration	Closed	Open	Open
Tip speed (m/s)	< 3	~ 10-15	~ 8
Media type	Steel/chrome	Ceramic, sand, slag	Ceramic, sand, slag
Media size (mm)	9-20	1-3	1-3
Separation of product from media	Settling zone	Accelerating gap	Screens
Typical grind sizes (P_{80}s in μm)	20-40	7-20	7-20
Available units (kW)	Up to 930	Up to 4000	Up to 1100

2.3 Stirred Milling and Downstream Processing

2.3.1 Flotation

The purpose of comminution is to adequately liberate target minerals for separation from gangue. If a valuable mineral is locked with gangue, the particle may report to the

concentrate or to the tailings. If these locked particles report mostly to the concentrate, concentrate grade will suffer. If they report mostly to the tailings, recovery will be compromised. Target grade and recovery in a flotation circuit is achieved by grinding to the liberation size of the mineral and by maintaining a narrow particle size distribution. At a given grind size (e.g. defined by a P_{80}) a wider particle size distribution is detrimental to flotation performance. Issues caused by an excessive proportion of ultrafine particles include entrainment and sliming. Misclassification of these fine particles can result in the recovery of gangue particles to the concentrate regardless of flotation chemistry. Fine particles also have high specific surface areas and therefore require higher doses of reagents (Pease et al, 2006). It is important to achieve liberation of the target mineral at the coarsest grind size possible to avoid issues related to over-grinding.

While a high proportion of fines relative to a given grind size is undesirable; the presence of fine particles is not in itself detrimental to flotation. The McArthur River Mine floats a bulk lead/zinc concentrate with a P_{50} of 2.5μm. Overall recovery is 85% and 96% of the particles floated are below 2.5μm (Pease et al, 2006). Provided a narrow particle size distribution is maintained, fine particles can be floated effectively; therefore, it is important to separate fines from coarse composite particles in order to achieve good recoveries. Circulating loads should be minimized through open circuit grinding and appropriate placement of the regrind mills in circuit. For instance, it is better to regrind cleaner feed rather than cleaner tails. The primary concern should be to achieve the correct mineral liberation at the most efficient point in the circuit (Pease et al, 2006).

Grinding products should have clean surfaces and should be floated quickly before oxidation of surfaces can occur (Pease et al, 2006). Stirred mills assist in achieving clean surfaces by using inert media and by polishing of surfaces through attrition grinding. The primary benefit of inert media is that no iron contaminates the product; therefore, no electrochemical interactions occur between the sulphide minerals and the reactive steel grinding media. These interactions often produce oxidized iron species which form hydrophilic slime coatings on sulphide minerals such as galena and sphalerite, thus decreasing recoveries (Cullinan et al, 1999). Steel media is used in ball mills and tower mills, although the use of chrome media can minimize contamination.

Column flotation cells are often used to improve recovery of ultrafine particles. Columns provide improved separation performance for fine materials along with additional benefits of low capital and operating costs, small footprint and ease of automation (Wills, 1997).

2.3.2 Leaching/Pre-oxidation

Stirred mills can be used to improve the kinetics of leaching and pressure oxidation processes by increasing the surface area to volume ratio of the particles. They are used for grinding the feed to a pressure autoclave for pre-oxidation prior to cyanidation. Stirred mills can also be used as a replacement for pressure oxidation provided that the reduction in particle size sufficiently improves cyanidation kinetics. The KCGM Gidji Roaster uses an 1120kW IsaMill for ultrafine grinding of gold-bearing sulphide ore prior to cyanidation (Xstrata, 2006). Both vertical and horizontal stirred mills were used in the Tati Hydrometallurgical demonstration plant for ultrafine grinding of nickel sulphide concentrates prior to pressure oxidation (Nel et al, 2006). In leaching or oxidative applications, particle size distributions can be better characterized by their top size or P_{98} rather than their P_{80}. While coarse particles can still be recovered in a flotation circuit, they are not effectively leached.

2.3.3 Dewatering

A high proportion of ultrafine particles in a final concentrate may create a tenacious froth which is detrimental to effective dewatering by thickening or filtration (Pease et al, 2006). A narrow particle size distribution will minimize the amount of ultrafines in the slurry; however, an effective means of filtering fine particles is still important for fine grind sizes. As ultrafine particles accumulate during filtration, the filtrate becomes resistant to flow and thus slows the dewatering process. One method of improving the filtration rate is by cross-flow filtration. This technique decreases the accumulation of ultrafine particles by directing slurry flow parallel to the surface of the filter rather than perpendicular. Filtration occurs due to a pressure differential across the filter membrane. This prevents a build-up of fines at the membrane (Yan et al, 2003).

Thickening of ultrafine particles can be problematic due to their low settling velocity. Increased flocculation or coagulation is necessary to correct the problem. Launders may also need to be cleaned out more regularly due to the tenacity of fine froths.

Energy input to stirred mills is limited by the maximum operating temperature of the mill. A high temperature differential across a mill for a given energy input will limit the pulp density as a lower than optimum pulp density may be required to prevent overheating. Low density slurry will require additional thickening. In a study of vertical and horizontal stirred mills for use in a hydrometallurgical pilot plant, it was found that the horizontal stirred mill had a higher temperature differential (roughly double) for a given specific energy input than the vertical stirred mill. This was due primarily to the higher exposed surface area in the vertical stirred mill (Nel et al, 2006).

2.4 Energy Requirements for Stirred Mills

Stirred mills are designed to produce fine particle sizes in an energy efficient manner. The type of stirred mill and operating conditions used influence specific energy consumption. Predicting full-scale specific energy requirements requires a procedure for scale-up of laboratory results.

2.4.1 Effect of Mill Type on Energy Requirements

Specific energy consumption in ball mills rises sharply below 75μm and grinding using these mills becomes uneconomical below 30μm. Stirred mills are more energy efficient than ball mills even at relatively coarse P_{80}s of up to 100μm (Jankovic, 2003). The ability of tumbling mills to transmit energy to media is limited compared to stirred mills (Napier-Munn, 1999). High-speed stirred mills are able to grind efficiently due to their design and the small size of the media used. Nesset et al (2006) found that the specific energy for size reduction of a zinc regrind concentrate in the SMD, IsaMill and laboratory ball mill was the same, while that for the tower mill was 57% lower. The main differentiating factor between the four technologies in that study was their power intensity. While the tower mill has better energy efficiency, a much larger tower mill would be required than an IsaMill or SMD for the same size reduction. Nesset proposed that the better energy efficiency in the tower mill was due to less energy being directed towards fluid movement and more

towards ball-particle interaction. Energy intensity does not have a strong influence on the relative performance of different stirred mills. The low intensity tower mill can operate as efficiently as the high intensity mills (Lichter et al, 2002). A comparison of three stirred mills at the Tati hydrometallurgical demonstration plant indicated that the high-speed vertical stirred mill had the lowest specific energy consumption for grinding a nickel sulphide concentrate (Nel et al, 2006).

2.4.2 Effect of Operating Conditions on Energy Requirements

Throughput, impeller speed, pulp density, circuit configuration, media size and media type can all affect stirred mill energy requirements.

Media size is often the primary factor limiting the fineness of grind possible in a mill and has a large impact on grinding efficiency (Lichter et al, 2002). The major media parameters that should be considered are size, type, competency and hardness (Lichter et al, 2002). There is a wide variation in cost between the types of media which must also be taken into account. Media commonly used in the high-speed stirred mills include high competency sand, ceramic and slag. Tower mills typically use steel or chrome steel media. Sand has the advantage of relatively low cost (US$0.1 per kilogram); however, there are a limited number of sites which can produce sand with the desired size distribution and competency. Milling efficiencies and specific cumulative breakage rates are decreased by using sand rather than ceramic media due to energy dissipation in media abrasion (Nel et al, 2006). When a constant agitator speed or mill power is maintained, the specific breakage rate decreases as the proportion of fines in the media increases. There is an optimum media size for a given feed size with respect to particle breakage rate, product size and size distribution. The optimum ratio of media size to feed size is approximately 20:1 (Yue, 2003). Selecting a media that is too coarse will reduce the probability of media/particle collisions and reduce energy efficiency (Murphy et al, 2000). The number of mechanical stress actions decreases linearly with increasing media size, thus decreasing the media size is the effective way to increase the frequency of grinding events and decrease the energy per event (Karbstein et al, 1995; Lichter et al, 2002). There is a limit to the benefit of decreasing media size with efficiency decreasing at media sizes smaller than 0.8 mm (Weller et al, 1999). Media with a lower specific gravity tends to grind by attrition rather than impact fracture. Attrition grinding is beneficial to grinding efficiency

(Andreatidis, 1995). However, the Netzsch mill operating guide recommends using a higher specific gravity media for better energy efficiency (Netzsch, 1996).

Tests using a horizontal stirred mill have shown that a higher flow rate results in lower specific energy requirements (Weller et al, 1999). The resulting higher pressure in the mill might accelerate particle breakage; however, too high a flow rate would cause media packing at the mill discharge, and excessive media and impeller wear (Weller et al, 1999). Increasing the tip speed for a given mill can decrease specific energy requirements (Weller et al, 1999); however, the tip speed is usually limited by such factors as heat generation in the horizontal stirred mill, media-product separation in the tower mill and the formation of a vortex in the SMD.

The effect of slurry density on energy requirements depends on the material being ground. In the case of sulphide ores, where the volumetric density of material will be much less than the mass density, energy requirements do not change greatly with slurry density (Nesset et al, 2006).

It has been shown that when operating conditions are optimized in a stirred mill with regards to energy requirements they are also optimized with regard to particle size distribution, i.e. the distribution is at its narrowest (Yue, 2003; Nesset et al, 2006). It is therefore possible to minimize energy requirements without compromising the quality of the product with respect to downstream processing.

2.4.3 Scale-up of Laboratory Stirred Mill Energy Requirements

Breakage in a laboratory stirred mill should relate closely to that in a full-scale mill as media size, media velocity and mill energy intensity are consistent between laboratory and full-scale mills (Andreatidis, 1995). This allows grinding energy requirements to be readily scaled-up from laboratory to full-scale mills. This is not the case for laboratory ball mills which have lower energy intensity than full-scale ball mills (Andreatidis, 1995). The number of particles in a lab stirred mill is also much greater than for an equivalently sized lab ball mill, thus making it easier to obtain a representative sample for scale-up purposes (Davey, 2002).

Energy requirements measured for a batch 1.5L Netzsch mill have been successfully scaled-up for a M3000 IsaMill. Energy versus P_{80} relationships were on a straight line for

both mills on a log-log scale (Gao et al, 1998). However, energy requirements for the IsaMill are typically determined using a continuous Netzsch mill (Weller et al, 1998). Energy requirements for the stirred media detritor have been successfully scaled-up from a 1.5L batch mill (Davey, 2002). While manufacturers claim that no special correction factors are necessary for scale-up of stirred mills, a comparative study (Nesset et al, 2006) indicated that this may not be the case depending on the method of power measurement used. The reaction table torque technique used for the SMD was shown to overestimate the no-load power, resulting in a substantial underestimation of the shaft input torque (Nesset et al, 2006). Weller et al (1998) found that different methods of measuring energy requirements for the Netzsch mill (by a clip-on power meter, an in-line torque meter and a power meter supplied with a variable speed drive) produced similar results that were scalable. Accurate measurement of particle size distributions is also important for scale-up. The laser diffractometer is the standard for measuring ultrafine particles. This instrument consistently reports a coarser distribution than a sieve analysis of the same material. This is believed to be due to non-spherical particles appearing spherical when spinning in water in the laser diffractometer (Nesset et al, 2006). The cyclosizer is also used for sizing ultrafine material. This instrument classifies by density as well as size, and the effect of density must be corrected for when interpreting cyclosizer results.

2.5 Stirred Milling and Particle Breakage

2.5.1 Effect of Mill Type on Breakage Mechanisms

Particle breakage behavior can impact grinding efficiency, particle size distributions and mineral liberation. Andreatidis defines the three possible breakage mechanisms as follows: Impact breakage results from the rapid compression of particles between media and mill liners. This breakage mechanism is most associated with conventional ball mills. Low pressure attrition results when there are no significant compressive forces within the mills (i.e. when low density media is used). Grinding occurs due to differences in acceleration between media and particles. This results in a polishing action which is otherwise known as abrasion. This breakage mechanism is most associated with high-speed stirred mills. High pressure attrition occurs when particles are compressed under high pressure. It results in

chipping or "rounding" of the particles. This breakage mechanism is most associated with tower mills and SAG mills (Andreatidis, 1995). While attrition (high or low pressure) is the breakage mechanisms most associated with stirred mills, some studies have shown that impact breakage is also present in these mills (Kwade et al, 1999; Yue, 2003). Andreatidis found that high-speed stirred mills grind primarily by attrition while tower mills grind with a combination of attrition and impact (Andreatidis, 1995). Yue found that impact breakage was the dominant breakage mechanism in a high-speed horizontal stirred mill for coarser grind sizes. This conclusion was based on the occurrence of first-order breakage when grinding quartz in a Netzsch mill as well as the lack of a bimodal particle size distribution at these grind sizes. If attrition breakage were the primary breakage mechanism, disappearance and appearance rates would accelerate resulting in non-first-order breakage (Yue, 2003). Solid tracer studies in a Sala agitated vertical mill have shown that first-order breakage also occurs in vertical stirred mills and that the population balance model provided a reasonable model for this breakage (Weller et al, 2000).

Stress intensities vary widely with mill type and grinding conditions. For a given stress intensity a relationship exists between product fineness and specific energy consumption. At a given stress intensity this relationship is only slightly influenced by differences in stirrer and grinding chamber geometry. There is an optimal stress intensity for a given grinding application. Product fineness at a given specific energy consumption increases with increasing stress intensity until this optimum is reached and then decreases relatively slowly with increasing stress intensity (Kwade, 1996).

The stress intensity in a horizontal stirred mill is proportional to media diameter, media density and stirrer tip speed according to the following formula (Kwade et al, 2002):

$$SI \, \alpha \, SI_{GM} = d_{GM}^{3} \rho_{GM} \upsilon_{t}^{2}$$

, where SI_{GM} = stress intensity of grinding media (Nm)

d_{GM} = diameter of grinding media (m)

ρ_{GM} = density of grinding media (g/m^{3})

υ_{t} = stirrer tip speed (m/s)

Therefore, if the same media is used, a 5-fold increase in tip speed will result in a 25-fold increase in stress intensity in a horizontal stirred mill.

Positron emission particle tracking in a batch SMD indicated that the type of particle motion varied between three zones in the mill. It was believed that these zones reflect differences in breakage mechanisms. It was found that varying the impeller speed altered the relative size and location of these regions. As the distribution of these regions was found to influence breakage mechanisms in the mill, impeller speed can be used as a means of controlling breakage mechanisms (Conway-Baker et al, 2002).

2.5.2 Effect of Breakage Mechanisms on Mineral Liberation

Stirred mills, particularly the IsaMill, operate at considerably higher stress intensities than traditional mills. The difference in stress intensities between ball, tower and stirred mills could significantly affect breakage mechanisms. An ore that has been ground to the same particle size in two different mills may have improved mineral liberation in one mill due to differences in these breakage mechanisms. Breakage along grain boundaries is preferred over breakage across grains in terms of maximizing mineral liberation for a given grind size. One study comparing breakage and mineral liberation in a bead mill to that in a ball mill found that results varied depending on the ore (Andreatidis, 1995). When grinding a relatively simple zinc rougher concentrate, the particle size-liberation relationship was not affected by differences between the mills. However, tests on a low-grade rougher concentrate consisting of middling particles showed improved liberation when a bead mill was used rather than a ball mill to produce the same P_{80} of 8µm (Andreatidis, 1995). This result indicates that the mineral size-liberation relationship can be improved by using a bead mill; however, the improvement is dependent on the characteristics of the ore. In the case of the above study, the bead mill was most beneficial for grinding complex ores. Liberation of silica and sphalerite was increased in -10µm particles when stirred milling was used compared to ball milling. This was attributed to the low energy attrition breakage promoted by the stirred mill which attritted silica from the surface of sphalerite grains, thereby increasing the liberation for both these phases in fine particles. The IsaMill is believed to selectively grind coarser particles which results in improved mineral liberation (Gao et al, 2002).

2.5.3 Effect of Stirred Mills on Particle Size Distributions

High-speed stirred mills can produce narrow particle size distributions without further size classification. Ball mills and tower mills require closed circuit operation with a hydrocyclone. It is difficult to operate the small (down to 2" diameter) hydrocyclones required at ultrafine particle sizes; therefore, poor classification can hurt the performance of fine grinding technologies (Pease et al, 2006). In the case of horizontal stirred mills, a narrow particle size distribution is achieved through stage-by-stage grinding between the impeller discs (Gao et al, 2002). This grinding behavior results in a narrow residence time distribution and, therefore, a narrow particle size distribution. At very fine grind sizes, attrition grinding occurs in high-speed horizontal stirred mills which results in bimodal particle size distributions (Yue, 2003). Tower mills have a tendency to over-grind fines and therefore have a long tail at the finer end of their particle size distributions (Gao et al, 2002).

The best function for characterizing the particle size distribution of an ultrafine product is the Rosin-Rammler-Bennett distribution rather than the Gaudin-Schuhmann distribution (Yue, 2003). This is an empirical distribution; however, it may have some basis in the population balance model of particle breakage (Wang et al, 2000).

Natural media (e.g. sand) tends to have a wide size distribution which negatively impacts grinding performance. Small media tends to produce a wider size distribution than coarse media at constant power in a horizontal stirred mill, possibly due to a lower stress intensity promoting attrition over massive fracture (Yue, 2003). There is an optimum media size for a given feed size with respect to particle breakage rate, product size and size distribution. The optimum ratio of media size to feed size is approximately 20:1 (Yue, 2003).

A horizontal mill will produce the narrowest particle size distribution under plug-flow conditions. It is therefore desirable that plug-flow be approximated in the IsaMill. Back-mixing can be minimized by increasing throughput and lowering impeller speed (Karbstein et al, 1996). Increasing throughput causes the residence time distribution in the Netzsch mill to become narrower (Weller et al, 2000). Uneven mixers in series have been used to successfully model residence time distributions in a Netzsch mill (Weller et al, 2000).

While both the SMD and the IsaMill can be operated without additional size classification, there are still benefits to be gained from using a hydroclassifier. Removing the fine material

prevents over-grinding, reducing the formation of problematic ultrafine material. The cut point of the hydroclassifier also limits the upper particle size obtained. As a result, a very steep particle size distribution can be obtained at comparable energy input to a situation where no additional classification is used (Karbstein et al, 1995). Although there are potential benefits to additional classification, it is not a necessity and therefore stirred mills are generally run in open circuit (Murphy et al, 1999; Davey, 2002). Grinding tests using a horizontal stirred mill have shown that a lower pulp density will produce a narrower particle size distribution, particularly at $P_{80}s$ below 10µm (Yue, 2003). Impeller speed also has an effect on particle size distributions. Particle size distributions, as measured by the Rosin-Rammler-Bennett modulus, become narrower with increasing tip speed (Wang et al, 2000). The use of a higher impeller speed in a batch SMD has been shown to create a narrower particle size distribution (Conway-Baker et al, 2002).

2.6 Conclusions and Recommendations

Stirred milling technologies are becoming more common in metal mining operations. Research on stirred milling for these applications has focused on the effect of mill type and operating conditions on grinding energy requirements, breakage mechanisms and product particle size distributions.

There is little research quantifying changes in mineral liberation with particle size in the ultrafine grinding range. Andreatidis performed work relating mineral liberation to grind size and breakage mechanism; however, the need to use point-counting limited the number of samples that could be analyzed. New image analysis technologies allow much larger quantities of liberation data to be gathered than is feasible using conventional point-counting techniques. These technologies include QEM-SEM and the JKTech Mineral Liberation Analyser. Both technologies have improved diagnostic metallurgy. The present study uses these technologies to relate mineral liberation to grind size, stress intensity and mill type.

The most common technologies for regrinding flotation streams are the ball mill, tower mill, Stirred Media Detritor and IsaMill. These mills differ in terms of stress and power intensity, media size and flow behavior. These variables affect breakage mechanisms and

rates as well as product characteristics such as particle size distributions and mineral liberation. A key focus of the present study is the effect of mill stress intensities on energy requirements, particle size distributions and mineral liberation.

CHAPTER 3 Experimental Program

3.1 Introduction

Different stirred mill technologies were evaluated in terms of grinding energy requirements, particle size distributions, mineral liberation and mineral breakage rates. The relationship between stress intensity, mineral hardness and mineral breakage rate is investigated in Chapter 4. The effect of stirred milling on energy requirements is described in Chapter 5. The effect of stirred milling on product particle size distributions is discussed in Chapter 6. The relationship between stirred milling and mineral liberation is discussed in Chapter 7.

3.2 Test Program

Table 2 provides a summary of the grinding trials and the analyses that were performed on the products. The grinding trials have been divided into two phases according to their objectives.

Table 2. Summary of test program

Phase	Mill Type	Objective	Media	Feed Material
Mineral breakage rates	Netzsch	Effect of stress intensity and mineral hardness on mineral breakage	1mm ceramic	Synthetic mixture of silica, calcite and magnetite (6:1:1)
Stirred mill comparison	Netzsch, SMD	Energy consumption, particle size distributions, mineral liberation	Colorado river sand	Zinc 1st retreat concentrate Zinc 2nd rougher concentrate Lead cleaner column tails

3.3 Laboratory Stirred Mills

A continuous Netzsch LME 4 horizontal stirred bead mill was used to approximate an IsaMill during the grinding trials. The Netzsch mill is shown in Figure 4.
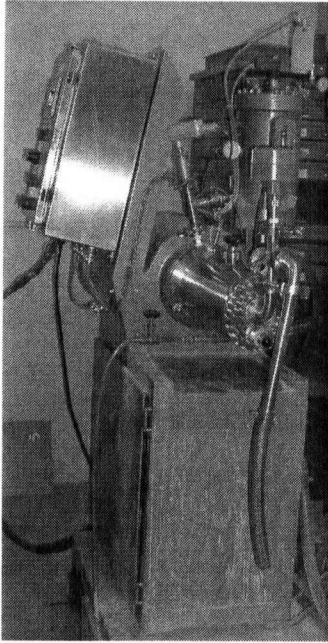
Figure 4. Netzsch LME 4 horizontal stirred mill

Slurry throughput can be varied to affect particle residence time which changes the grind size. The mill impeller speed can be varied between 600 to 2500 rpm. A dynamic media cartridge separator is used to accelerate media away from the mill discharge without using screens as a separation device, a feature which is also found in the full-scale IsaMill.

A Metso Minerals batch laboratory stirred media detritor was used for scaling-up to a full-scale SMD. The laboratory SMD has an effective chamber volume of 1.5L. Mill retention time is varied to achieve different grind sizes. The mill has a fixed impeller speed of 555 rpm. A reaction table torque meter is used to determine power requirements. The laboratory SMD is shown in Figure 5.
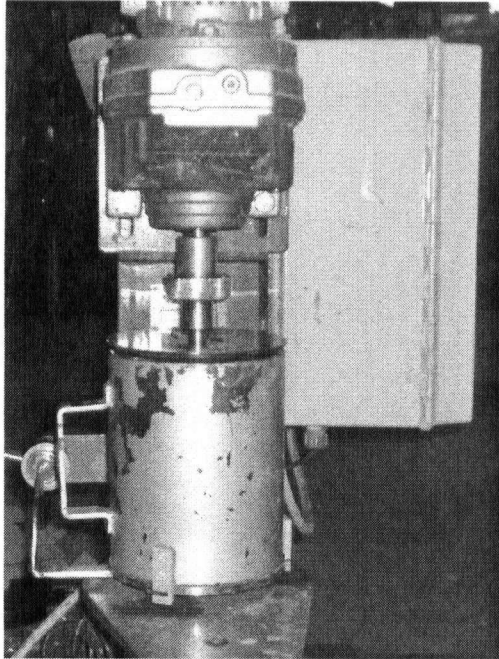
Figure 5. Laboratory 1.5L batch SMD

3.4 Product Characterization

3.4.1 Particle Size Analysis

Measurements of particle size distributions were performed using a Malvern Mastersizer 2000 laser particle size analyzer. Ultrasound and dispersant were added to break up agglomerates prior to analysis. A demagnetizing coil was used to disperse aggregates of magnetite.

3.4.2 BET Specific Surface Area Measurement

The specific surface areas of the grinding products were measured using a Quantasorb BET surface area analyzer. Samples were degassed for a minimum of 2 hours at 50°C prior to a measurement. Repeat cuts from a single sample resulted in a 95% confidence interval of ±0.01 m^2/g.

3.4.3 Mineral Liberation Analysis

Samples were divided into size fractions prior to the preparation of transverse mounts. Size fractionation was performed using a Warman Cyclosizer. Mineral liberation of the individual

size fractions was analyzed using a JKTech MLA (Mineral Liberation Analyser). It should be noted that the finest (-5 μm or C7) size fractions were not analyzed with the MLA. The MLA does not have the resolution necessary to resolve particles finer than 5 μm. In most cases, there was little +38 μm material to analyze. As a result, liberation was based on an analysis of the particles between 5 and 38 μm for all samples with the exception of the zinc 1st retreat concentrate, the zinc 2nd rougher concentrate, and the coarsest zinc 2nd rougher concentrate laboratory mill products. The +38 μm fractions were analyzed for these samples. The C1 and C2 cyclosizer fractions were combined prior to analysis due to their small mass.

The geometric mean particle sizes by mineral for each cyclosizer fraction were calculated based on pure mineral density and are given in Table 3.

Table 3. Geometric mean particle size by cyclosizer fraction

Size Fraction	Geometric Mean Particle Size(μm)			
	Sphalerite	Galena	Pyrite	Quartz
C1/2	34	26	31	42
C3	23	15	19	30
C4	15	10	13	20
C5	11	7	9	14
C6	7	5	6	9
C7	3	2	2	4

3.4.4 Particle Size Distribution Functions

The Rosin-Rammler distribution function was fitted to the product particle size distributions for each mill in order to compare the widths of the distributions (based on the distribution coefficient). This is the preferred function for approximating particle size distributions at these fine sizes (Yue, 2003). The Rosin-Rammler function is as follows:

$$W_r = 100 \exp[-(x/a)^b] \%$$

Where W_r = wt % retained

x = particle size

a = size at which 36.8% particles retained

b = distribution coefficient

The fit of the Rosin-Rammler distributions was determined using the coefficient of determination as follows:

$$R^2 = \frac{\sum\limits_{i=1}^{n}(Y_i - \overline{Y})^2 - \sum\limits_{i=1}^{n}(Y_i - \hat{\beta}_0 - \hat{\beta}_1 X_i)^2}{\sum\limits_{i=1}^{n}(Y_i - \overline{Y})^2}$$

$$\hat{Y} = \hat{\beta}_0 + \hat{\beta}_1 X_i$$

, where $\hat{\beta}_0$ = intercept of the fitted regression line

$\hat{\beta}_1$ = slope of the fitted regression line

X_i and Y_i = values of the corresponding point (X_i, Y_i)

$\overline{Y}$ = sample mean of the observations on Y

$\hat{Y}$ = estimated response at X_i based on the fitted regression line (Yue, 2003)

Figure 6 plots the correlation of the Rosin-Rammler distribution to the actual distribution versus P_{80} for the zinc 1st retreat concentrate products.

Figure 6. Fit of Rosin-Rammler distributions for zinc 1st retreat concentrate

The Rosin-Rammler distribution becomes less effective at describing the actual size distribution as grind size decreases. There is a steep drop in the coefficient of determination at P_{80}s of less than $10\mu m$. This trend was also observed for the zinc 2nd rougher concentrate and lead cleaner column tails streams.

3.5 Mineral Breakage Rates

Grinding trials were performed to relate mineral breakage rates to differences in mineral hardness and impeller speed.

3.5.1 Feed Material

An 8 kg mixture of silica (Moh's hardness 7), calcite (Moh's hardness 2.5) and magnetite (Moh's hardness 5.5) was prepared for each test according to the weight ratio of 6:1:1. This mixture was then slurried to a pulp density of 30%. The particle size distribution of each component was measured prior to mixing.

Figure 6. Fit of Rosin-Rammler distributions for zinc 1st retreat concentrate

The Rosin-Rammler distribution becomes less effective at describing the actual size distribution as grind size decreases. There is a steep drop in the coefficient of determination at P_{80}s of less than 10µm. This trend was also observed for the zinc 2nd rougher concentrate and lead cleaner column tails streams.

3.5 Mineral Breakage Rates

Grinding trials were performed to relate mineral breakage rates to differences in mineral hardness and impeller speed.

3.5.1 Feed Material

An 8 kg mixture of silica (Moh's hardness 7), calcite (Moh's hardness 2.5) and magnetite (Moh's hardness 5.5) was prepared for each test according to the weight ratio of 6:1:1. This mixture was then slurried to a pulp density of 30%. The particle size distribution of each component was measured prior to mixing.

3.5.2 Grinding Media

A 1.0-1.6mm silica-alumina-zirconia ceramic media was used at 80% by volume loading. Ceramic media was used instead of Colorado River sand in order to prevent contamination of the quartz product by grinding media.

3.5.3 Operation of Mills

The feed was passed through the mill three times for each test. Approximately 1L of slurry was sampled from each pass. Each sample was dried and riffled into two portions. A Davis tube (an oscillating tube which uses an electromagnet to recover magnetic material) was used to remove the magnetite, and the magnetite's particle size distribution was measured. Calcite was dissolved in dilute hydrochloric acid to separate it from the silica. The particle size distribution of the silica was measured and that of the calcite was calculated by difference based on its mass fraction. After this analysis was done for each pass, the breakage rates of each mineral could be determined. The procedure was repeated for a total of five impeller speeds (1000, 1200, 1400, 1700 and 2000 rpm). Figure 7 outlines the procedure used.
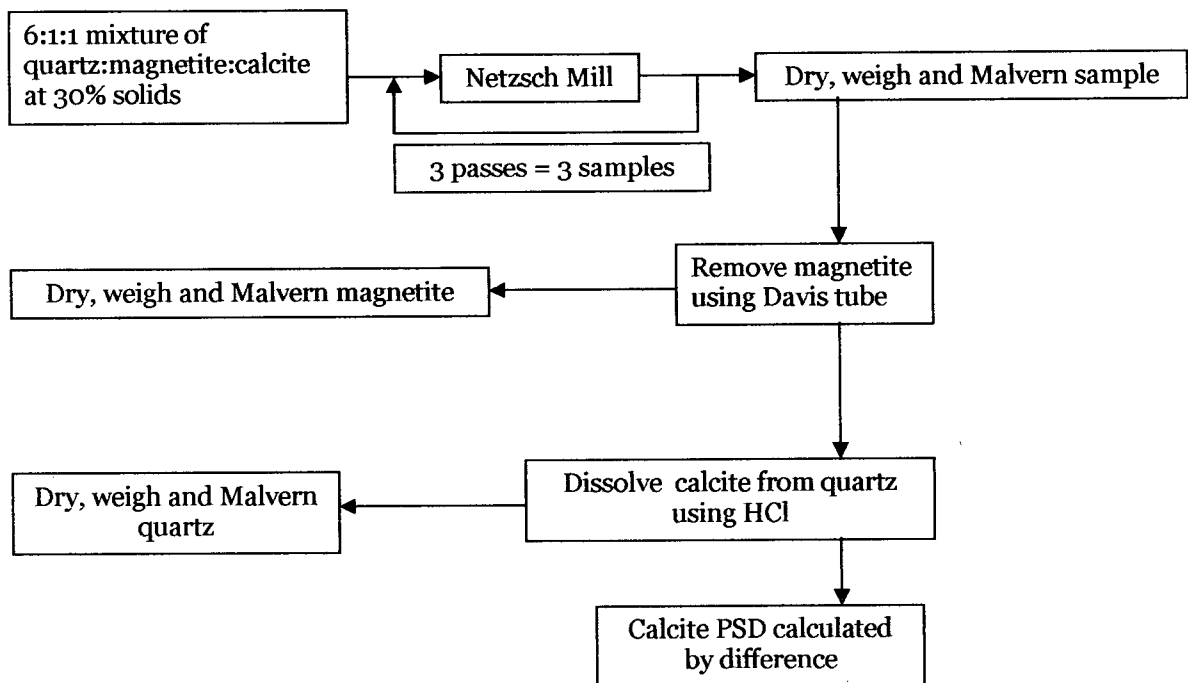
Figure 7. Mineral breakage rate testing procedure

3.6 Stirred Mill Comparison

Grinding trials were performed to compare the two laboratory stirred mills in terms of energy requirements, particle size distributions and mineral liberation.

3.6.1 Feed Material

Samples were obtained of the overall feed streams to the three regrind circuits at the Red Dog concentrator. These streams are referred to as lead cleaner column tails, zinc 2nd rougher concentrate and zinc 1st retreat concentrate, and the flow sheets for each circuit can be found in appendices A, B and C, respectively. Approximately 400 kilograms of sample were provided for each stream. Assays were performed on these samples (see appendices A, B and C for assay results).

Table 4 presents the F_{80}s for these three samples.

Table 4. F_{80}s of tower mill circuit feeds used in experiments

Feed Material	P_{80} (μm)
Zinc 2nd Rougher Concentrate	49
Zinc 1st Retreat Concentrate	29
Lead Cleaner Column Tails	26

3.6.2 Grinding Media

A Colorado River sand media with a P_{80} of 2.7mm was used in both the stirred media detritor and the Netzsch mill.

3.6.3 Operation of Mills

Netzsch mill:

Media was added to fill 80% of the effective mill volume by bulk. Approximately 8kg of feed material in 40% solids slurry was used as feed for each test. The slurry was agitated in a baffled tank and fed to the mill using a positive displacement pump. Power draw, pressure, temperature, impeller speed and pump speed were read from the mill control panel. The impeller speed was set at 1500 rpm. Product flow rate was measured using a

stopwatch and a graduated cylinder. Samples were taken after 3 minutes of grinding (to allow the mill to reach steady state operation). Pulp density was determined by drying a portion of each grind product in the oven. Specific energy consumption was calculated by dividing the net power draw (actual power draw less no-load power draw) by the solid flow rate.

Stirred Media Detritor:

Feed material and water were mixed together in the mill for 2 minutes. After the pre-mixing step, media was added to the mill such that the volume of media equaled the volume of slurry, and the mill was restarted. A reading of the cumulative kWhr was displayed on the control panel, and samples were taken at intervals based on the desired kWhr/t (specific energy consumption). Samples were taken one of two ways: by syringe at intervals (as recommended by Metso Minerals) or by removing the entire grind product and taking a cut. Syringe testing could be used for determining specific energy consumption and particle size distributions. In order to obtain sufficiently large samples for mineral liberation analysis or specific surface area measurement, it was necessary to stop the mill at the desired specific energy consumption and screen the media out of the product. A fresh feed would then be used for the next test. Differences in the results obtained using the two methods are noted in chapters 5 and 6.

CHAPTER 4 Stress Intensity, Mineral Hardness and Breakage Rates

4.1 Introduction

A test program was conducted to assess the effect of stress intensity on breakage rates for minerals of different hardness. Stress intensity is an important parameter in determining mineral breakage rates. The optimum stress intensity for efficient particle breakage depends on the mineral hardness. Harder minerals will require higher stress intensity for efficient breakage. Table 5 lists the Moh's hardness for minerals in the Red Dog flotation concentrates.

Table 5. Moh's hardness of minerals

Mineral	Moh's Hardness
Sphalerite	3.5-4
Pyrite	6.5
Quartz	7
Galena	2.5

(www.webmineral.com, 2006)

Stirred mills have higher stress intensities than ball mills. A low intensity mill could be expected to preferentially grind softer minerals. As a result, hard minerals, such as quartz, would be less liberated compared to softer mineral, such as sphalerite, after the ore is ground in a ball mill circuit. This outcome would be exacerbated by the presence of classifying cyclones in ball mill circuits. Classifying cyclones sort particles by both size and density; therefore, dense minerals, such as sulphides, are more likely to be reground in a ball mill while low density quartz reports to the cyclone overflow. Liberation of quartz is therefore likely to be lower than for sulphide minerals upon reaching the flotation circuit. Stirred mills could rectify this problem in two ways. Firstly, they are run in open circuit, thus avoiding the effect of classifying cyclones. Secondly, the high stress intensity in these mills would be expected to break both hard and soft minerals effectively. The second hypothesis was tested in the mineral breakage rates phase of the grinding trials.

28

4.2 Experimental Procedure

Section 3.5 describes the procedures for conducting this stage of the grinding trials. For this study, calcite was the soft mineral (Moh's hardness 2.5), magnetite (Moh's hardness 5.5) was the moderately hard mineral and quartz was the hardest mineral (Moh's hardness 7).

4.3 Results and Discussion

Mineral P_{80} is plotted versus residence time for each impeller speed in Figures 8 through 12. Stirred mill stress intensity increases proportionally with the square of impeller speed. As the impeller speed increases, the slopes ("breakage rates") of the three minerals should converge. While lower impeller speeds would preferentially break the softer minerals, all minerals should break at higher impeller speeds.
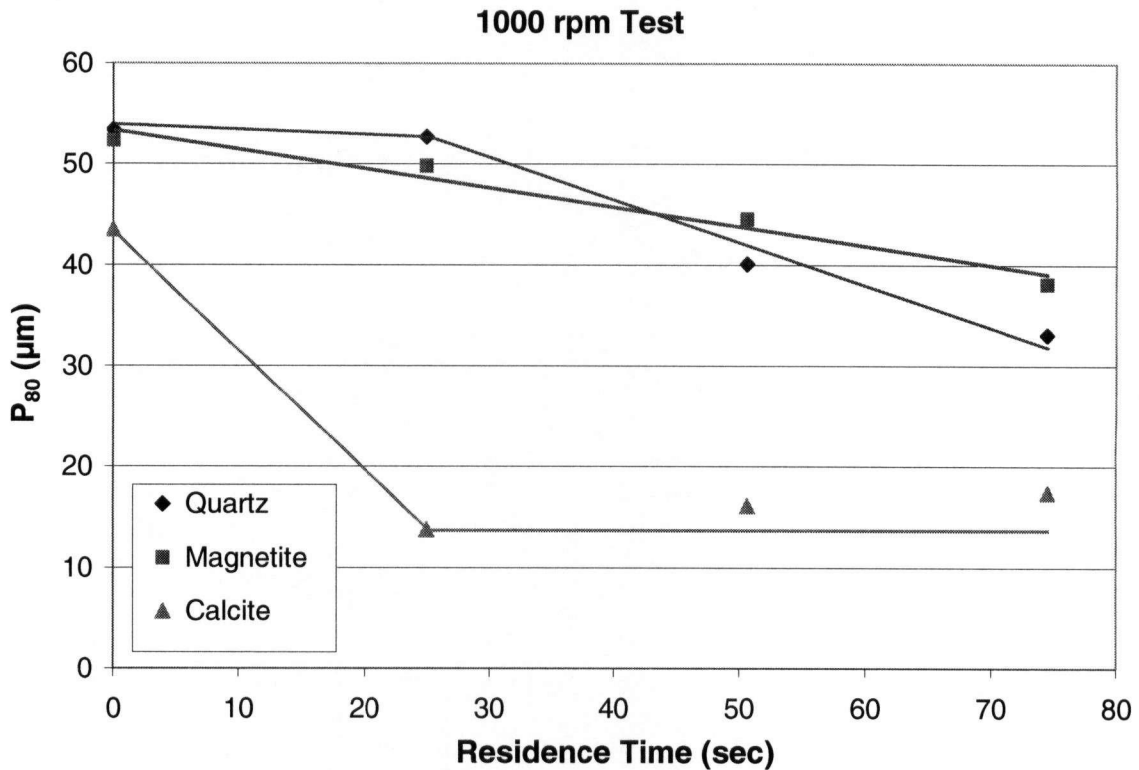
Figure 8. P_{80} vs. residence time for 1000 rpm test

At an impeller speed of 1000 rpm, calcite breaks more quickly than quartz and magnetite. Calcite breakage levels off after the first pass through the mill. This is due to breakage by cleavage in calcite. When cleavage breakage is no longer possible, breakage rates for calcite slow dramatically. This type of breakage is also found in galena.

29
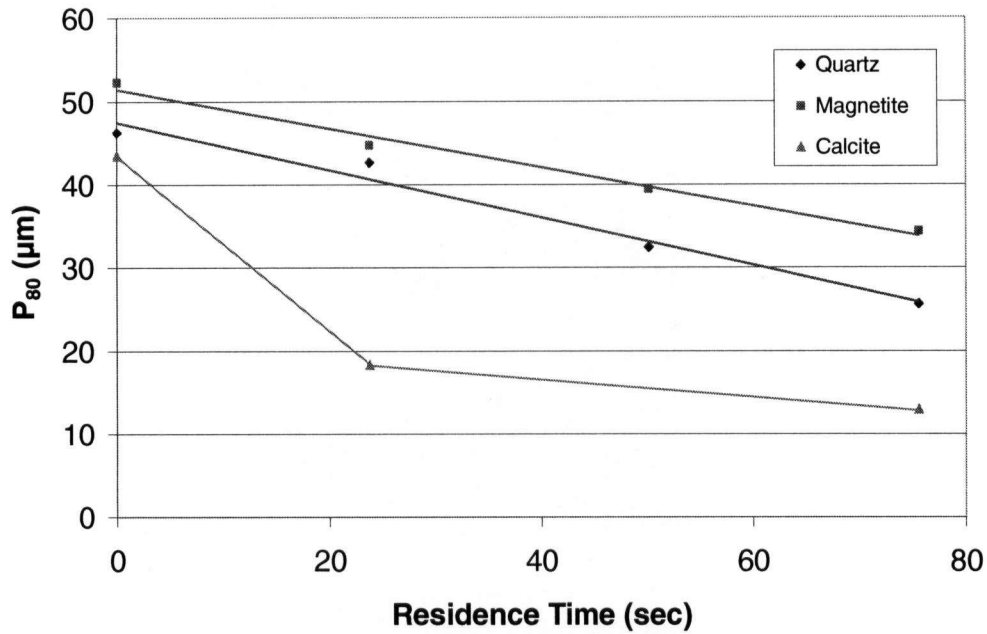
Figure 9. P_{80} vs. residence time for 1200 rpm test

The calcite point for the second pass of the 1200 rpm test appears to be an outlier. This could be due to issues associated with separating the three minerals prior to particle size analysis. In this test, calcite still has a higher breakage rate than the harder minerals.
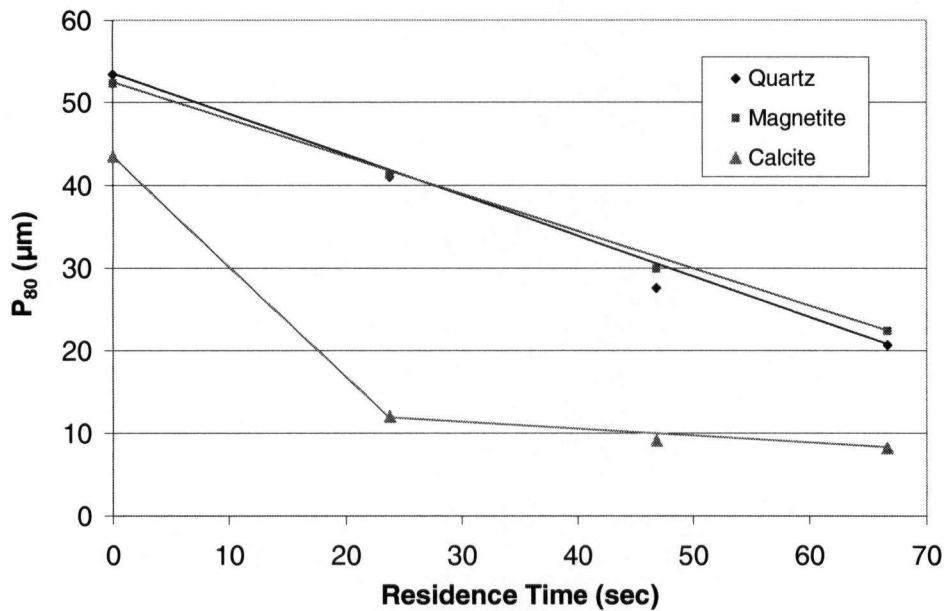
Figure 10. P_{80} vs. residence time for 1400 rpm test

At an impeller speed of 1400 rpm, the three slopes are closer than they were for the 1000 and 1200rpm tests, indicating that breakage of the harder minerals is improving with higher stress intensity.
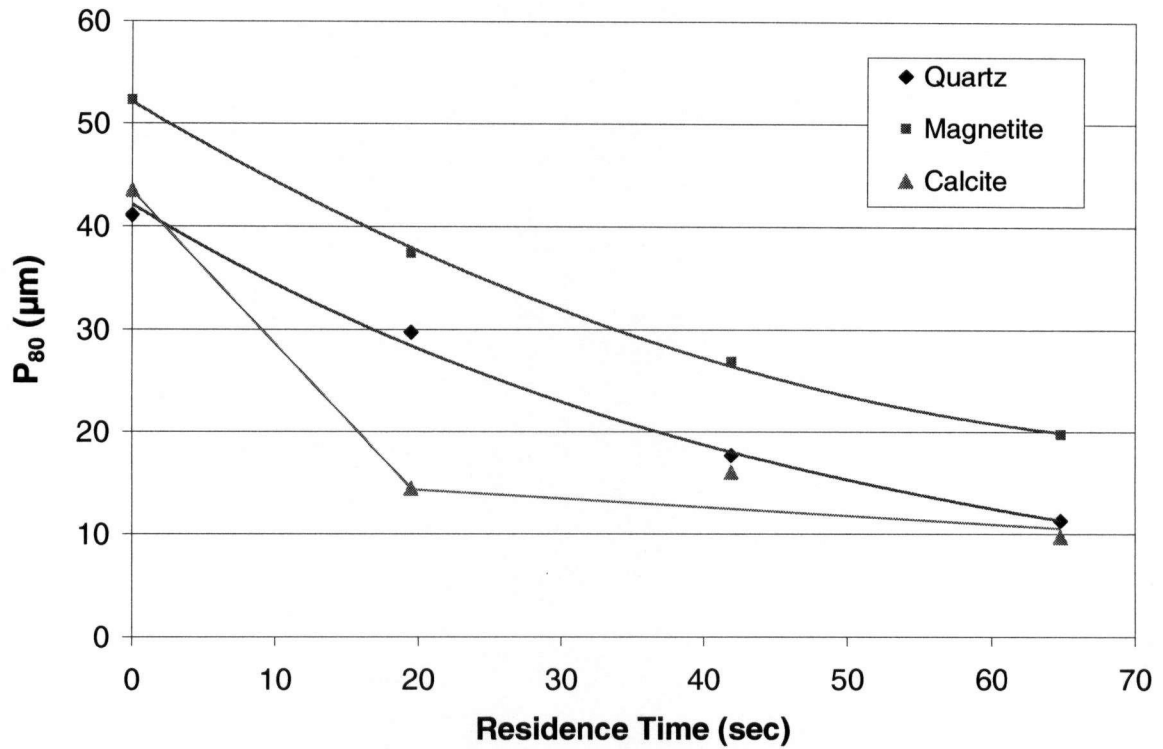
Figure 11. P_{80} vs. residence time for 1700 rpm test

At an impeller speed of 1700 rpm, there is an improvement in breakage rate for the harder minerals, particularly magnetite.
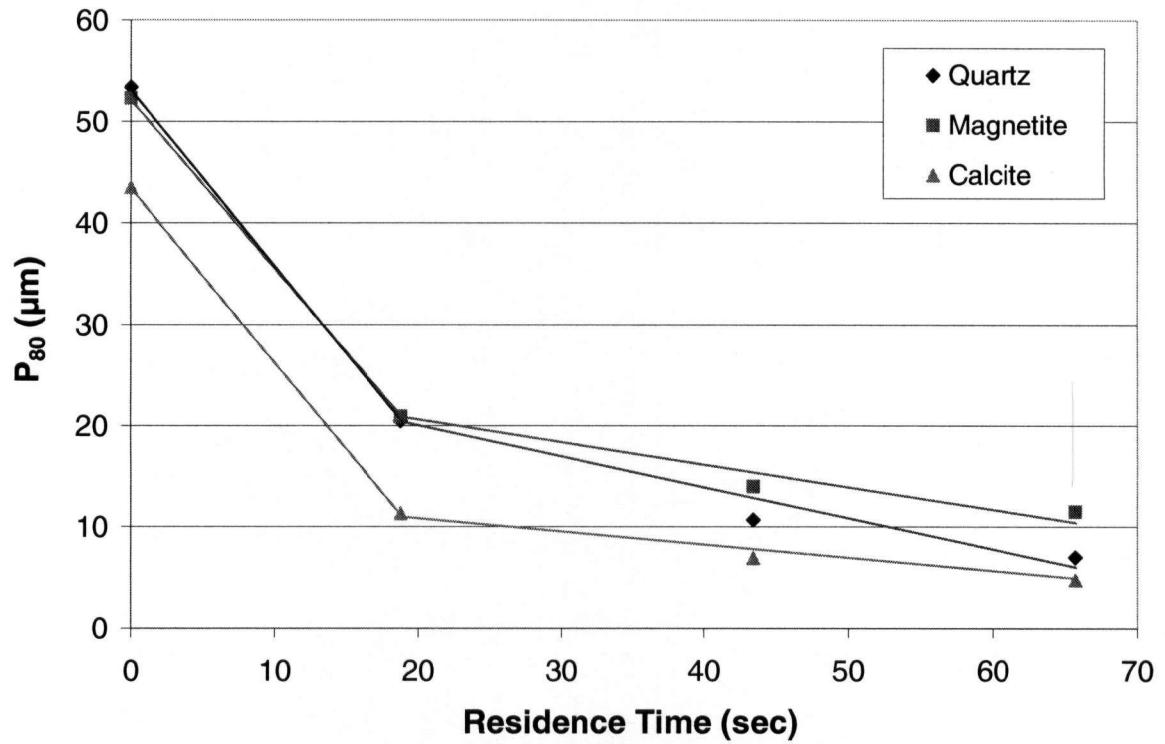
Figure 12. P_{80} vs. residence time for 2000 rpm test

At an impeller speed of 2000 rpm, the slopes for the three minerals are very similar. The hardness of the mineral no longer influences breakage rate.

Figure 13 plots the slopes from the previous graphs versus impeller speed for each mineral.
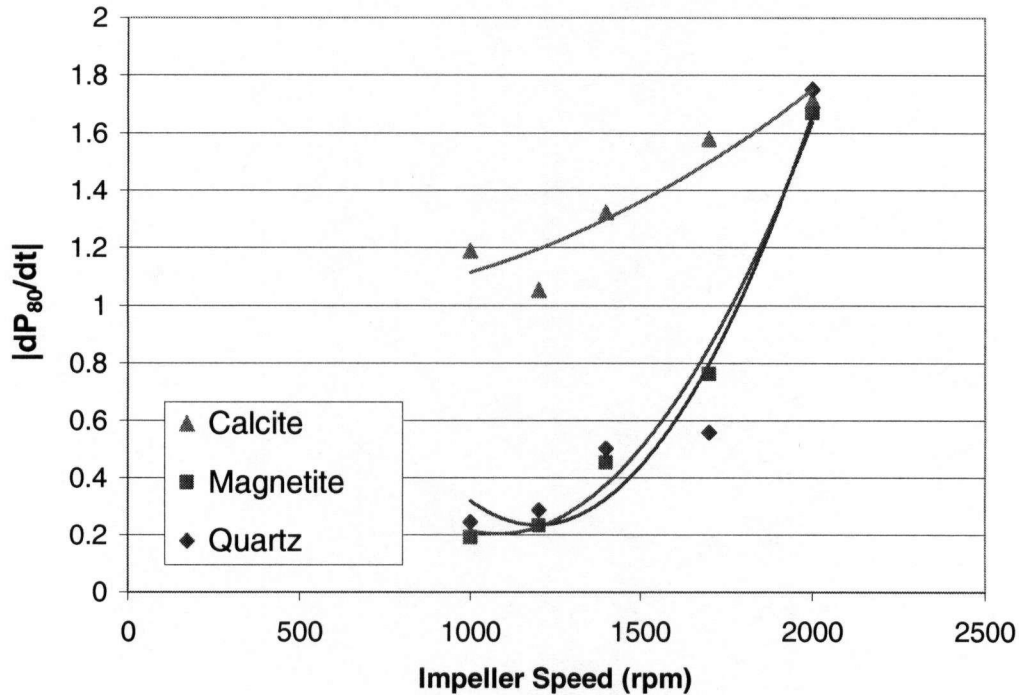
Figure 13. $|dP_{80}/dt|$ vs. Impeller Speed

The breakage rate of calcite is faster than those of magnetite and quartz for all impeller speeds except for 2000 rpm. The breakage rates of the hard and soft minerals gradually converge up to an impeller speed of 1700 rpm at which point the breakage rates of the harder minerals increase dramatically. Breakage rates (as measured by slope of P_{80} vs. residence time curves) seem to converge at higher stress intensity for minerals of different hardness. The results suggest that the optimal stress intensity for grinding the harder minerals is achieved at close to 2000rpm while that of calcite is reached at a lower impeller speed. If magnetite or quartz liberation were important, the optimal impeller speed would be higher than if calcite liberation was the primary concern.

Previous studies have shown that quartz breakage rates are increased by an order of magnitude when grinding in a horizontal stirred mill compared to a ball mill (Ma et al, 1998).

4.4 Conclusions

Increasing the stress intensity in a horizontal stirred mill causes the breakage rates of minerals of different hardness to converge. Relatively low intensity ball and tower mills over-grind

softer minerals compared to harder minerals. This effect is exacerbated by the preferential recovery of dense minerals, such as galena, to the hydrocyclone underflow for regrinding while lighter minerals, such as quartz, are sent to the flotation circuit at a relatively coarse grind size. The stirred mill avoids these problems when used in regrind applications due to their high stress intensity and open circuit configuration. By selecting an appropriate stress intensity (via the impeller speed), it would be possible to preferentially grind hard or soft minerals depending on the liberation requirements for a particular flotation stream.

4.5 Recommendations

The changes in stress intensity obtained by varying the Netzsch mill impeller speed cannot be compared directly to those in high-speed or low-speed vertical stirred mills due to differences in hydrodynamics compared to a horizontal stirred mill. A synthetic mixture should be tested in a variable speed vertical stirred mill using the same method as was used for the Netzsch mill in the present study.

CHAPTER 5 Effect of Mill Type on Grinding Energy Requirements

5.1 Introduction

Specific energy consumptions for two high-speed stirred mills were compared for grinding the three feeds to the Red Dog regrind circuits. Energy requirements were determined using procedures recommended by the manufacturers of each mill.

5.2 Experimental Procedure

Energy requirements for the Netzsch mill and the SMD were measured during the mill comparison phase of the grinding trials as described in section 3.6.

5.3 Results and Discussion

Data on energy requirements for each mill can be found in appendices A, B and C. Specific energy consumption for the SMD was measured using both syringe samples and screened samples (see section 3.6.3 for an explanation of sampling methods). Results indicated that particle size analysis of syringe samples was more variable than for screened samples, suggesting that syringe samples may not be representative; therefore, the screened sample curves are referred to in the discussions.

Figure 14 plots specific energy consumption versus P_{80} for grinding the zinc 1st retreat concentrate to different P_{80}s using each mill. The current specific energy consumption for the tower mill circuit (obtained from the Red Dog concentrator) is also shown.
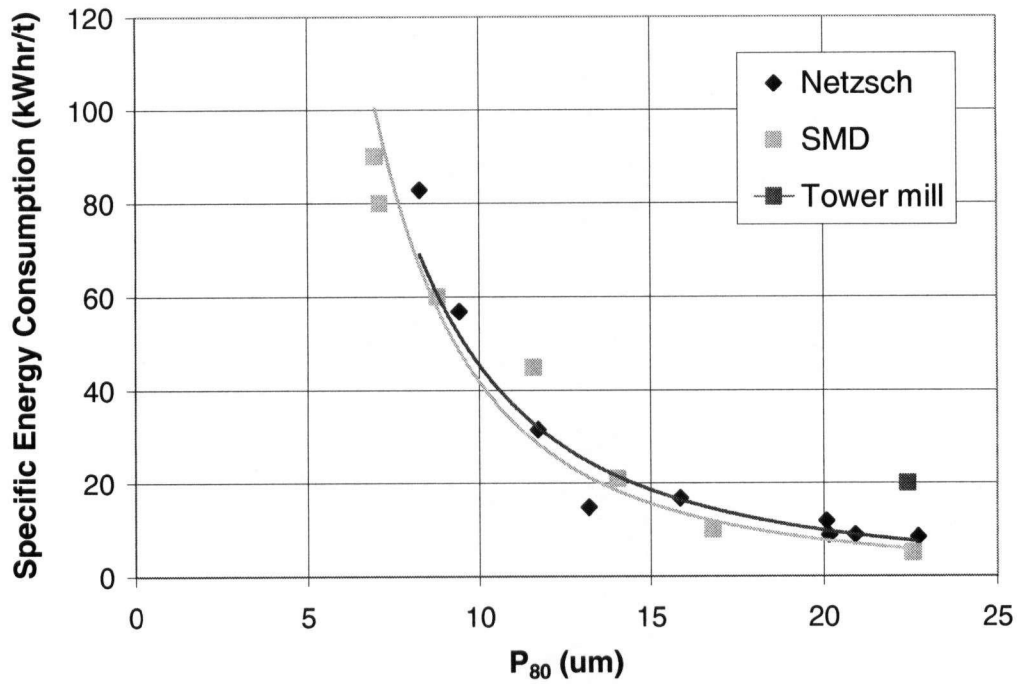
Figure 14. Specific energy consumption versus P_{80} for zinc 1st retreat concentrate

There is a large reduction in energy consumption for the high-speed stirred mills compared to the tower mill in operation. It should be noted that this is a comparison between laboratory and operating data; however, the lab-scale results are scalable according the mill manufacturers. The tower mills currently consume 20kWhr/t to grind from a F_{80} of 29μm to a P_{80} of 22μm. The stirred mills were able to grind to approximately the same size ($P_{80} \sim 23$μm) using less than 10kWhr/t. Specific energy consumption was similar for the SMD and the Netzsch across the range of grind sizes measured.

Figure 15 plots specific energy consumption versus P_{80} for the zinc 2nd rougher concentrate. Data on tower mill specific energy consumption for this circuit is not available.
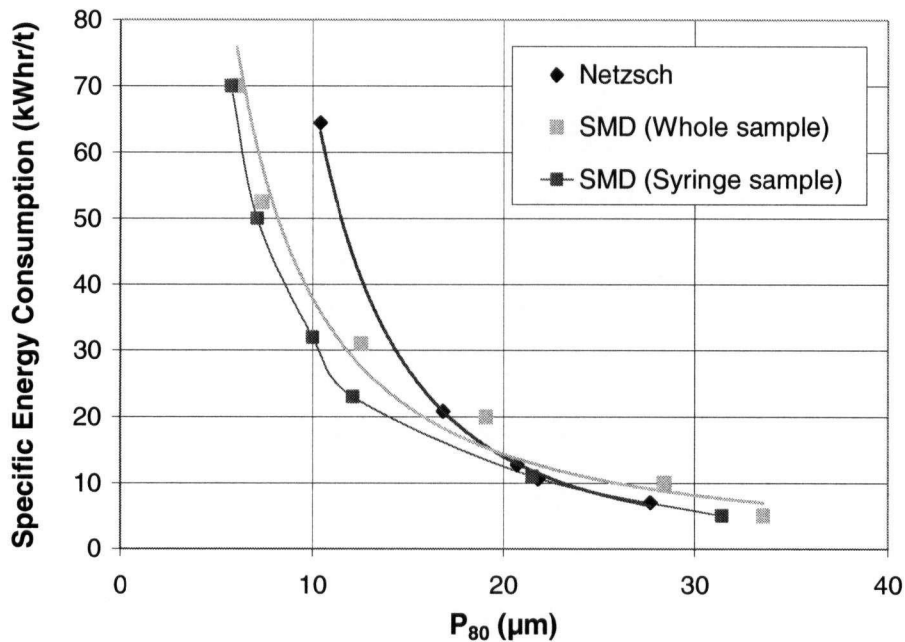
Figure 15. Specific energy consumption versus P_{80} for zinc 2nd rougher concentrate

The curves for the Netzsch mill and the SMD were similar for grinding to P_{80}s above ~12μm. At finer grind sizes, the SMD appears to have lower energy requirements.

Figure 16 plots specific energy consumption versus P_{80} for grinding the lead cleaner column tails. The current tower mill data is also plotted. The cyclone overflow product sample sent to UBC had a P_{80} of 21.6μm; however, the usual P_{80} as reported by the Red Dog mine is approximately 17μm. Both points are shown on the plot. In either case the SMD and Netzsch mill offer significantly decreased specific energy consumptions compared to the tower mill.
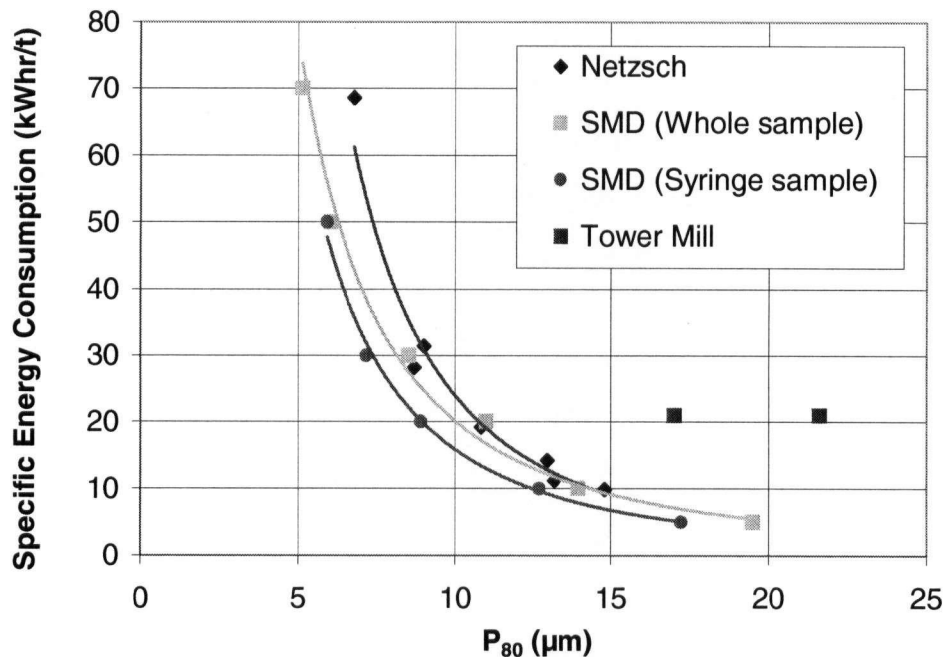
Figure 16. Specific energy consumption versus P_{80} for lead cleaner column tails

Except for the finest grind sizes ($P_{80}<8\mu m$), the Netzsch mill and the SMD had similar specific energy consumptions. The SMD had lower specific energy consumptions for the finest grind size.

Generally, higher stress intensity in a mill is associated with higher energy efficiency; therefore, the Netzsch mill might be expected to produce a smaller grind size for a given energy input than the SMD. Based on the results obtained for the three streams, this is not the case. One possible reason for the similarity between the curves relates to the existence of an optimum stress intensity. According to Kwade (1996), for a given energy input, there is an optimum stress intensity which will produce the finest particle size. This optimum stress intensity decreases with increasing specific energy input and product fineness. When the stress intensity is increased beyond this optimum, energy utilization starts to decrease. The stress intensity is proportional to the impeller tip speed (see 2.5.1 for equation) which is ~8 m/s for the SMD and 10-15 m/s for the IsaMill. Therefore, if the stress intensity in the SMD is close to the optimum, the higher stress intensity in the Netzsch mill would not further reduce energy consumption. With increasing specific energy input, and therefore decreasing particle size, the

optimum stress intensity decreases (Kwade et al, 1996). This could explain the lower specific energy requirements of the SMD at the finer grind sizes. Other studies have shown that energy efficiency does not necessarily improve with increasing power intensity (Nesset et al, 2006; Lichter et al, 2002).

Another factor to consider when comparing the mills is the scale-up issue described by Nesset whereby energy consumption is underestimated by 30-40% using the grinding chamber reaction torque measurement. This method of measuring power draw was used for the SMD and assumes that impeller shaft torque is equal to the grinding chamber reaction torque. Nesset (2006) found that this assumption is not valid, and a correction factor should be used to adjust the grinding chamber reaction torque measurement. If that scale-up issue is present in this case, the full-scale IsaMill would be expected to have lower specific energy consumption than the SMD. Concern regarding the common method of measuring power in the SMD should be balanced against previous successful scale-ups of batch laboratory SMD results to continuous pilot-scale (Davey, 2002). An additional issue arises from comparing a batch mill to a continuous mill. As the SMD is being operated in batch mode, short-circuiting of particles is not possible; however, this problem could arise in full-scale continuous operation and influence energy requirements.

5.4 Conclusions

At coarser grind sizes, the specific energy consumptions of the vertical and horizontal stirred mills were similar. At P_{80}s below ~8-10μm, the SMD tended to have lower specific energy requirements than the Netzsch mill. Given the different procedures used to measure power draw for each mill and issues associated with scale-up for the SMD, the differences between the two mills are likely not significant. Therefore, over the stress intensity range covered during testing with the SMD and Netzsch mill, there was no significant difference in energy utilization.

5.5 Recommendations

Further confirmation of the accuracy of the SMD scale-up procedure would be valuable. New comparative studies should be conducted to compare energy usage in a batch laboratory SMD to that in a full-scale operating SMD. Testing should investigate the effect of impeller speed on energy utilization to determine whether there is an optimal stress intensity.

CHAPTER 6 Effect of Mill Type on Product Particle Size Distributions

6.1 Introduction

The particle size distributions of the horizontal and vertical stirred mill products were characterized in order to evaluate the effect of stirred milling on downstream processes. In general, grinding should reduce particle sizes to provide adequate liberation without producing excessive amounts of fines that negatively affect flotation and dewatering. The comparison was based on measurement of the product specific surface areas, Rosin-Rammler distribution functions and the P_{80}:P_{20} ratio.

6.2 Experimental Procedure

Particle size distributions for the mills were determined during the mill comparison phase of the grinding trials as described under section 3.6.

6.3 Results and Discussion

6.3.1 Comparison of laboratory and tower mill particle size distributions

A wide particle size distribution is undesirable for most downstream processes, particularly flotation and dewatering. Figure 17 plots the particle size distributions of the cyclone overflow from the tower mill circuit, and the coarse grind products from the SMD and the Netzsch mill for the zinc 1st retreat concentrate grinding trials at a comparable P_{80} of 23μm.
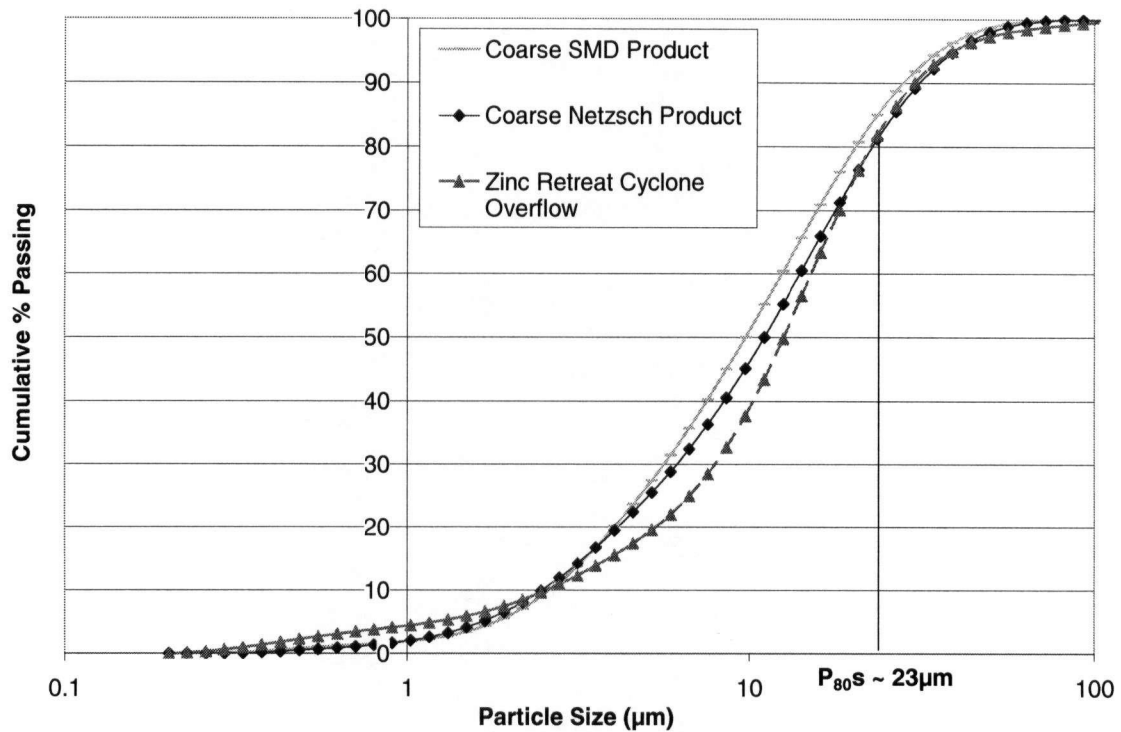
Figure 17. Particle size distributions for coarse stirred mill products and cyclone overflow (zinc 1st retreat circuit)

The cyclone overflow had a slightly narrower particle size distribution at a P_{80} of 22-23µm than the other mills based on the P_{80}:P_{20} ratios. This could be expected as the tower mill is operated in closed circuit with the classifying cyclones, while the Netzsch mill was operated in open circuit. The SMD was operated in batch mode which is neither open nor closed circuit. The Netzsch mill produced a similar particle size distribution to the tower mill despite being operated in open circuit. In full-scale operations, the IsaMill and the SMD are typically run in open circuit. High reduction ratios for either mill may require a closed circuit configuration or a mills operating in series. The ability to produce a narrow particle size distribution without additional size classification is a major benefit of high-speed stirred mills (Weller et al, 1999).

6.3.2 Rosin-Rammler distribution functions

The Rosin-Rammler distribution function was fitted to the product particle size distributions for each mill. A higher Rosin-Rammler distribution coefficient indicates a narrower particle

size distribution. Particle size distribution characterization data can be found for each stream in appendices A, B and C. Figure 18 plots the Rosin-Rammler distribution coefficient versus P_{80} for the SMD and Netzsch mill zinc 1st retreat concentrate grinding products.
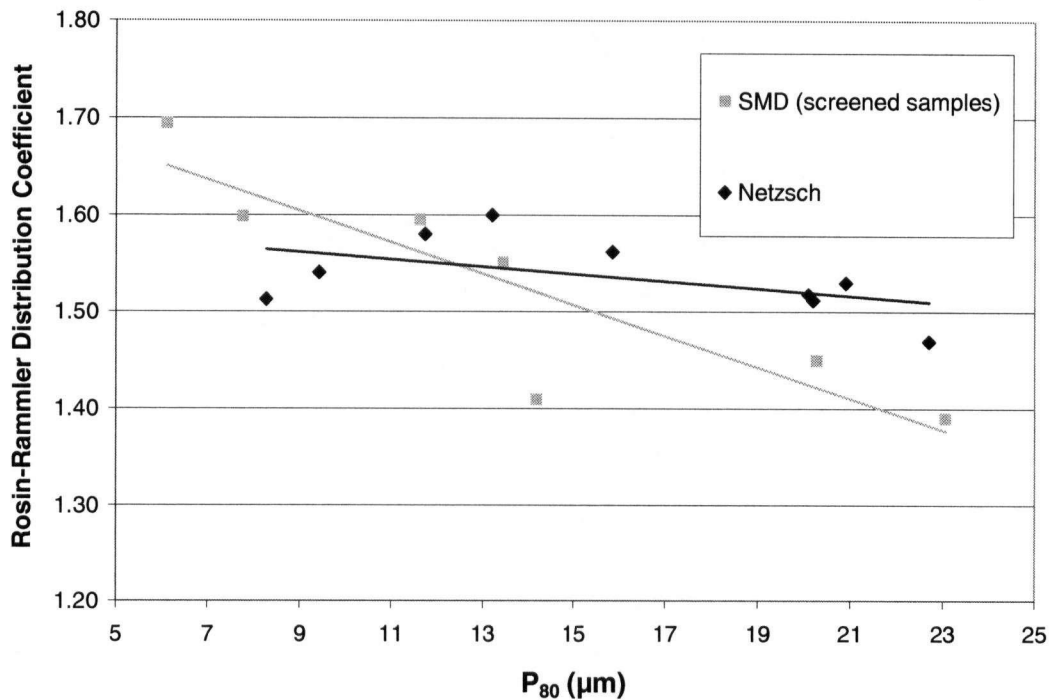
Figure 18. Rosin-Rammler distribution coefficient versus P_{80} for zinc 1st retreat concentrate products

The Rosin-Rammler function fit the particle size distributions best at P_{80}s above ~10μm. The SMD has a wider size distribution at coarser grind sizes (P_{80}>12μm), and a narrower size distribution at finer sizes. The widths of the Netzsch product size distributions are fairly consistent across the range of grind sizes. One explanation for the unexpected narrowing of the particle size distribution of the SMD at finer grind sizes is the use of a batch mill for lab testing. It is believed that higher stress intensities are required to grind finer particles – the stress intensities in the SMD may be too small to grind the finest particles due to the lower stirrer speed. As a grinding limit is reached for particles at the fine end of the distribution, only coarse particles are ground which would create a narrower size distribution.

Figure 19 plots the Rosin-Rammler distribution coefficient versus P_{80} by mill type for the zinc 2nd rougher concentrate products.
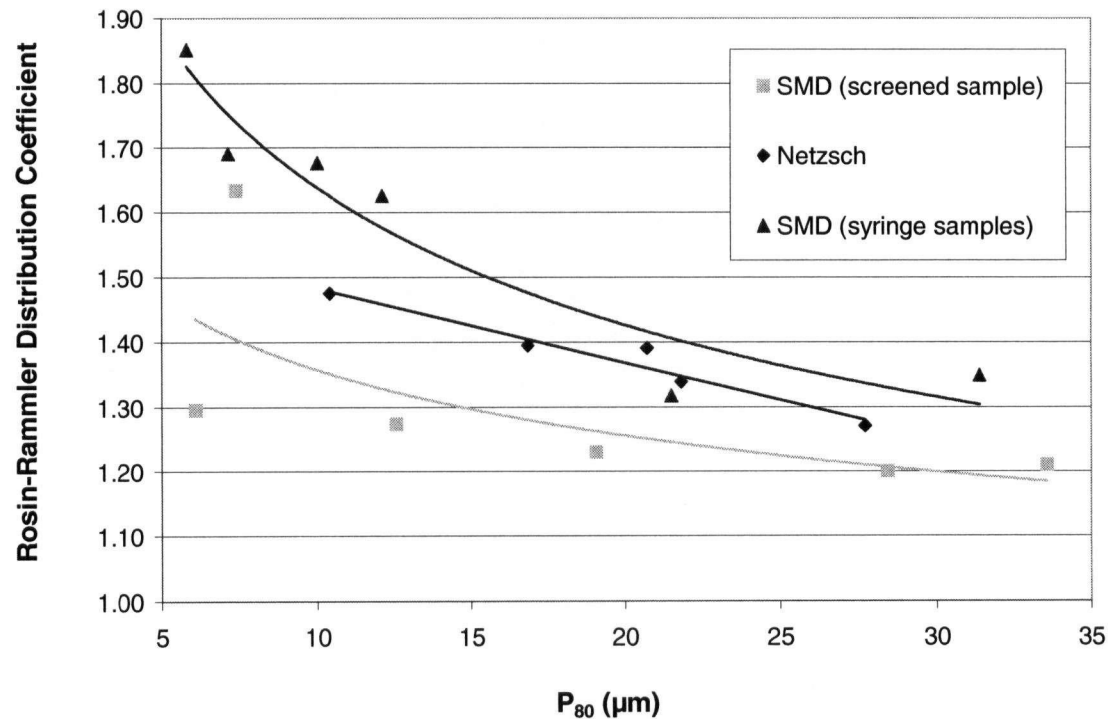
Figure 19. Rosin Rammler distribution coefficient versus P_{80} for zinc 2nd rougher concentrate

There was a discrepancy between the syringe and screened samples from the SMD. The size distributions of the syringe samples are narrower than those of the screened samples. This indicates a potential sampling error in the syringe sampling procedure. It is possible that due to hydrodynamics the syringe is more likely to take particles from a particular size range. Based on the screened SMD samples, the Netzsch products have narrower particle size distributions for most grind sizes, particularly at P_{80}s greater than 10µm where the Rosin-Rammler distribution fits the data best.

Figure 20 plots the Rosin-Rammler distribution coefficient versus P_{80} by mill type for the lead cleaner column tails products.
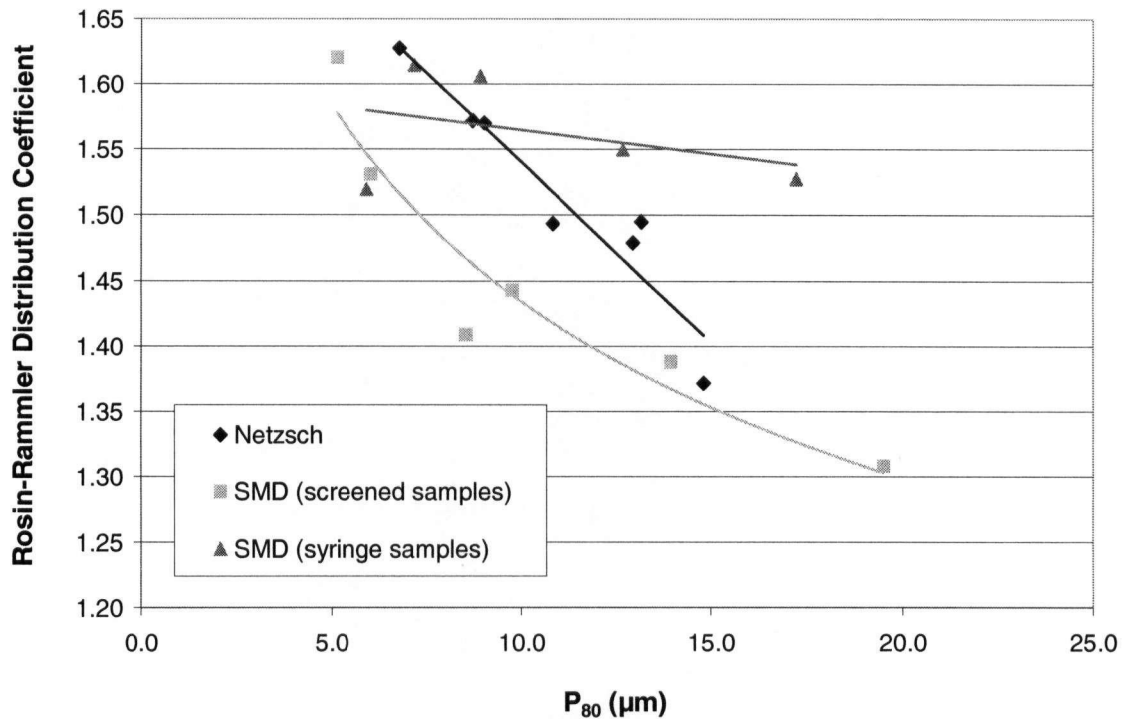
Figure 20. Rosin Rammler distribution coefficient versus P_{80} for lead cleaner column tails

Similar to the zinc 2nd rougher concentrate products, the syringe method of sampling produced narrower particle size distributions than the screened samples. Based on the SMD screened samples, the Netzsch mill produced narrower particle size distributions than the SMD for the lead cleaner column tail products. The particle size distributions become narrower for both mills as the grind size decreases. In the case of the SMD this result suggests that a grinding limit has been reached in the batch mill. In the case of the Netzsch mill, this result confirms Xstrata's claim that the particle size distribution narrows with decreasing grind size (Young, 2005). According to Yue and Klein (2005), there is an optimum feed size to media size ratio. The progeny particles from grinding fall outside of this limit; therefore, below a certain particle size, regrinding of the progeny becomes less efficient thereby narrowing the size distribution.

6.3.3 P_{80}:P_{20} ratio

An alternative method of measuring the spread of particle size distributions is to divide the P_{80} by the P_{20} for each sample. This ratio can be plotted versus P_{80} as shown in Figures 21 through 23.
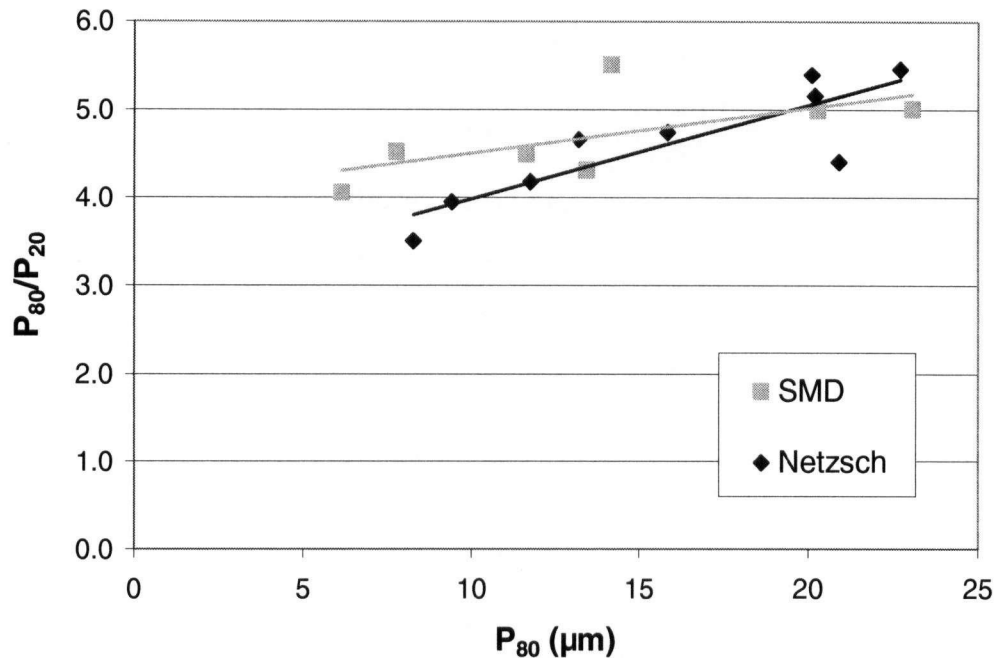
Figure 21. P_{80}/P_{20} vs. P_{80} for zinc 1st retreat concentrate mill products

For the zinc 1st retreat concentrate, contrary to the Rosin-Rammler distribution coefficient curves (Figure 18), the width of the size distributions are similar except for the finest products. At P_{80}s less than ~10μm, the SMD produces slightly wider size distributions.
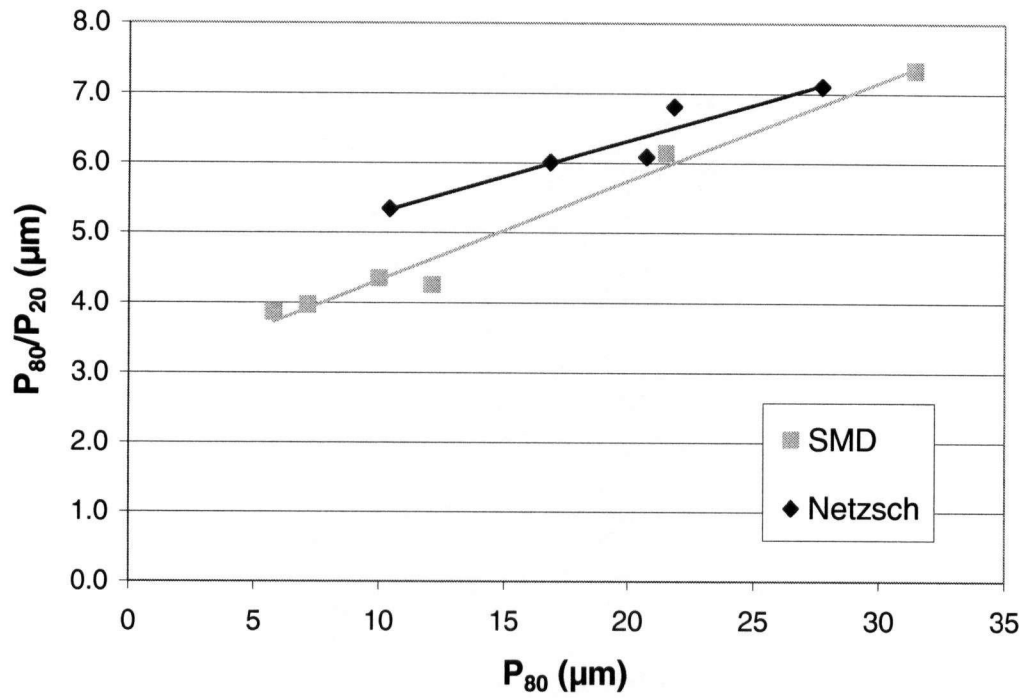
Figure 22. P_{80}/P_{20} vs. P_{80} for zinc 2nd rougher concentrate mill products

The Rosin-Rammler results showed that the Netzsch products had narrower size distributions at all grind sizes (Figure 19); however, the $P_{80}:P_{20}$ ratio plot shows that the Netzsch mill products have wider distributions, particularly at finer P_{80}s.
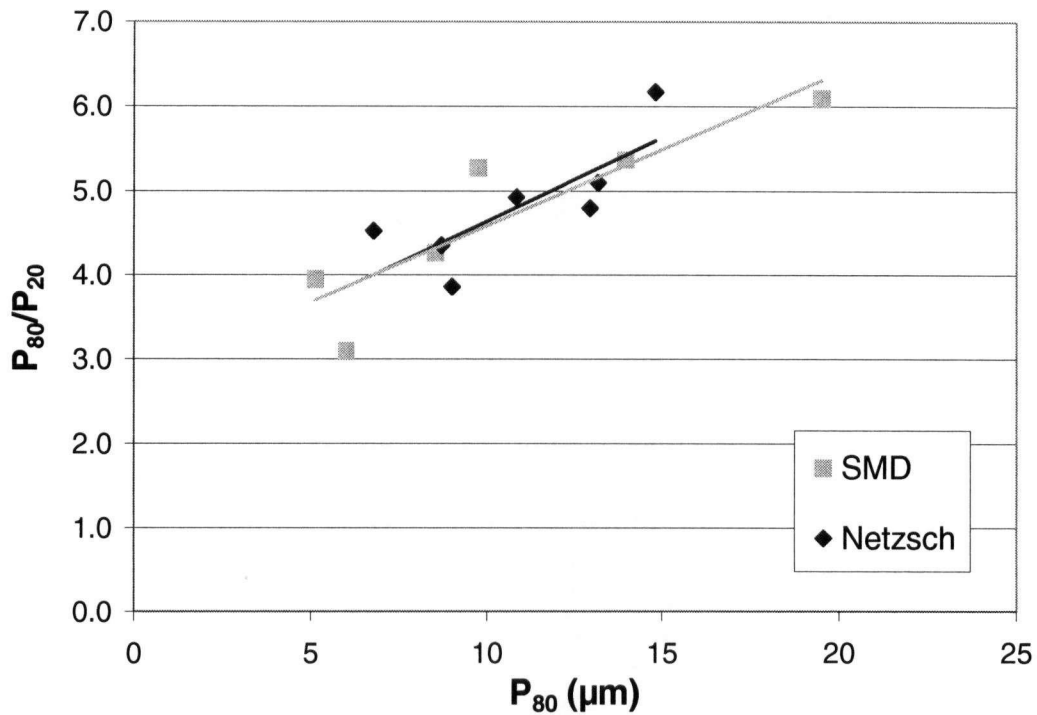
Figure 23. P_{80}/P_{20} vs. P_{80} for lead cleaner column tails mill products

The widths of the lead cleaner column tails product size distributions are similar for both mills according to the P_{80}:P_{20} plot.

6.3.4 Specific Surface Area Measurements

The specific surface area was measured for the screened samples from each mill. At comparable P_{80}s, a high specific surface area indicates a higher fines content and thus a wider size distribution.

Figure 24 plots specific surface area versus P_{80} for the zinc 1st retreat concentrate products. The SMD curve appears to be slightly higher than that of the Netzsch mill at the finer grind sizes; however, the curves are very close. This indicates that the products have similar proportions of ultrafine particles for a given P_{80}.
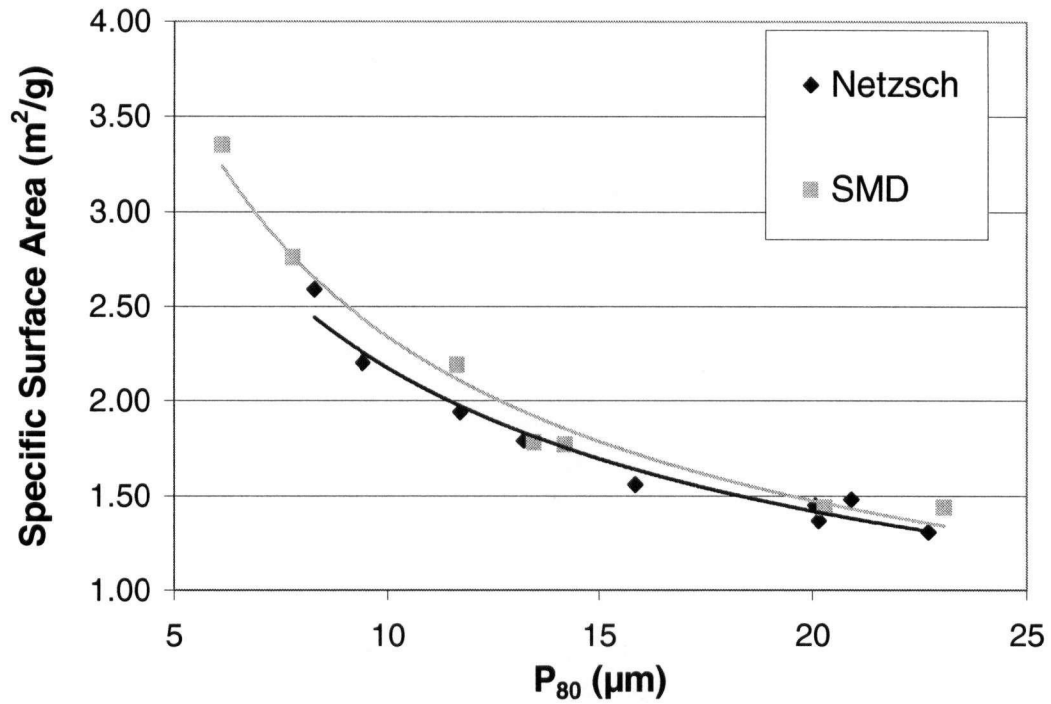
Figure 24. Specific surface areas versus P_{80} for zinc 1st retreat concentrate products

Figure 25 plots specific surface area versus P_{80} for the zinc 2nd rougher concentrate products. There is no clear trend that would indicate a difference between the mills. While the Netzsch mill products follow a similar trend to that for the other two circuit feeds, the SMD curve is very scattered. In this case, the specific surface area measurements are not able to provide information on differences between the mills.
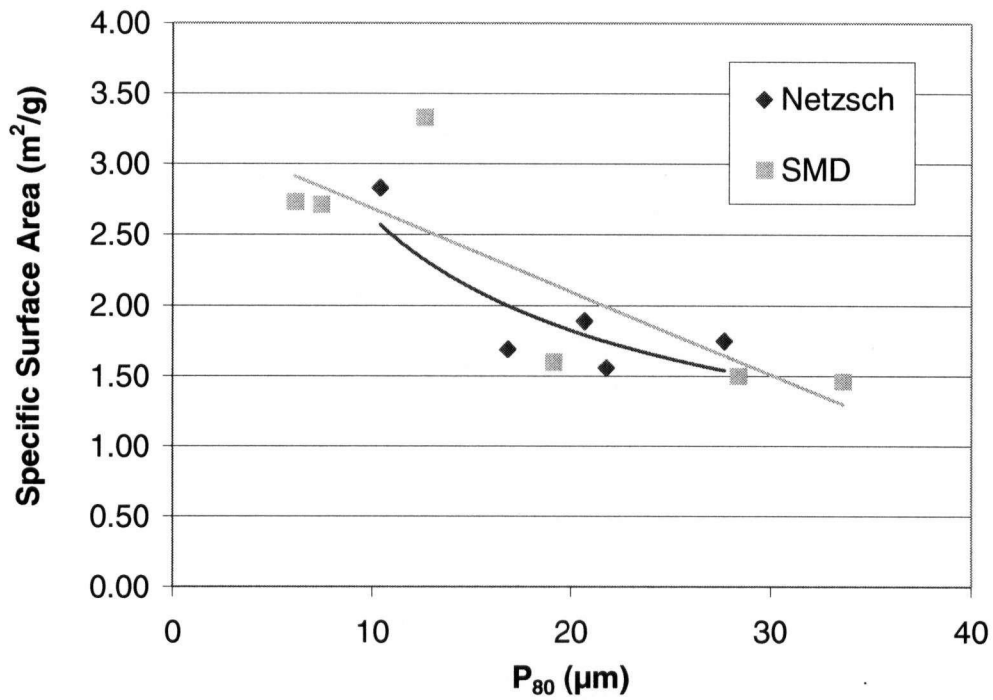
Figure 25. Specific surface area versus P_{80} for zinc 2nd rougher concentrate products

Figure 26 plots specific surface area versus P_{80} for the lead cleaner column tails products. The curves are similar except for the finest grind sizes ($P_{80}<7\mu m$) where the SMD product has a higher specific surface area than the Netzsch mill product. This is indicative of a higher proportion of ultrafine particles in the SMD product.
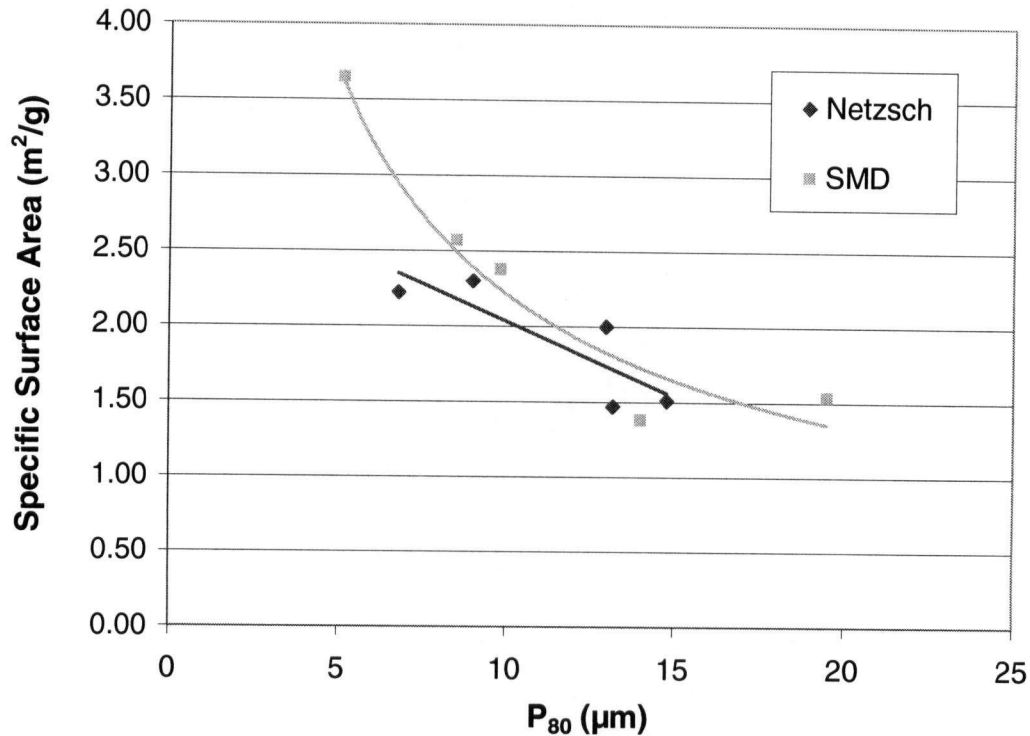
Figure 26. Specific surface area versus P_{80} for lead column tail products

6.4 Conclusions

The particle size distributions of the mill products were characterized using different methods. Rosin-Rammler distributions indicated that the SMD produced wider particle size distributions than the Netzsch mill for the three regrind feeds. Decreasing the grind size resulted in a narrower size distribution for both mills. The ratio of P_{80}:P_{20} was plotted against P_{80} to characterize the spread of the distributions. These plots did not indicate any differences between the mills that were consistent for the three samples. The specific surface areas of the mill products indicated that the SMD produced a greater proportion of fines when grinding the lead cleaner column tails below 10μm. This trend was seen to a lesser extent in the zinc 1st retreat concentrate products, and it was not apparent for the zinc 2nd rougher concentrate products. The trend in the lead samples could be due to over-grinding of the softer galena mineral in the batch mill. In general, the SMD appeared to produce a higher proportion of ultrafine particles for a given grind size than the Netzsch mill.

In order to understand these results, it is important to consider differences in the operation of the two mills. In this study, a batch mill (SMD) was compared to a continuous mill (Netzsch).

Batch operation of the SMD could result in over-grinding of the fines as all particles stay in the mill for the full residence time. The Netzsch mill better approximates plug flow than the SMD which would be expected to result in a narrow particle size distribution. The results may also indicate a difference in breakage mechanisms between the two mills. The lower stress intensity in the SMD produces more ultrafines which indicates that attrition grinding predominates. The higher stress intensity in the Netzsch mill possibly results in a combination of impact and attrition breakage. This would produce a narrower size distribution as impact breakage tends to create more uniformly sized progeny particles compared to attrition grinding. The mineral composition of the three streams may also play a role. Streams with a high ratio of quartz (hard) to sulphide (soft) would have a range of breakage rates. The range of breakage rates would decrease at high stress intensities (see Chapter 4); therefore, low stress intensity mills could be expected to have a wider size distribution than high stress intensity mills.

6.5 Recommendations

Continuous testing of an SMD unit would avoid the issues of over-grinding and grinding limits that are present in the batch unit. The effect of short-circuiting on the particle size distributions could also be determined. A study should be conducted to compare a batch and a continuous SMD in terms of energy, particle size distributions, mineral liberation and mineral breakage rates. The most appropriate method of characterizing a particle size distribution depends on the application. The Rosin-Rammler distribution coefficient and the $P_{80}:P_{20}$ ratio measure the entire distribution, so a distribution could be wide due to excessive coarse particles or excessive fine particles. The specific surface area data provides additional information as it is a measure of the amount of fines; therefore, this method best reflects behavior at the fine end of the distribution. The Rosin-Rammler distribution fits relatively poorly at the fine end of the distribution. In the case of flotation, the relative amount of fines is the most important characteristic of the distribution; therefore, the specific surface area is the most suitable method of characterization.

CHAPTER 7 Effect of Ultrafine Grinding on Mineral Liberation

7.1 Introduction

Mineral liberation analysis was performed on products from the laboratory high-speed stirred mills. Mineral liberation, associations and texture were related to changes in mill type and grind size. Further grinding trials were conducted to relate mineral liberation behavior to mineral hardness and mill stress intensity.

7.2 Experimental Procedure

Samples for mineral liberation analysis were obtained from the mill comparison phase of the grinding trials according to the procedures outlined in section 3.6. Mineral liberation analysis was performed on the samples as described in section 3.4.3.

7.3 Results and Discussion

7.3.1 Zinc 2nd Rougher Concentrate

7.3.1.1 Feed Characterization

A mineral liberation analysis was performed on zinc 2nd rougher concentrate. Table 6 shows the modal mineralogy for this sample based on MLA measurements (minerals are identified based on their X-Ray spectrum).

Table 6. Modal mineralogy for zinc 2nd rougher concentrate

Mineral	Weight %
Sphalerite	65
Pyrite	16
Quartz	15
Galena	2

The overall liberation of sphalerite is approximately 82%. Despite high sphalerite liberation, this stream contains significant amounts of contaminant minerals as shown in Table 6. These results suggest that a significant portion of the contaminant minerals occur as free particles (i.e. not attached to sphalerite). Their presence could be due to either entrainment or inadvertent surface activation causing flotation.

Figure 27 plots the liberation of each mineral versus mean particle size (by cyclosizer fraction) along with the overall weight distribution by size. The weight distribution does not add up to 100% as the -5 μm material is not included.
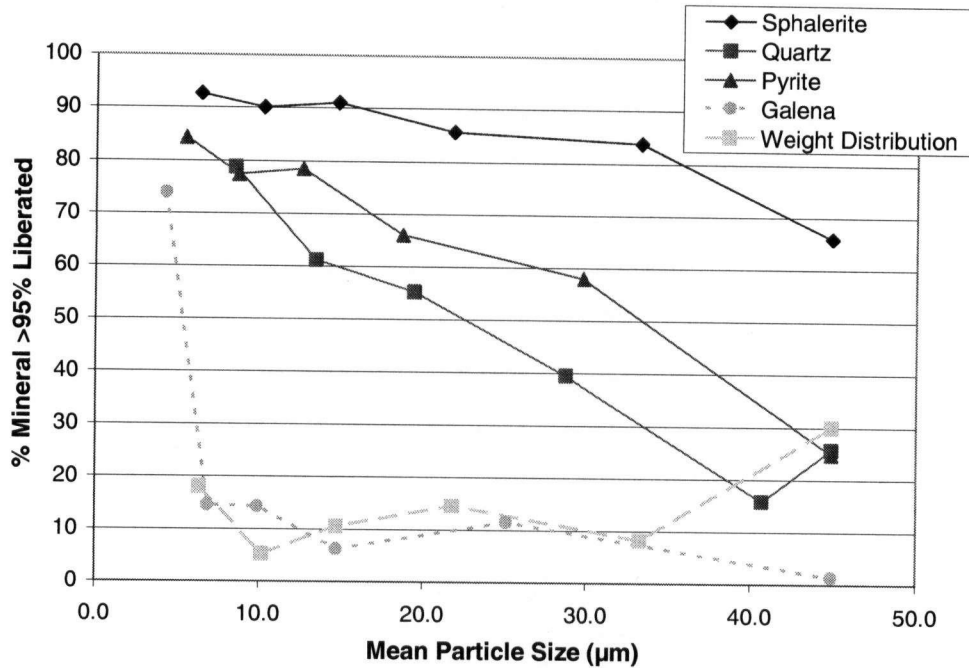
Figure 27. Mineral liberation by size fraction for zinc 2nd rougher concentrate

While liberation increases for all minerals with decreasing particle size as expected, the amount of the increase varies. For the sphalerite, liberation increased from about 85% in the C1/2 cyclosizer fraction to about 93% in the C6 fraction. Pyrite liberation increased from 58% to 84% over this size range, although the increase was much larger when the +38μm material is taken into account. For quartz and galena, the change in liberation was much greater over the C1/2 to C6 size range. For quartz, liberation increased from 15% to almost 80% and for galena from 12% to about 75%. It should be noted that quartz liberation improved in an almost linear manner with decreasing particle size, while galena liberation only improved in the finest fraction. These results suggest that there is potential significant benefit in grinding quartz to finer sizes as it would lead to an incremental improvement in quartz liberation and therefore quartz rejection. However, for galena, the zinc 2nd rougher concentrate would have to be ground below 10 μm to achieve a significant increase in liberation.

7.3.1.2 Mineral Associations

When determining whether ultrafine grinding would improve flotation performance, it is important to consider how gangue minerals are recovered to the concentrate. There are three mechanisms by which this deportment occurs: entrainment, activation and locking (i.e. flotation due to association with the mineral to be concentrated). If gangue mineral recovery is due to entrainment or activation, increasing gangue liberation will probably not improve gangue rejection. If the problem is locking, increasing gangue liberation may improve gangue rejection.

Although Figure 27 shows the liberation of quartz, pyrite and galena, it does not show if these minerals are associated with sphalerite. Mineral association is quite important. For instance, while quartz-sphalerite composite grains need to be ground to improve gangue rejection, there is likely no need to grind quartz-pyrite composite grains. Therefore, it is important to determine the amount of quartz and pyrite that are attached to sphalerite.

Figures 28 and 29 show the distributions of liberated and locked quartz and pyrite along with the associations of these gangue minerals. Since the amount of galena present is small (2%), its association distribution was not analyzed.
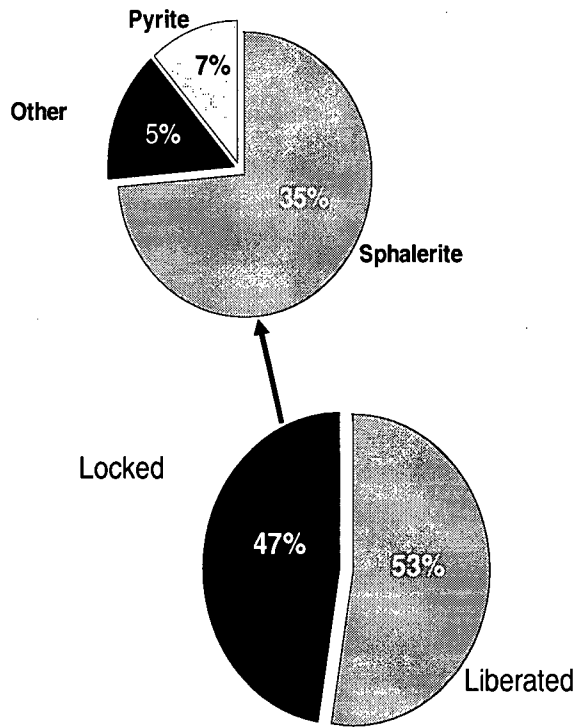
Figure 28. Minerals associated with locked quartz
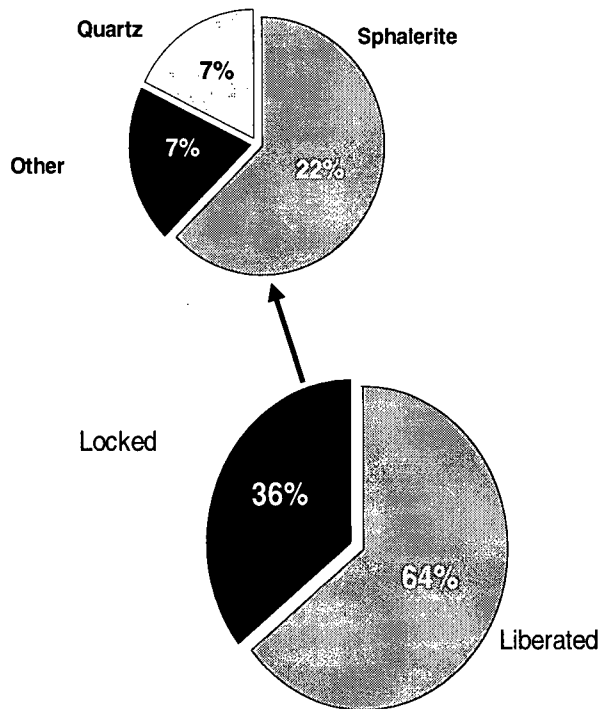
Figure 29. Minerals associated with locked pyrite

Figure 28 shows that 53% of quartz is liberated and that 47% is locked. A closer examination of the locked grains shows that 12% is locked with pyrite and galena leaving 35% of the quartz attached to sphalerite. This suggests that improving quartz liberation would improve sphalerite liberation and decrease quartz contamination of the zinc concentrate.

Figure 29 shows that 64% of the pyrite is liberated, 14% is locked with quartz or other gangue minerals and 22% is locked with sphalerite. While the majority of locked pyrite is associated with sphalerite, the degree of liberation of pyrite is higher than for quartz; therefore, improving pyrite liberation would not be as beneficial to the zinc concentrate. Pyrite may also float due to inadvertent activation, so improving pyrite liberation might not significantly improve pyrite rejection.

These results suggest that 73% of the quartz and 82% of the pyrite can be rejected without the need for finer grinding. For pyrite, chemical depression would be required. For quartz, entrainment is likely the reason for contamination of the product. It should, however, be noted that the measurement of the degree of liberation is based on two-dimensional

sections. This method can overestimate the degree of liberation by up to 10%. Therefore, the actual liberation of quartz and pyrite is likely lower than indicated by these numbers.

Figures 30 and 31 show the association of pyrite and quartz with sphalerite by locking class and size fraction. These data provides information on the association of gangue minerals with valuable minerals. For instance, in Figure 30, particles containing 20-40% pyrite in the 12-18 μm size fraction will contain ~40wt% sphalerite. The remaining 60wt% is composed of pyrite and other gangue minerals.
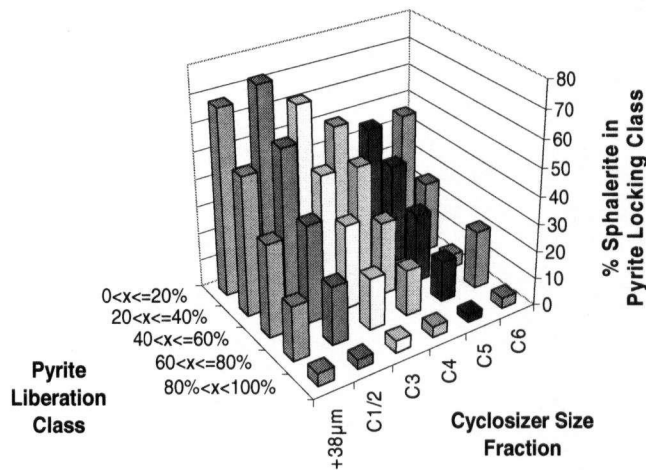
Figure 30. Association of sphalerite with locked pyrite in zinc 2nd rougher concentrate
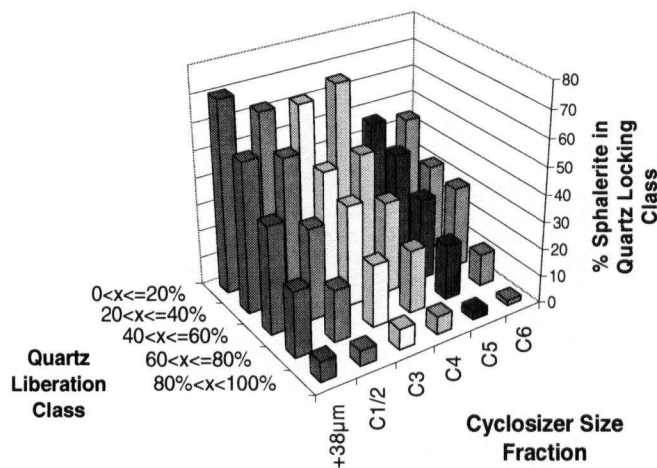
Figure 31. Association of sphalerite with locked quartz in zinc 2nd rougher concentrate

58

These plots show that quartz and pyrite become less associated with sphalerite as particle size decreases. The proportion of quartz or pyrite associated with sphalerite is lower in the finest cyclosizer fraction (C6) than in the coarser fractions. This indicates that finer grinding would reduce locking of sphalerite with gangue minerals. Improved liberation of quartz and pyrite would allow for better rejection and therefore improve the grade of the zinc concentrate from cleaning flotation.

7.3.1.3 Texture

Mineral liberation gives an indication of the amount of comminution required to achieve a specific metallurgical target, however, it does not take mineral texture into account. Figure 32 shows two locked sphalerite-quartz particles from the zinc 2nd rougher concentrate. These particles are in the 26-38μm cyclosizer fraction (C1/2).

32(a)   32(b)
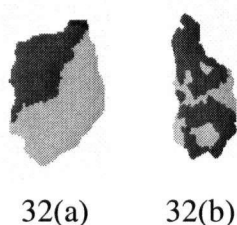
Figure 32. Locked quartz-sphalerite particles from the zinc 2nd rougher concentrate a) simple texture b) complex texture (26-38μm particle size range)

These are false colour images produced by the MLA using grey-scale SEM images. In Figure 32, quartz and sphalerite grains are grey and black, respectively. Particle 32(a) would be more easily liberated by further grinding than particle 32(b) which has a more complex texture. The zinc flotation streams used for this study contained a mixture of both simple and complex textures.

Table 7 tabulates the grain size of the minerals in the zinc 2nd rougher concentrate. The data clearly show that the grain size of galena is finer than that of pyrite and quartz. This indicates that the galena texture is finer than that of the other minerals. This may in part explain why galena liberation is not achieved until the particle size is less than 10 μm.

Table 7. D_{50} grain size by mineral in zinc 2nd rougher concentrate

	Sphalerite	Quartz	Pyrite	Galena
D_{50} Grain size (μm)	17.0	15.6	12.4	3.1

The fineness of galena is also apparent from MLA images. Figure 33 shows two particles which are indicative of lead sulphide texture in the 26-38μm particle size range. Sphalerite, pyrite and galena are shown as dark grey, light grey and black, respectively.

33(a)   33(b)
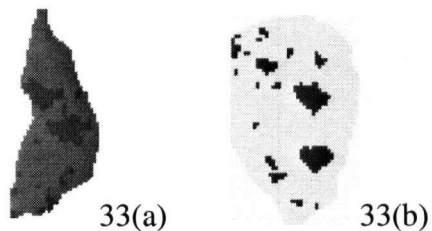
Figure 33. Particles containing galena in coarsest size fraction 33(a) sphalerite-galena 33(b) pyrite-galena (26-38 μm particle size range)

Liberation classes can be used to better understand the distribution of minerals within particles. If a large proportion of a mineral is 0-20% liberated, this indicates that there is a small amount of that mineral in a large number of particles as opposed to a large amount of that mineral in a smaller number of particles. The distribution of mineral by liberation class also indicates how easily the mineral can be separated. Figure 34 plots the distribution of minerals by liberation class in the zinc 2nd rougher concentrate.
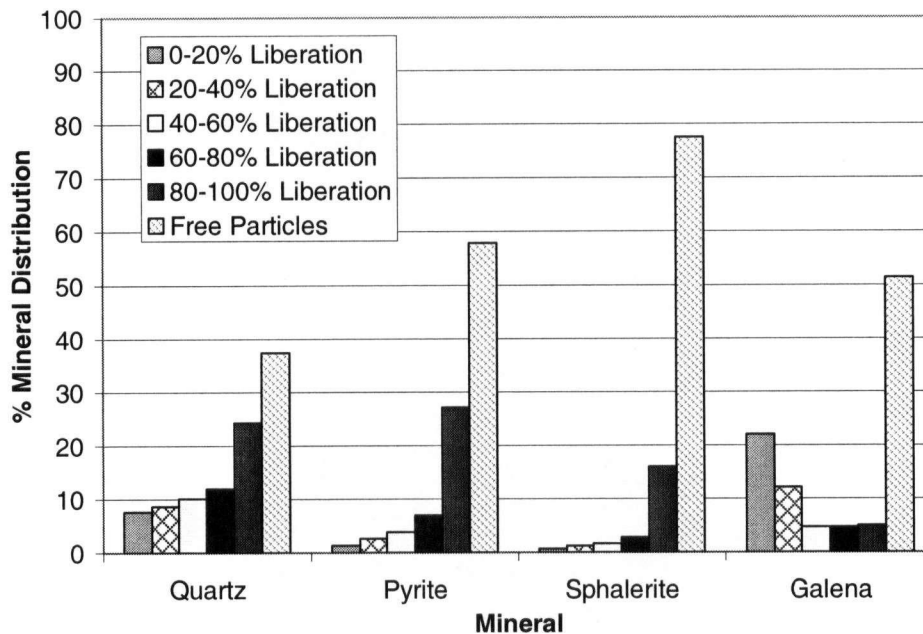
Figure 34. Mineral by liberation class in zinc 2nd rougher concentrate

The majority of sphalerite is present in free particles, while the majority of locked sphalerite is in the 80-100% liberation class. This indicates both that the sphalerite will be easy to recover by flotation and that the locked sphalerite has a coarse grain size. Therefore, improving sphalerite liberation will be relatively easy. In the case of quartz, there is a greater chance to improve liberation as a large proportion is currently locked. Of the locked quartz, the majority is in the 60-100% liberation class which indicates a relatively coarse grain size. The most interesting result in terms of texture is for galena. The liberation class distribution for galena is bimodal with 51% in the free particle class and 36% in the 0-40% liberation class. This result, together with the observations from Figures 27 and 33, shows that a very small grind size would be necessary to improve the degree of liberation of galena due to its fine grain size; however, a significant amount of galena may be rejected by chemical depression (lime addition).

7.3.1.4 Product Characterization

The zinc 2nd rougher concentrate was ground using both the Netzsch mill and the SMD to a fine, medium and coarse size. Table 8 lists the grind sizes analyzed for each mill.

Table 8. Grind sizes of mill products

Mill	Grind Size, P_{80} (μm)		
	Fine	Medium	Coarse
Netzsch (IsaMill)	10	21	28
SMD	13	19	28

Figures 35 and 36 plot mineral liberation (>95% liberated) versus P_{80} for the SMD and Netzsch mill products. The error bars represent the 95% confidence intervals.
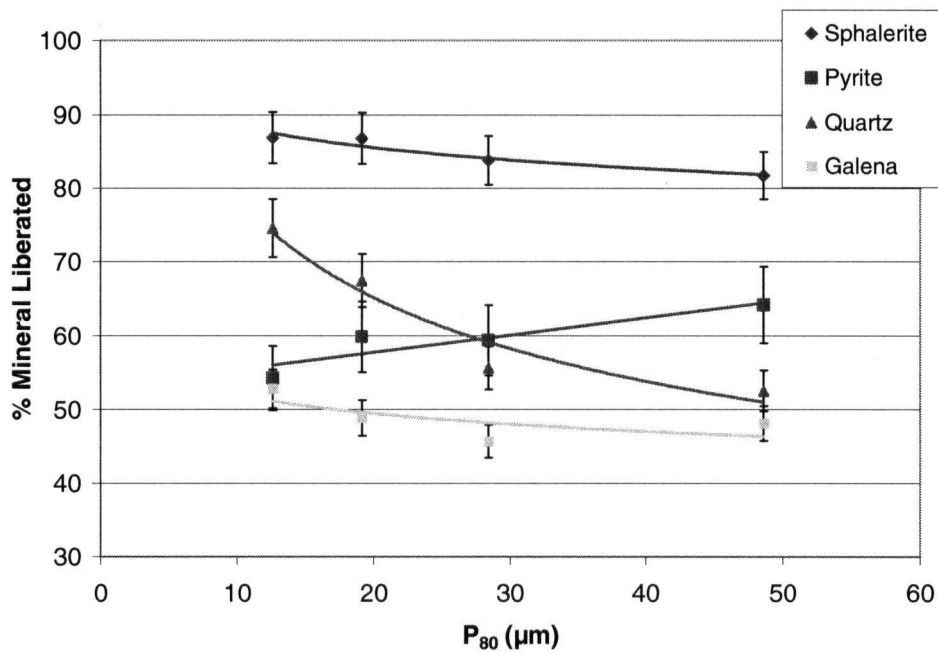
Figure 35. Mineral liberation versus P_{80} for SMD products
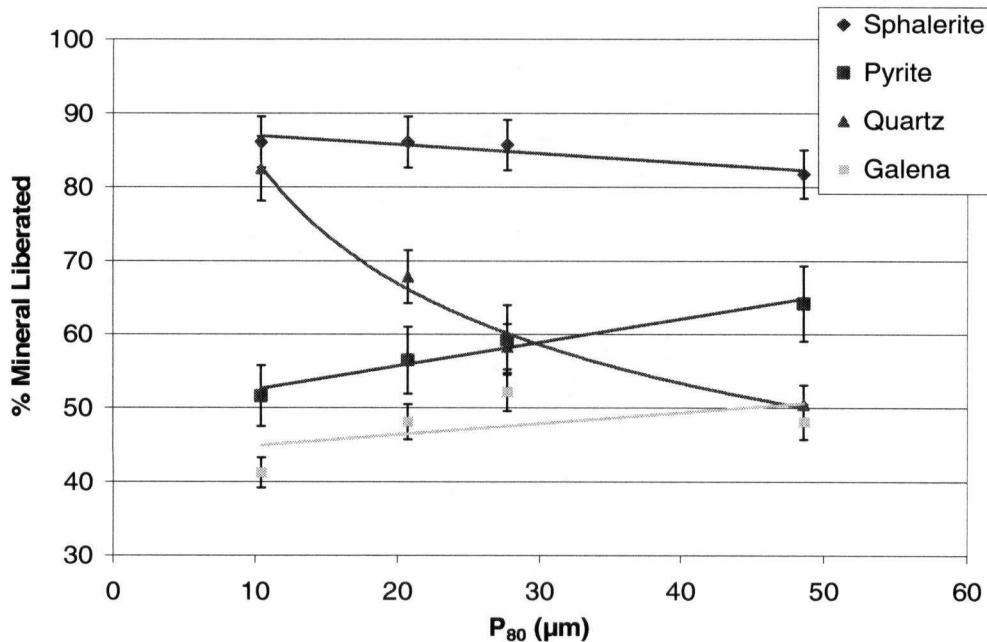
Figure 36. Mineral liberation versus P_{80} for Netzsch mill products

Figures 35 and 36 show that for both the SMD and Netzsch mills, quartz liberation increases significantly with decreasing grind size of the zinc 2nd rougher concentrate. Sphalerite liberation improves by ~4-5% by grinding the feed to a P_{80} of 10-13μm. However, the liberation of the sulphide gangue minerals appears to decrease with decreasing grind size, indicating experimental error in the measurement of liberation. The trend is believed to be a result of assuming that liberation in the finest size fraction (C7) is equivalent to that in the next coarsest size fraction (C6). When liberation in the C7 fraction is set at a higher value than C6, the pyrite and galena liberation curves are flat or increase slightly with decreasing particle size which is a more reasonable trend.

There are three possible explanations for the behaviour of quartz presented in Figures 35 and 36. Firstly, the liberation/size data given in Figure 27 strongly suggest that quartz is the mineral that is most impacted by finer grinding. Secondly, the stress intensity in both the SMD and Netzsch mills were sufficiently high to liberate quartz. Thirdly, because of differences in mineral hardness, attrition may be directed towards the sulphides on the surface of the quartz rather than the quartz itself. Sulphides may be attritted off the surface of quartz, thus improving quartz liberation.

Preventing quartz from reporting to the final zinc concentrate is important as it is a penalty element in smelter contracts. Previous work by AMIRA on the Red Dog zinc rougher regrind circuit has also shown that the primary benefit of regrinding is the improvement in quartz liberation rather than sphalerite liberation (Davey et al, 1993).

In general, the effect of both the Netzsch mill and SMD on mineral liberation is similar. For both mills, quartz liberation was significantly improved while sulphide mineral liberation was not. Although high-speed stirred mills may not improve sulphide mineral liberation, sulphide kinetics would still likely benefit from high-speed grinding. The use of inert media would minimize the release of iron ions and thus minimize the formation of iron hydroxide precipitates which could adsorb on particle surfaces. Tower mills do not use inert media. Also, the attritive action of high-speed stirred mills promotes the cleaning of particles surfaces (Pease et al, 2006).

7.3.2 Zinc 1st Retreat Concentrate

7.3.2.1 Feed Characterization

A mineral liberation analysis was performed on zinc 1st retreat concentrate. Table 9 shows the modal mineralogy for this sample based on MLA measurements.

Table 9. Modal mineralogy for zinc 1st retreat concentrate

Mineral	Weight %
Sphalerite	64
Pyrite	20
Quartz	10
Galena	3

The overall liberation of sphalerite is approximately 81%. Similar to the zinc 2nd rougher concentrate, significant amounts of pyrite and quartz contamination are present despite good sphalerite liberation. Therefore, the recovery of these minerals to the concentrate indicates problems with entrainment or inadvertent surface activation.

Figure 37 plots the liberation of each mineral versus mean particle size (by cyclosizer fraction) along with the overall weight distribution by size. The weight distribution does not add up to 100% as the -5 μm material is not included.
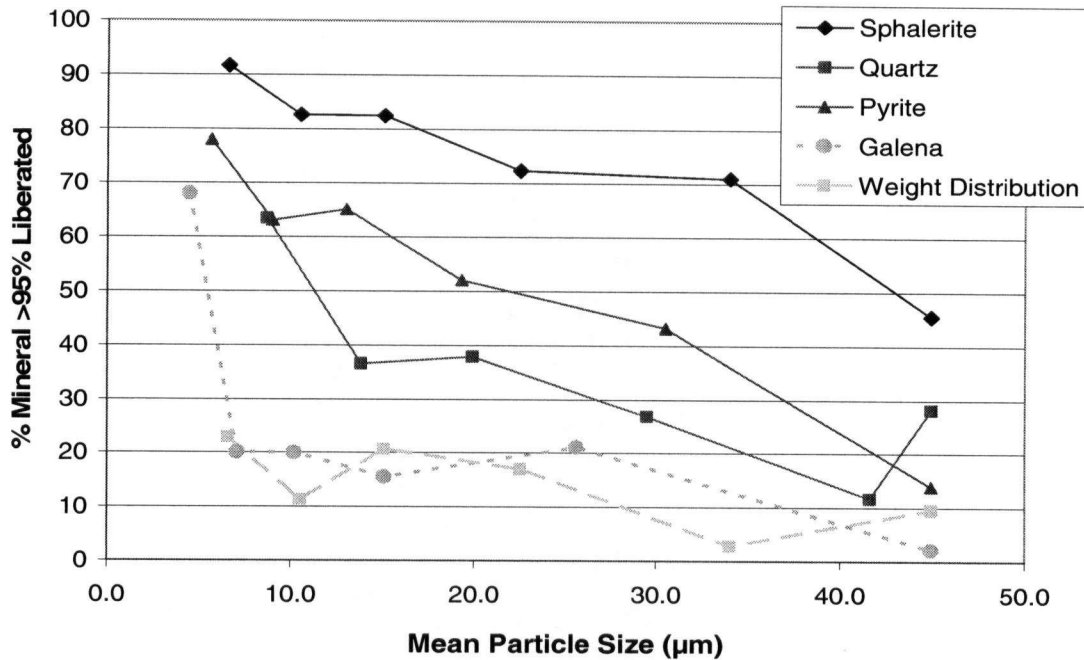
Figure 37. Mineral liberation by size fraction for zinc 1st retreat concentrate

The behavior of minerals with changes in particle size is similar to that in the zinc 2nd rougher concentrate. Sphalerite shows the smallest improvement in liberation with decreasing grind size as it is mostly liberated. Galena liberation only improves in the finest cyclosizer fraction, indicating a finely grained texture. Quartz shows the greatest improvement in liberation between the C1/2 and C6 fractions (from 16% to 79%), although pyrite also shows a similar improvement when the +38µm material is taken into account.

7.3.2.2 Mineral Associations

Figures 38 and 39 show the distributions of liberated and locked quartz and pyrite along with the associations of these gangue minerals. This is important for determining whether finer grinding would improve gangue rejection from the final zinc concentrate.
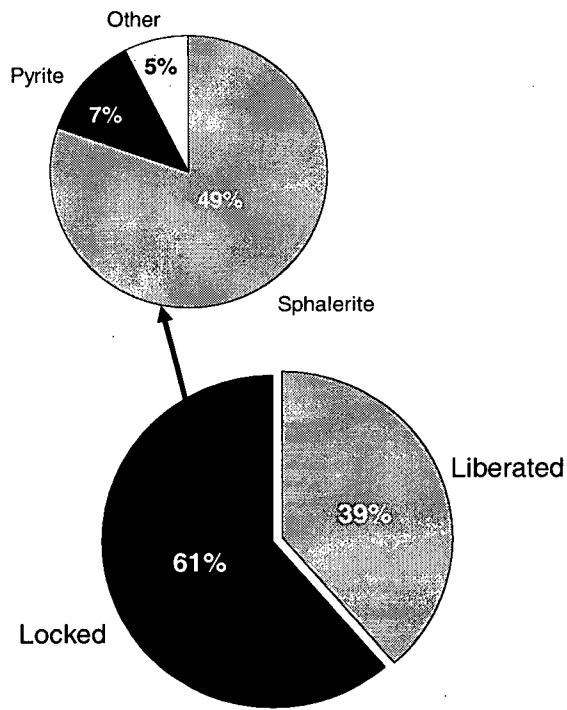
Figure 38. Minerals associated with locked quartz
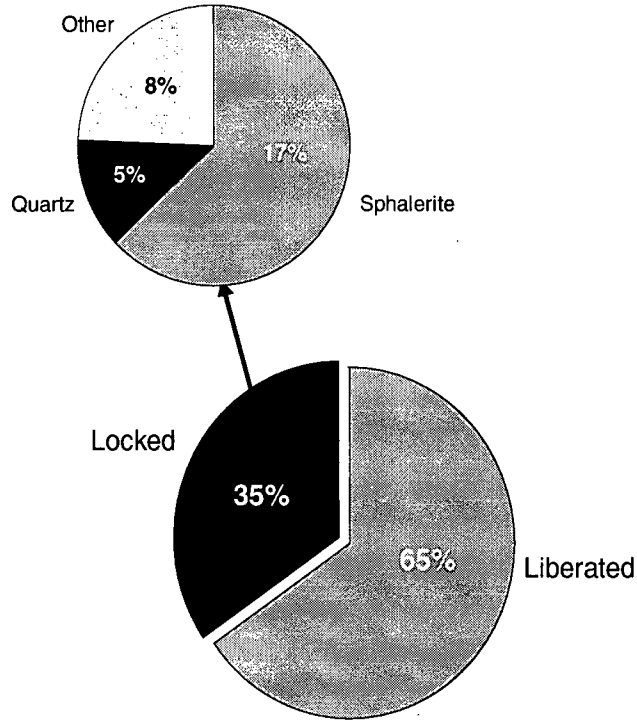
Figure 39. Minerals associated with locked pyrite

The greatest benefit of finer grinding would be improved quartz rejection from the concentrate. Figure 38 shows that 49% of quartz is locked with sphalerite. Figure 39 shows that a relatively small amount, 17%, of pyrite is locked with sphalerite. These results suggest that 51% of the quartz and 78% of the pyrite can be rejected without the need for finer grinding. Finer grinding would have a greater benefit for the zinc 1st retreat concentrate than for the zinc 2nd rougher concentrate as a larger part of the quartz contamination problem is due to locking with sphalerite.

7.3.2.3 Texture

Table 10 tabulates the grain size of the different gangue minerals in the zinc 1st retreat concentrate.

Table 10. D_{50} grain size by mineral in zinc 1st retreat concentrate

	Galena	Pyrite	Sphalerite	Quartz
D_{50} Grain Size (μm)	3.0	7.7	9.4	17.3

As was found in the zinc 2nd rougher concentrate, galena has the finest grain size. Quartz has the coarsest grains. Unlike the zinc 2nd rougher concentrate, sphalerite has a relatively fine texture compared to quartz.

Figure 40 is a plot of mineral distribution by liberation class for the zinc 1st retreat concentrate.
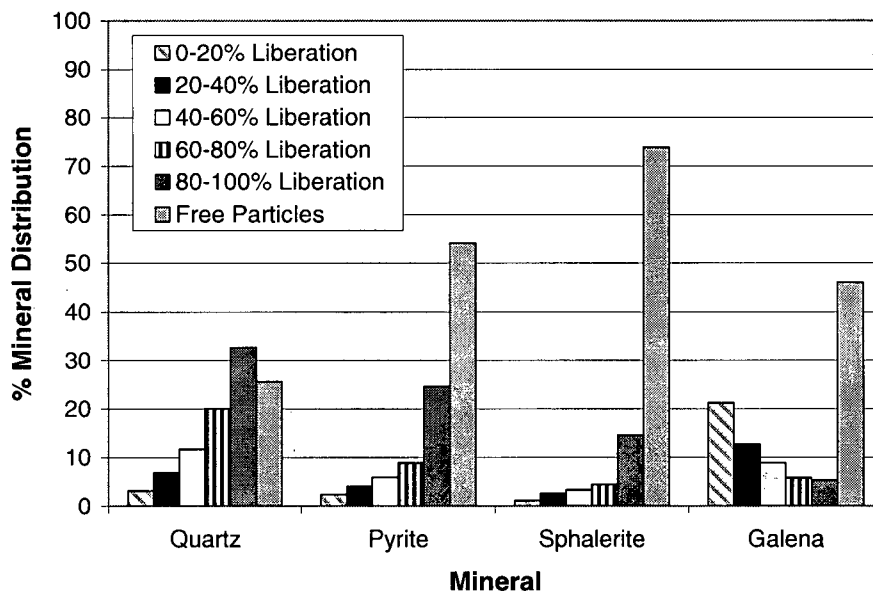
Figure 40. Mineral by liberation class in zinc 1st retreat concentrate

Similar to the zinc 2nd rougher concentrate, sphalerite and pyrite in the zinc 1st retreat concentrate are mostly liberated or in 80-100% liberated grains. Quartz has a lower degree of liberation than the sulphide minerals but has a large amount of material in the 80-100% liberation class. This indicates that the quartz is relatively coarse grained, and improvements in liberation should occur at a relatively coarse grind size. Galena has a bimodal distribution as in the zinc 2nd rougher concentrate. This indicates that the degree of galena liberation will not improve until a very fine grind size (<10μm).

7.3.2.2 Product Characterization

The zinc 1st retreat concentrate was ground using both the Netzsch mill and the SMD to fine, medium and coarse sizes. Table 11 lists the grind sizes analyzed for each mill.

Table 11. Grind sizes of mill products

	Grind Size, P_{80} (µm)		
Mill	Fine	Medium	Coarse
Netzsch (IsaMill)	8	16	23
SMD	8	14	23

Figures 41 and 42 plot mineral liberation (>95% liberated) versus P_{80} for the SMD and Netzsch mill products. The error bars represent a 95% confidence interval.
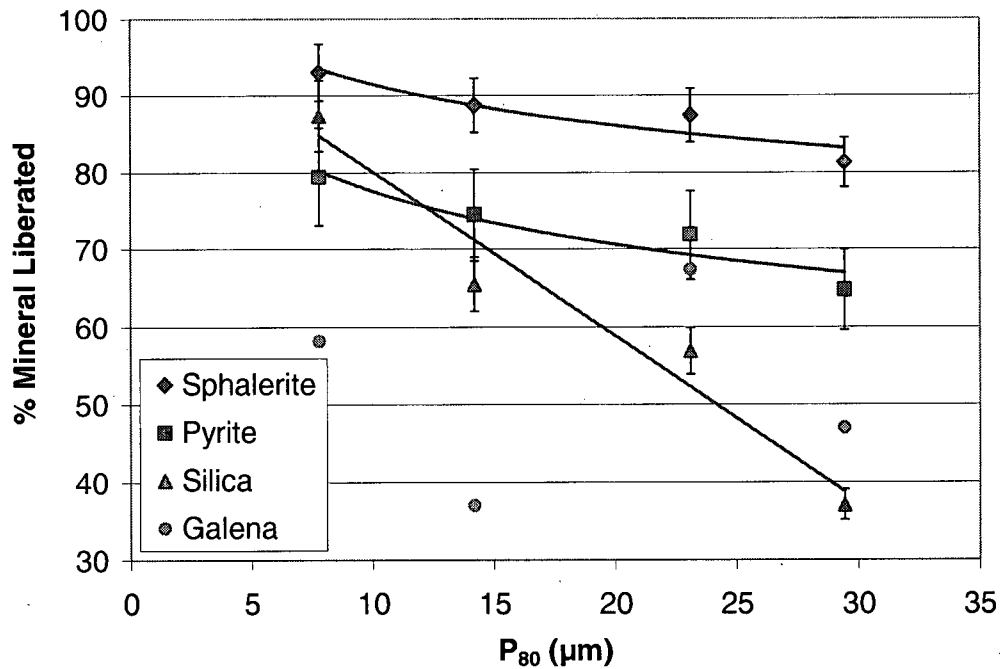
Figure 41. Mineral liberation versus P_{80} for SMD products

69
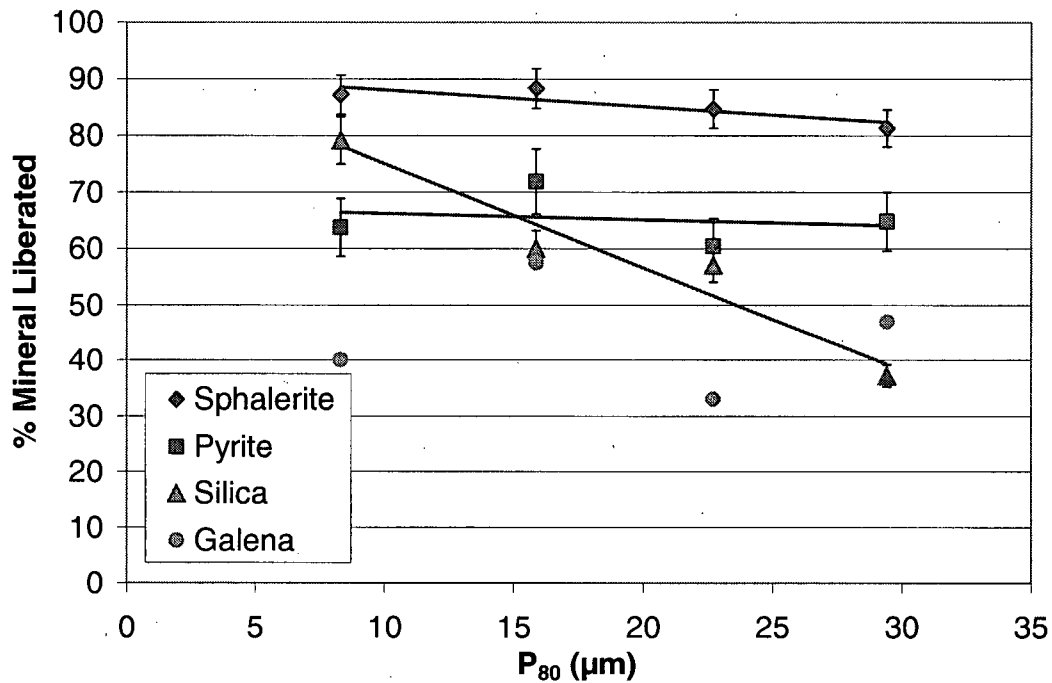
Figure 42. Mineral liberation versus P_{80} for Netzsch mill products

Sphalerite liberation improves by 6% for the Netzsch mill and by 11% for the SMD by grinding to a P_{80} of ~8μm. Quartz liberation improves significantly for both mills (50% for SMD and 42% for Netzsch). Pyrite liberation improves with decreasing grind size for both mills except for the finest Netzsch mill grind size. Based on the liberation of pyrite in the coarser Netzsch products, this point is likely an outlier. Galena liberation is very scattered. The poor curve obtained for this mineral could be attributed to the small quantity of galena in the sample (~3%). This makes it more difficult to obtain a representative analysis.

Regrinding the zinc 1st retreat concentrate stream to a finer grind size using either of the high-speed mills would be beneficial. Improving the degree of quartz liberation would increase quartz rejection from the zinc concentrate. Improving pyrite liberation would also be beneficial to the zinc concentrate grade.

The liberation behavior of the grinding products support the idea that the high stress intensities in stirred mills provide improved quartz liberation without excessive grinding of the sulphides as indicated by the results of the stress intensity, mineral hardness and breakage rate study (Chapter 4).

7.3.3 Lead Cleaner Column Tails

7.3.3.1 Feed Characterization

A mineral liberation analysis was performed on lead cleaner column tails. Table 12 shows the modal mineralogy for this sample based on MLA measurements.

Table 12. Modal mineralogy for lead cleaner column tails (MLA)

Mineral	Weight %
Sphalerite	34.4
Pyrite	30.9
Quartz	4.7
Galena	27.4

Pyrite and sphalerite are the primary contaminants in this stream.

Figure 43 plots the liberation of each mineral versus mean particle size (by cyclosizer fraction) along with the overall weight distribution by size. The weight distribution does not add up to 100% as the -5μm and +38μm material is not included.

Figure 43. Mineral liberation by size fraction for lead cleaner column tails

71

7.3.3 Lead Cleaner Column Tails

7.3.3.1 Feed Characterization

A mineral liberation analysis was performed on lead cleaner column tails. Table 12 shows the modal mineralogy for this sample based on MLA measurements.

Table 12. Modal mineralogy for lead cleaner column tails (MLA)

Mineral	Weight %
Sphalerite	34.4
Pyrite	30.9
Quartz	4.7
Galena	27.4

Pyrite and sphalerite are the primary contaminants in this stream.

Figure 43 plots the liberation of each mineral versus mean particle size (by cyclosizer fraction) along with the overall weight distribution by size. The weight distribution does not add up to 100% as the -5μm and +38μm material is not included.

Figure 43. Mineral liberation by size fraction for lead cleaner column tails

71

The greatest improvement in mineral liberation with decreasing particle size was for quartz. The sulphide minerals also improved to a lesser extent with decreasing particle size. Quartz, sphalerite and pyrite liberation increase fairly linearly, while galena liberation only improves at particle sizes below 15μm. However, compared to the zinc regrind streams, galena liberation improved at a relatively coarse grind size.

7.3.3.2 Mineral Associations

Figures 44 through 46 show the distributions of liberated and locked sphalerite, quartz and pyrite along with the associations of these gangue minerals.
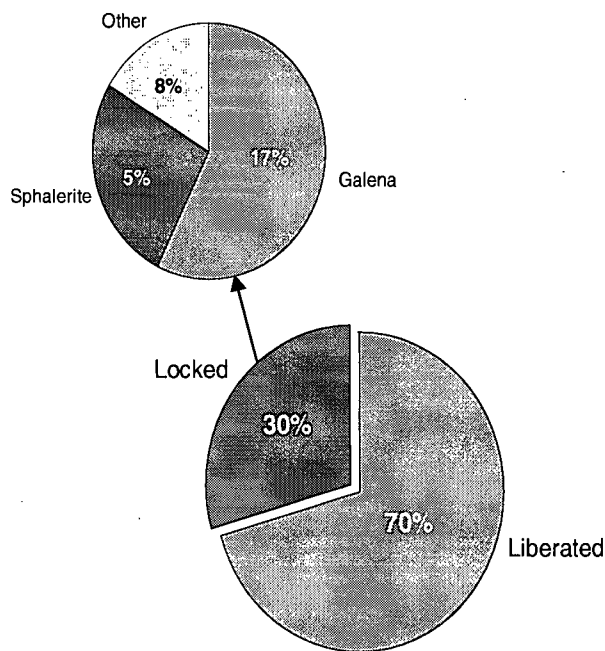
Figure 44. Minerals associated with locked pyrite
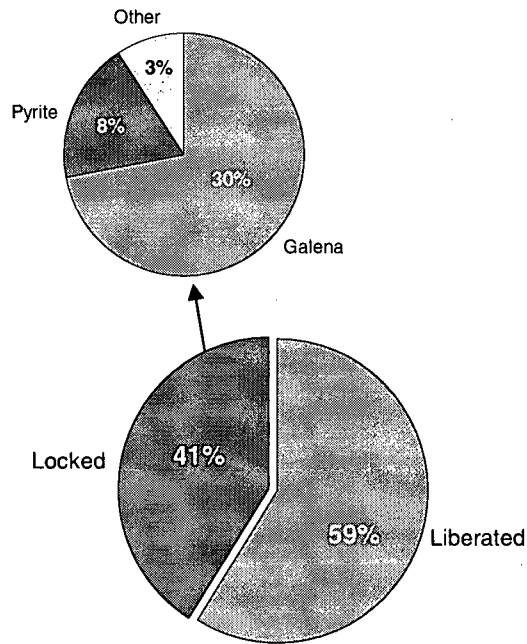
Figure 45. Minerals associated with locked sphalerite
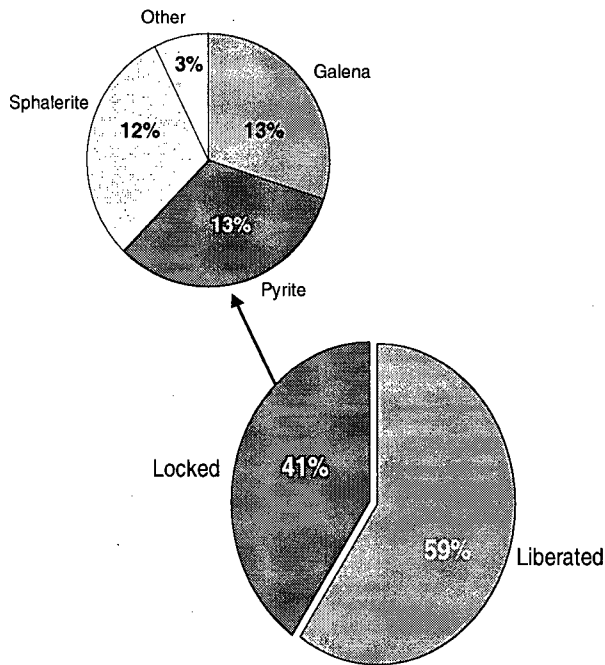
Figure 46. Minerals associated with locked quartz

Figure 44 shows that 70% of pyrite is liberated, indicating that the majority of the pyrite contamination issue is due to entrainment or surface activation. Figure 45 shows that 59% of sphalerite is liberated. While this is a high degree of liberation, 30% of sphalerite is locked with galena; therefore, increasing sphalerite liberation further would result in improved rejection of this gangue mineral from the lead concentrate. Quartz has the same degree of liberation as sphalerite; however, only 13% of quartz is locked with galena. Therefore, improving quartz liberation would not be as beneficial as improving sphalerite liberation. These results suggest that 83% of the pyrite, 70% of the sphalerite and 87% of the quartz can be rejected without the need for finer grinding.

7.3.3.3 Texture

Table 13 tabulates the grain size of the different gangue minerals in the lead cleaner column tails.

Table 13. D_{50} grain size by mineral in lead cleaner column tails

	Galena	Sphalerite	Pyrite	Quartz
D_{50} Grain Size (μm)	5.5	8.6	8.9	6.8

Compared to the zinc regrind streams, the grain sizes are fairly even for the four main minerals. This likely indicates a similar texture for the minerals.

Figure 47 is a plot of mineral distribution by liberation class for the lead cleaner column tails.
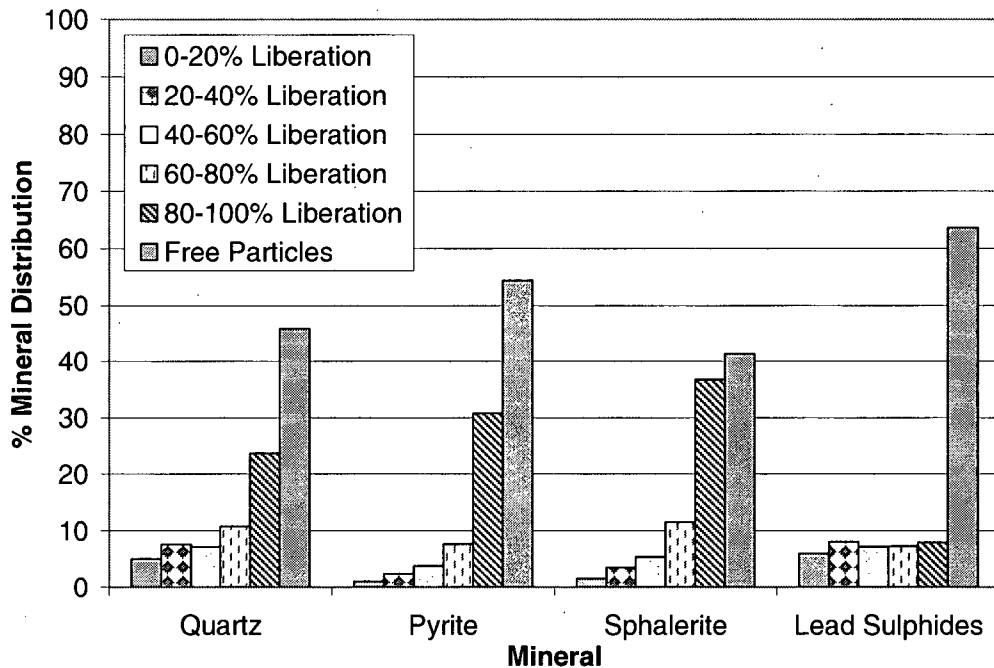
Figure 47. Mineral by liberation class in lead cleaner column tails

The three gangue minerals, quartz, pyrite and sphalerite, have similar distributions with high levels of liberation and nearly (80-100%) liberated grains. Galena does not have the bimodal distribution seen in the zinc regrind streams, indicating that the galena texture is coarser and liberation should improve more linearly with decreasing grind size.

7.3.3.2 Product Characterization

The lead cleaner column tails stream was ground using both the Netzsch mill and the SMD to a fine, medium and coarse size (two coarse sizes were analyzed for the Netzsch mill). Table 14 lists the grind sizes analyzed for each mill.

Table 14. Grind sizes of mill products

	Grind Size, P_{80} (μm)		
Mill	Fine	Medium	Coarse
Netzsch (IsaMill)	7	9	13 and 15
SMD	6	14	20

A wider range of grind sizes was analyzed using the SMD due to difficulties obtaining coarser sizes using the Netzsch mill. The Netzsch mill grind size could only be changed by adjusting the throughput as impeller speed and media load were kept constant.

Figures 48 and 49 plot mineral liberation (>95% liberated) versus P_{80} for the SMD and Netzsch mill products. The error bars represent a 95% confidence interval.
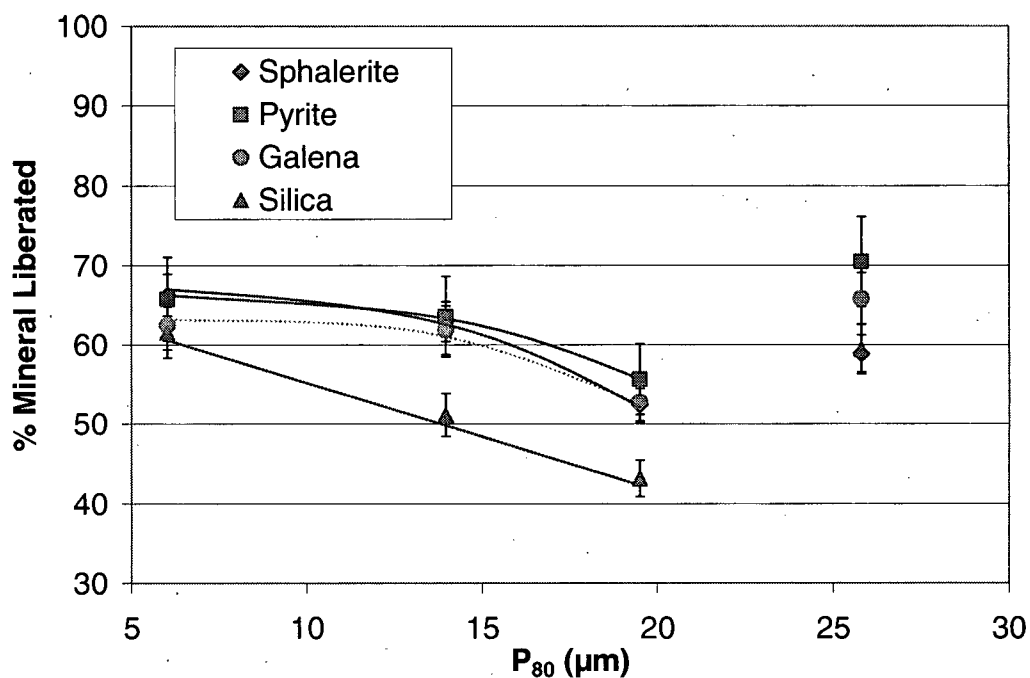

Figure 48. Mineral liberation versus P_{80} for SMD feed and products
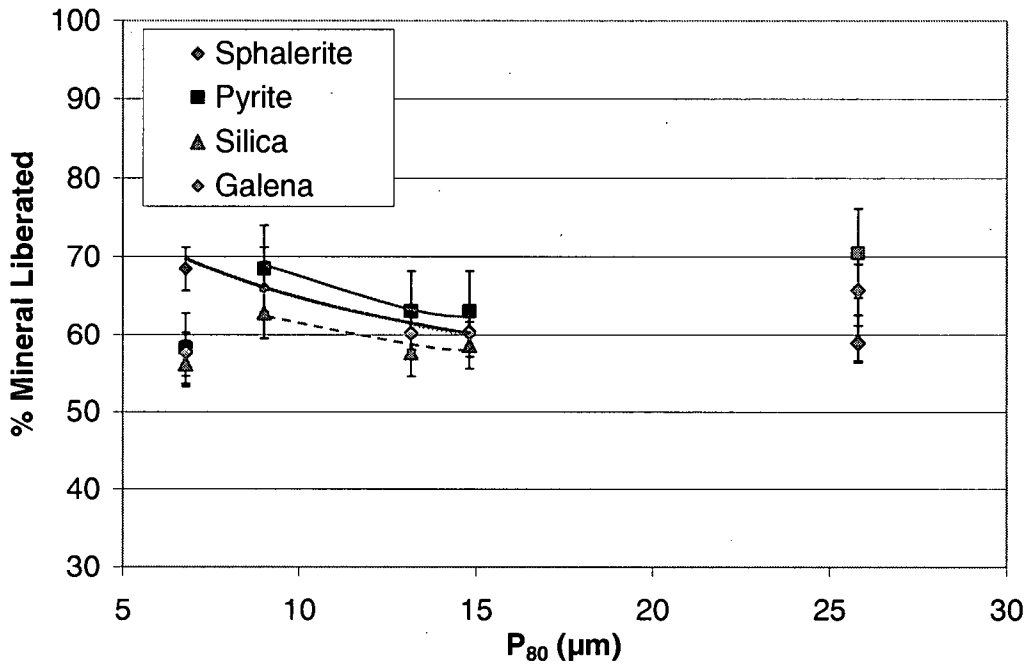
Figure 49. Mineral liberation versus P_{80} for Netzsch mill feed and products

There is a discrepancy between mineral liberation in the feed and that in the products. This could be due to agglomeration in the feed. This makes it difficult to compare liberation in the tower mill products to that in the laboratory mill products; therefore, only the results for the products will be discussed. The finest Netzsch mill sample also appears to be an outlier with liberation decreasing compared to the next coarsest sample. When only the three coarsest Netzsch mill products are considered, there is an increase in liberation for all four minerals with decreasing grind size for both mills. The SMD products show a larger improvement in sulphide mineral liberation between the coarse and medium grind size than between the medium and fine grind size, indicating that the benefit of finer grinding is reaching a limit. It is difficult to determine a trend for the Netzsch mill data; however, minerals in the three coarsest grind sizes have similar degrees of liberation to similar grind sizes in the SMD. For the SMD, the greatest increase in liberation between the coarsest and finest grind sizes was for quartz (19% for SMD). A similar trend might have been found for the Netzsch mill had a wider range of grind sizes been available.

7.4 Conclusions

For all regrind circuit feeds, the greatest benefit of finer grinding was improved quartz liberation. Therefore, ultrafine grinding could benefit flotation selectivity by increasing quartz rejection.

High-speed stirred mills could be beneficial for improving non-sulphide gangue rejection in the zinc 2nd rougher concentrate and zinc 1st retreat concentrate streams at the Red Dog mine. The benefits are less clear for the lead cleaner column tails stream where quartz contamination is less of an issue. Although the greatest benefit of ultrafine grinding was quartz rejection, there were also smaller increases in sulphide mineral liberation. A greater issue than locking for sulphide minerals is the high proportion of free sulphide gangue minerals reporting to the concentrate. In particular, inadvertent activation of pyrite is a problem in all three regrind circuits. Similar grind size-liberation trends were found for both types of high-speed stirred mills.

7.5 Recommendations

In the case of the Red Dog zinc regrind circuits, high stress intensity stirred milling would be appropriate for improved liberation of quartz. Quartz liberation would be improved without over-grinding of the softer sulphide minerals. In the case of the Red Dog lead regrind circuit; quartz liberation is less important. A lower stress intensity stirred mill would selectively grind the softer galena without grinding the harder minerals (i.e. quartz) needlessly. A suitable stress intensity could be obtained by using different types of stirred mill for the zinc and lead regrind circuits or by adjusting the impeller speed on the same type of stirred mill.

When investigating liberation in flotation streams, it may be more appropriate to look at the effect of operating conditions on gangue liberation rather than only liberation of the mineral to be floated. This is particularly important when penalty elements are present in the flotation stream.

Flotation streams of different mineralogy should be ground at various stress intensities in the same mill. Mineral liberation analysis would determine whether there are optimum stress intensities for grinding different flotation streams based on the hardness of the minerals requiring improved liberation. Flotation testing should be conducted on stirred mill products

of different grind sizes in order to confirm the trends observed using mineral liberation analysis.

CHAPTER 8 Conclusions and Recommendations

8.1 Conclusions

The following conclusions could be drawn based on this study:

1) Grinding tests using synthetic mixtures of minerals demonstrated that mineral breakage rates increase with stress intensity. At lower stress intensities, soft minerals grind faster than hard ones, but as stress intensity is increased, breakage rates of hard minerals approach those of soft minerals. By selecting an appropriate stress intensity (via the impeller speed), it is possible to preferentially grind hard or soft minerals depending on the specific mineral liberation requirements. If increased liberation of a hard mineral is required, a higher stress intensity should be used. If liberation of a softer mineral is required, a lower stress intensity should be used to avoid grinding the harder minerals.

2) The high-speed stirred mills both offer significantly decreased specific energy requirements (by approximately 50%) compared to the tower mills currently in operation at the Red Dog Mine. Specific energy requirements are similar for both laboratory mills, except at the finest grind sizes where the SMD was more energy efficient than the Netzsch mill. However, issues relating to scale-up need to be addressed for the SMD.

3) Based on characterization of mill products using the Rosin-Rammler distribution function, the SMD products have wider particle size distributions than the Netzsch mill products. Specific surface areas were higher for the fine lead cleaner column tails SMD products than for the Netzsch products; however, the results for the zinc products were inconclusive. The greater proportion of fine particles in the SMD products could be due to three operational factors: lower stress intensity, perfect mixing of SMD versus plug flow of Netzsch, and batch operation of the laboratory SMD unit. The higher stress intensity in the Netzsch mill possibly results in a combination of impact and attritive breakage which minimizes the amount of fines produced, while the lower stress intensity in the SMD may only break particles via attrition. Also, at lower stress intensity (SMD), differences in mineral hardness create a range of breakage rates (hard minerals grind slower than soft ones) resulting in a wide size distribution.

4) The two laboratory stirred mill products showed similar grind size-mineral liberation behavior.

5) For the three streams tested in this study the high stress intensity improved liberation of the hard quartz particles the most. This result was most beneficial and significant for the two zinc circuits which contained a large amount of un-liberated quartz. For the lead circuit, where quartz is less of an issue and complex fine grained galena texture is of greater concern, the results indicate that a lower stirrer speed is preferable.

8.2 Recommendations

Future work on the relationship between ultrafine grinding mills and downstream processing would be beneficial in the following areas:

1) The changes in stress intensity obtained by varying the Netzsch mill impeller speed cannot be compared directly to those in high-speed or low-speed vertical stirred mills. A synthetic mixture should be tested in a variable speed vertical stirred mill using the same method as was used for the Netzsch mill in the present study.

2) Tests to determine energy requirements should be conducted in parallel using a batch SMD and a full-scale SMD at a concentrator in order to evaluate scale-up accuracy.

3) For flotation streams, the optimum stress intensity will depend on specific mineralogical factors such as hardness and grain size. Grinding studies should be conducted on flotation streams with varying mineralogies over a range of impeller speeds (stress intensities). Mineral liberation would be measured to determine whether there are optimum stress intensities based on the hardness of the minerals requiring liberation.

4) To confirm that grinding conditions can be optimized for a stream with a specific mineralogical composition, flotation testing should be conducted on stirred mill products at different grind sizes produced over a range of stress intensities.

5) Based on the results of this study, for the zinc 2nd rougher concentrate and the zinc 1st retreat concentrate, a relatively high stress intensity should be used to improve quartz liberation without over-grinding of the softer sulphide minerals.

6) For the lead cleaner column tails, grinding should be conducted at a lower stress intensity to selectively liberate the softer galena, which has a complex fine grained texture, without needlessly grinding the harder minerals such as quartz.

7) Continuous Netzsch mill products should be compared to those from a continuous SMD when evaluating the effect of mill type on energy requirements and particle size distributions. The best method of comparing particle size distributions for flotation feeds is the specific surface area.

8) When optimizing comminution conditions based on mineral liberation, it may be more appropriate to investigate the effect of operating conditions on gangue mineral liberation rather than solely on liberation of the mineral to be floated.

Bibliography

Andreatidis, J., 1995. *Breakage Mechanisms and Resulting Mineral Liberation in a Bead Mill*, M.Eng.Sc. thesis, University of Queensland, Brisbane, Australia.

Barthelmy, D. *Mineralogy Database,* <http://www.webmineral.com/determin/non-metallic_minerals_by_hardness.shtml>
Access March 27th, 2006.

Conway-Baker, J., Barley, R.W., Williams, R.A., Jia, X., Kostuch, J., McLoughlin, B. & Parker, D.J., 2002. *Measurement of the motion of grinding media in a vertically stirred mill using positron emission particle tracking (PEPT)*, Minerals Engineering, Vol. 15, pp. 53-59.

Cullinan, V.J., *Improving the flotation response of fine galena*, PhD thesis. 1999, University of South Australia.

Davey, G. 2002, *Ultrafine and fine grinding using the METSO Stirred Media Detritor (SMD)*, Proceedings of the 34th Annual Meeting of the Canadian Mineral Processors, Ottawa, Canada, pp. 153-169.

Davey, K.J. & Frew, J.A., 1993. *The Effect of Regrinding on Zinc Rougher Concentrate Flotation at Cominco's Red Dog Mine*, AMIRA Rep 799 Project P336, CSIRO, Australia.

Harbort, G., Murphy, A., Vargas, A. & Young, M., 1999. *The Introduction of the IsaMill for Ultrafine Grinding in the Mt Isa Lead/Zinc Concentrator*, Extemin99, Peru.

Gao, M., Young, M., Cronin, B. & Harbort, G., 1998. *IsaMill medium competency and its effect on milling performance*, Proceedings of the SME Annual Conference, Salt Lake City, Utah, USA.

Gao, M., Young, M. & Allum, P., 2002. *IsaMill Fine Grinding Technology and its Industrial Applications at Mount Isa Mines*, Proceedings of the 34th Annual Meeting of the Canadian Mineral Processors, Ottawa, Canada.

George, P., Nguyen, A.V. & Jameson, G.J., 2004, *Assessment of true flotation and entrainment in the flotation of submicron particles by fine bubbles,* Minerals Engineering, Vol. 17, pp. 847-853.

Greet, C.J., Small, G.L., Steiner, P. & Grano, S.R., 2004. *The Magotteaux Mill®: investigating the effect of grinding media on pulp chemistry and flotation performance.* Minerals Engineering Vol. 17, pp. 891-896.

Jankovic, A. 2003, *Variables affecting the fine grinding of minerals using stirred mills,* Minerals Engineering, Vol. 16, pp. 337-345.

Karbstein, H. et al, 1996, *Scale-up for Grinding in Stirred Ball Mills,* Aufbereitungs-Technik, Vol. 37, No. 10, pp. 469-479.

Karbstein, H. et al, 1995, *Producing Suspensions with Steep Particle Size Distributions in Fines Ranges,* Aufbereitungs-Technik, Vol. 36, No. 10, pp. 464-473.

Klimpel, R.R. 1998, *Evaluating comminution efficiency from the point of view of downstream froth flotation,* Minerals & Metallurgical Processing, Vol. 15, No. 4, pp.1-8.

Kwade, A. Blecher, L. & Schwedes, J. 1996, *Motion and stress intensity of grinding beads in a stirred media mill. Part 2: Stress intensity and its effect on comminution,* Powder Technology 86, pp. 69-76.

Kwade, A., 1999. *Determination of the most important grinding mechanism in stirred media mills by calculating stress intensity and stress intensity,* Powder Technology 105, pp.382-388.

Kwade, A. Schwedes, J., 2002, *Breaking characteristics of different materials and their effect on stress intensity and stress number in stirred media mills,* Powder Technology 122, pp. 109-121.

Lichter, J.K.H. & Davey, G., 2002, *Selection and Sizing of Ultrafine and Stirred Grinding Mills,* Mineral Processing Plant Design, Practice, and Control Proceedings, SME, USA, pp. 783-800.

Lofthouse, C.H, Johns, F.E., 1999, *The Svedala (ECC International) Detritor and the Metals Industry,* Minerals Engineering, Vol. 12, No. 2, pp. 205-217.

Ma, Z., Hu, Sian, Zhang, Shaoming & Pan, X. 1998, *Breakage behavior of quartz in a laboratory stirred ball mill,* Powder Technology, Vol. 100, pp.69-73.

Metso Minerals,

http://www.metsominerals.com/inetMinerals/MaTobox7.nsf/DocsByID/53B338EE821B
F913C1256C5A002E37C1/$File/Stirred_Media_Detritor_EN.pdf

Access July 28, 2006

Murphy, A. et al, 2000, *IsaMill: New Tool for Improving Plant Recoveries,* www.xstratatech.com/doc/im_newtool_en.pdf

Napier-Munn, T.J. 1999, *Mineral Comminution Circuits: Their Operation and Optimisation,* JKMRC, Queensland, Australia.

Nel, G., Swarts, A., Doriegan, S. & Johnson, G., 2006, *Comparing the Milling Efficiencies of Pilot Scale Horizontal and Vertical Ultrafine Grinding Mills for Tati Sulphide Concentrate,* Proceedings of the Randol Innovative Metallurgy Forum 2005, Perth, Australia.

Nesset, J., Radziszewski, P., Hardie, C. & Leroux, D., 2006, *Assessing the Performance and Efficiency of Fine Grinding Technologies,* Proceedings of the 38th Annual Canadian Mineral Processors Conference, Ottawa, Canada, pp. 283-309.

Netzsch Incorporated, 1996, *Dispersion Equipment Operating Instructions,* Exton, PA, USA.

Palmer, C.M. & Johnson, G.D., 2005. *The Activox® Process: Growing Significance in the Nickel Industry,* JOM, Vol. 57, No. 7.

Pease, J.D., Curry, D.C. & Young, M.F. 2006. *Designing flotation circuits for high fines recovery,* Minerals Engineering, Vol. 19, pp. 831-840.

Svedala Vertimill, http://www.svedala.de/inetMinerals/MaTobox7.nsf/DocsByID/318FF33277D44D6CC12 56DC800500D46/$File/Vertimill.pdf Access July 28, 2006

Wang, Y. & Forssberg, E., 2000. *Technical Note: Product Size Distribution in Stirred Media Mills,* Minerals Engineering, Vol. 13, No. 14, pp. 459-465.

Weller, K.R. & Gao, M. 1999, *Ultra-Fine Grinding,* CSIRO, Queensland, Australia. · www.xstratatech.com/doc/im_ultrafinegrinding_en.pdf Access December 15, 2005

Weller, K.R., Gao, M. & Allum, P. 1998, *Scaling-up Horizontal Stirred Mills from a 4-litre Test Mill to a 4000-litre "IsaMill",* www.xstratatech.com/doc/im_scaleup_en.pdf Access December 15, 2005

Weller, K.R.., Spencer, S.J., Gao, M.W. & Liu, Y., 2000, *Tracer Studies and Breakage Testing in Pilot-Scale Stirred Mills,* Minerals Engineering, Vol. 13, No. 4, pp. 429-458.

Wills, B., 1997. *Mineral Processing Technology*, Butterworth Heinemann, Oxford, UK.

Xstrata Technology, 2006. http://www.xstratatech.com/en/t_isamill_technology.html
Access July 28, 2006

Xstrata Technology, 2006.
http://www.isamill.com/index.cfm?action=dsp_content&contentID=28
Access July 31, 2006

Yan, D., Parker, T. & Ryan. S., 2003, *Dewatering of fine slurries by the Kalgoorlie Filter Pipe,* Minerals Engineering, Vol. 16, pp. 283-289.

Young, M., 2005, *Fine Grinding as Enabling Technology*, Presentation at McGill University, Montreal, QC.

Yue. J., 2003. *Rheological Effects on Ultrafine Grinding in a Stirred Mills*, M.A.Sc. thesis, University of British Columbia, Vancouver, Canada.

Yue, J. & Klein, B. 2005, *Particle breakage kinetics in horizontal stirred mills*, Minerals Engineering, Vol. 18, pp. 325-331.

APPENDICES

Appendix A – Lead Cleaner Column Tails Regrind Circuit

Regrind Circuit Location

Lead Flotation Circuit
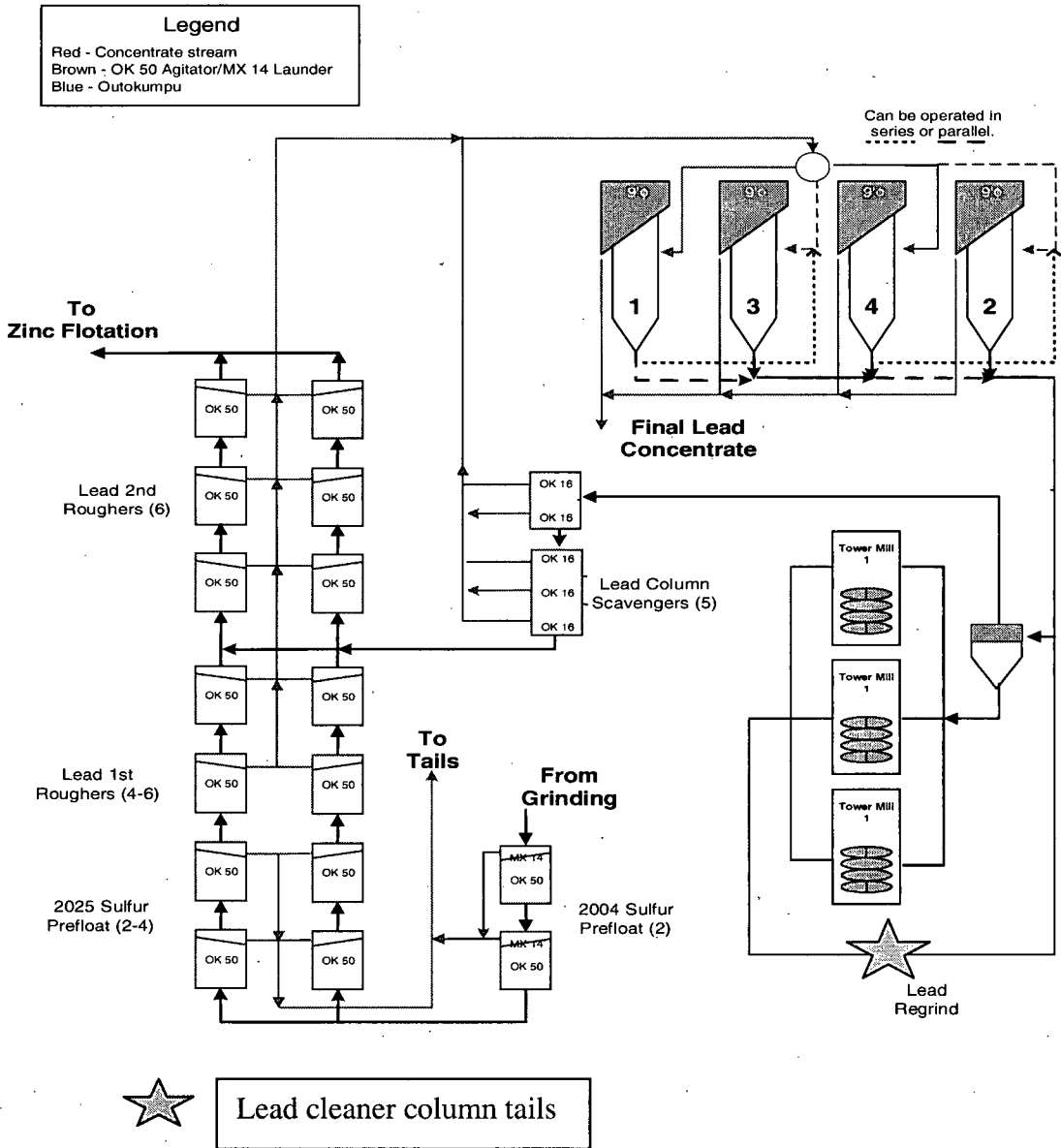
Figure A-I. Lead flotation circuit at the Red Dog Mine

Characterization of Circuit

Table A-I. Mineralogy of lead cleaner column tails

Head Assay (%)					Calculated Mineralogy (%)				MLA Modal Mineralogy (%)			
Pb	Zn	Fe	SiO_2	Ba	Galena	Sphalerite	Pyrite	NSG	Galena	Sphalerite	Pyrite	Quartz
21.6	22.7	14	5.8	1.4	24.9	35.5	27.7	11.9	27.4	34.4	30.9	4.7

Table A-II. Particle size distributions (Red Dog lead regrind circuit)

Regrind Circuit Sample	P_{80} (μm)	Specific Surface Area (m^2/g)	$P_{80}:P_{20}$	Rosin-Rammler Distribution		
				Size Coefficient, a	Width Coefficient, b	Coefficient of Determination, R^2
Lead cleaner column tails	25.8	1.30	5.9	17.05	1.27	0.999
Lead tower mill feed	52.5	0.95	6.1	31.22	1.21	0.993
Lead tower mill discharge	23.6	1.40	6.7	14.88	1.37	0.994
Lead scavenger feed (cyclone o/f)	21.6	1.44	6.0	14.61	1.35	0.997

Netzsch Mill Grinding Trials

Table A-III. Energy requirements (Lead regrind; Netzsch mill)

	Test	Pump (rpm)	Flow (L/min)	% solids	kW	F_{80} (μm)	P_{80} (μm)	Solid Flow (t/hr)	Specific Energy Consumption (kWhr/t)
	Empty				0.60				
	Run 1	200	1.27	37.9%	1.90	25.8	9.01	0.041	31.4
40% Solids	Run 2	600	3.58	35.7%	1.80	25.8	13.17	0.107	11.2
	Run 3	100	0.61	36.8%	1.90	25.8	6.78	0.019	68.6
	Run 4	400	2.61	36.6%	1.75	25.8	12.95	0.081	14.2
30% Solids	Pass 1	600	4.31	31.0%	1.65	25.8	14.81	0.106	9.9
	Pass 2	600	4.35	31.0%	1.60	25.8	10.83	0.107	19.2
	Pass 3	600	4.48	31.0%	1.60	25.8	8.70	0.111	28.2

Table A-IV. Particle size distributions (Lead regrind; Netzsch mill products)

Feed Sample (Netzsch)	P_{80} (μm)	Specific Surface Area (m^2/g)	$P_{80}:P_{20}$	Rosin-Rammler Distribution		
				Size Coefficient, a	Width Coefficient, b	Coefficient of Determination, R^2
	9.0	2.30	3.9	6.60	1.57	0.998
	13.2	1.47	5.1	8.56	1.50	0.997
Lead cleaner column tails	6.8	2.22	4.5	4.93	1.63	0.995
	13.0	2.00	4.8	8.70	1.48	0.998
	14.8	1.51	6.2	10.68	1.37	0.995

Stirred Media Detritor Grinding Trials

Table A-V. Energy requirements (Lead regrind; SMD using screened samples)

metso minerals

LABORATORY STIRRED MEDIA DETRITOR
TEST DATA SHEET

Project: UBC Fine Grinding   **Application:** Lead Column Tails   **% Solids:** 40%
Sampling: Screened   **Media:** Colorado River Sand

Details		FEED	1	2	3	4	5	6
Charge								
total volume	ml		1408	1408	1408	1408	1408	1408
media ratio	v/v		50%	50%	50%	50%	50%	50%
slurry volume	ml		704	704	704	704	704	704
media volume	ml		704	704	704	704	704	704
Media								
density	kg/m^3		2650	2650	2650	2650	2650	2650
mass	g		1866	1866	1866	1866	1866	1866
Feed								
dry solids density	kg/m^3	5000	5000	5000	5000	5000	5000	5000
liquid density	kg/m^3	1000	1000	1000	1000	1000	1000	1000
slurry solids content	% m/m	40.0	40.0	40.0	40.0	40.0	40.0	40.0
slurry density	kg/m^3	1471	1471	1471	1471	1471	1471	1471
slurry solids content	%v/v	11.8	11.8	11.8	11.8	11.8	11.8	11.8
slurry mass	g		1035	1035	1035	1035	1035	1035
solids mass - dry	g		414	414	414	414	414	414
powder moisture content	% m/m		6.0	6.0	6.0	6.0	6.0	6.0
solids mass - "wet"	g		441	441	441	441	441	441
water volume	ml		595	595	595	595	595	595
Work Input								
required work input	kWhr/t	0	5	10	20	30	50	70
required power	kWhr		0.0021	0.0041	0.0083	0.0124	0.0207	0.0290
Particle Size								
D80	µm	25.8	19.5	14.0	11.0	8.5	6.0	5.1

Table A-VI. Energy requirements (Lead regrind; SMD using syringe samples)

LABORATORY STIRRED MEDIA DETRITOR
TEST DATA SHEET

metso minerals

Project: UBC Fine Grinding **Application:** Lead Column Tails **% Solids:** 40%
Sampling: Syringe **Media:** Colorado River Sand

Details		FEED	1	2	3	4	5
Charge							
total volume	ml		1408	1408	1408	1408	1408
media ratio	v/v		50%	50%	50%	50%	50%
slurry volume	ml		704	704	704	704	704
media volume	ml		704	704	704	704	704
Media							
density	kg/m³		2650	2650	2650	2650	2650
mass	g		1866	1866	1866	1866	1866
Feed							
dry solids density	kg/m³	5000	5000	5000	5000	5000	5000
liquid density	kg/m³	1000	1000	1000	1000	1000	1000
slurry solids content	% m/m	40.0	40.0	40.0	40.0	40.0	40.0
slurry density	kg/m³	1471	1471	1471	1471	1471	1471
slurry solids content	%v/v	11.8	11.8	11.8	11.8	11.8	11.8
slurry mass	g		1035	1035	1035	1035	1035
solids mass - dry	g		414	414	414	414	414
powder moisture content	% m/m		0.0	0.0	0.0	0.0	0.0
solids mass - "wet"	g		414	414	414	414	414
water volume	ml		621	621	621	621	621
Work Input							
required work input	kWhr/t	0	5	10	20	30	50
required power	kWhr		0.0021	0.0041	0.0083	0.0124	0.0207
Particle Size							
D80	µm	25.8	17.2	12.7	8.9	7.2	5.9

Table A-VII. Particle size distributions (Lead regrind; SMD products)

Feed Sample (SMD)	P_{80} (µm)	Specific Surface Area (m²/g)	P_{80}:P_{20}	Rosin-Rammler Distribution		
				Size Coefficient, a	Width Coefficient, b	Coefficient of Determination, R^2
	19.5	1.54	6.1	13.19	1.31	0.995
	14.0	1.39	5.4	10.10	1.39	0.996
Lead cleaner column tails	9.8	2.38	5.3	7.05	1.44	0.994
	8.5	2.57	4.3	6.94	1.41	0.993
	5.1	3.65	3.9	3.91	1.53	0.987

Mineral Liberation Analysis

Table A-VIII. Mineral liberation analysis and assay results (Lead regrind circuit samples and mill products)

Sample Number	Sample Name	+38 μm	C1/2	C3	C4	C5	C6	C7	% Zinc Assay	% Zinc MLA	% Lead Assay	% Lead MLA	% Iron Assay	% Iron MLA	% Silica Assay	% Quartz MLA	Zn_Sulphide % Liberated	Zn_Sulphide % Binary	Pb_Sulphide % Liberated	Pb_Sulphide % Binary	Pyrite % Liberated	Pyrite % Binary	Quartz % Liberated	Quartz % Binary
490	Lead Column Tails	6.2	11.3	15.1	14.0	8.7	28.3	16.4	20.1	19.9	33.4	28.6	13.5	15.7	1.0	1.5	41.0	48.6	55.4	36.1	55.5	34.0	13.5	40.4
491									24.5	23.6	18.7	16.2	16.5	18.9	2.6	3.6	50.9	41.5	46.7	43.2	66.4	26.2	26.0	46.0
492									24.7	22.3	16.2	13.8	18.0	21.1	3.1	3.3	63.6	32.7	60.4	34.2	77.9	18.3	43.8	38.2
493									24.2	21.4	16.4	17.6	17.6	18.3	3.7	5.1	60.4	35.6	59.0	35.6	72.6	22.3	53.6	29.1
910									23.1	19.2	22.3	26.1	13.8	13.5	7.2	6.6	67.4	29.6	76.1	20.1	75.0	19.8	73.1	20.4
470	Lead Tower Mill Fd	36.9	13.3	24.9	6.3	3.0	8.5	7.1	11.1	11.4	48.9	46.7	11.4	12.3	0.3	0.4	30.7	56.3	68.9	26.3	52.5	37.4	3.7	45.5
471									21.7	17.4	30.9	29.1	15.3	17.2	0.4	1.4	42.2	47.5	59.9	32.3	61.4	30.1	24.9	43.5
472									24.4	20.8	20.6	19.6	17.0	19.1	2.7	3.1	62.2	33.1	66.5	28.1	74.8	20.1	42.2	39.6
473									24.4	19.9	20.6	19.0	17.0	19.0	2.7	4.0	60.0	34.6	60.8	32.5	72.6	21.8	43.0	34.7
911									24.0	18.8	23.4	24.9	13.1	14.4	5.2	5.3	62.5	31.4	62.8	30.1	60.7	31.6	50.2	33.2
480	Lead Tower Mill Disc	3.9	11.4	15.2	14.1	8.7	28.9	17.8	16.8	15.3	40.5	36.0	15.9	14.9	0.3	1.5	37.0	48.2	60.4	30.5	53.1	32.0	10.2	34.0
481									18.1	16.0	34.8	31.1	13.7	17.0	0.5	1.7	49.9	41.1	68.9	25.9	67.0	25.6	29.5	44.1
482									21.3	18.8	26.9	26.1	14.4	17.3	2.8	2.5	66.2	30.4	75.6	21.6	75.0	21.1	56.6	30.2
483									21.7	17.9	27.5	28.8	14.3	15.4	3.1	3.7	62.3	33.4	72.0	24.0	69.9	24.7	56.4	31.1
484									22.1	17.9	29.1	31.4	12.4	12.8	4.8	3.6	72.7	25.6	83.1	15.2	70.8	27.0	56.7	31.1
512	Lead Scav Feed	3.0	5.9	14.9	17.0	10.4	30.9	17.9	20.5	19.8	33.1	28.6	13.0	15.4	2.0	2.1	47.1	43.6	59.6	31.3	55.6	32.0	16.8	42.2
513									22.8	21.8	22.2	18.2	15.8	19.1	3.2	3.3	53.9	38.7	58.3	33.4	67.5	24.4	34.6	34.9
514									23.3	21.4	20.0	18.4	16.4	19.2	3.3	3.3	64.5	31.1	68.2	27.2	75.9	20.0	42.6	40.0
515									23.7	20.7	20.5	20.9	16.1	17.4	3.6	4.8	59.3	36.0	67.0	28.2	72.7	22.4	54.5	34.2
516									22.1	18.8	25.2	28.3	12.5	13.7	6.6	3.9	73.3	24.8	84.2	14.2	79.3	18.6	75.4	16.2
1023	Coarse SMD Product (P80=20μm)	2.5	3.1	9.1	15.1	10.2	39.8	20.4		17.1		24.0		20.4		1.2	40.1	45.9	47.8	39.8	56.8	32.2	11.4	46.8
1024									22.6	21.3	17.5	13.0	20.6	22.5	3.6	3.4	37.8	42.8	28.0	42.8	48.3	34.0	33.6	30.6
1025									24.4	21.7	15.5	12.6	19.5	22.3	3.9	3.4	55.7	34.7	38.9	44.9	61.4	29.1	47.9	35.4
1026									25.2	22.7	14.5	14.4	18.0	19.1	3.9	3.9	57.0	34.2	49.9	37.9	64.3	26.5	48.5	33.2
1027									24.2	19.5	21.8	27.4	13.4	12.9	7.5	2.3	54.0	33.7	56.8	31.4	52.4	33.3	43.5	30.8
1062	Medium SMD Product (P80=14μm)	1.8	1.8	2.9	9.0	10.2	45.5	28.8		17.7		12.8		25.0		4.0	45.2	38.6	35.7	40.2	59.6	28.3	40.9	38.1
1063									23.3	19.5	15.0	12.4	21.1	23.9	3.8	3.5	55.9	35.7	43.4	42.7	65.9	26.2	56.4	30.6
1064									25.1	20.6	15.7	16.2	18.9	19.9	3.9	3.8	60.7	31.6	54.3	34.9	67.7	25.7	48.9	31.0
1065									25.1	19.9	22.1	26.5	12.9	12.8	6.1	3.0	65.5	28.4	64.6	27.8	62.9	28.9	52.0	29.1
1010	Fine SMD Product (P80=6μm)	0.6	0.4	0.7	1.2	1.6	57.7	37.8		13.1		13.2		28.0		4.0	38.8	30.3	41.2	28.0	70.5	17.4	73.4	18.1
1011										7.1		7.1		34.3		5.1	54.0	28.7	38.3	37.2	81.6	14.1	77.3	16.6
1012									24.2	19.9	20.0	23.5	15.5	15.0	5.6	2.4	66.9	27.0	62.9	30.0	64.9	27.7	60.4	28.0
1066	Coarse Netzsch Product (P80=15μm; 30% solids)	0.5	0.5	4.7	13.1	11.9	46.8	22.4		18.4		15.5		22.5		4.6	42.1	41.2	33.3	46.3	54.9	31.8	39.7	33.5
1067									23.1	20.4	16.8	14.6	20.0	21.8	3.8	4.0	56.8	35.2	46.9	41.7	68.3	24.8	58.8	29.2
1068									25.1	21.3	17.6	17.3	18.7	18.9	4.0	4.0	58.5	34.9	51.3	39.4	68.1	24.8	52.4	30.8
1069									24.5	19.7	22.6	27.5	13.7	12.9	5.0	2.6	63.0	30.1	63.6	27.5	61.4	29.4	62.9	20.2
1033	Coarse Netzsch Product (P80=13μm)	0.2	0.2	3.4	12.0	11.7	48.4	24.1		19.1		14.7		22.5		4.4	49.7	41.2	42.5	45.3	65.9	25.8	49.7	33.2
1034									21.9	20.8	17.8	14.4	19.0	21.9	3.6	3.4	53.2	36.9	40.6	43.8	60.7	29.5	48.6	34.3
1035									24.6	21.4	17.1	17.9	18.4	18.7	3.4	3.6	56.8	36.5	53.8	37.8	69.1	23.8	53.7	26.6
1036									24.3	21.0	21.0	25.2	14.2	13.6	5.6	2.8	62.5	32.5	63.1	30.1	62.2	29.7	60.8	23.6
1049	Medium Netzsch Product (P80=9μm)	0.5	0.5	0.7	3.3	6.3	56.5	32.0		15.6		15.4		25.0		3.6	44.3	40.6	41.6	41.0	60.4	28.8	55.2	27.6
1050										17.6		18.7		21.2		3.1	61.5	32.5	57.5	35.6	74.3	21.3	60.7	26.5
1051									23.0	21.0	22.0	24.7	12.4	14.2	5.3	2.0	70.0	24.7	67.5	26.0	68.7	24.7	63.9	25.9
1045	Fine Netzsch Product (P80=7μm)	0.8	0.2	0.4	1.0	1.9	52.9	42.9		14.7		22.3		21.4		3.0	54.7	34.9	55.8	32.1	66.9	25.5	62.2	22.4
1046									23.4	20.4	20.5	23.7	15.6	14.9	5.4	2.3	62.1	29.2	57.5	31.8	57.7	31.5	55.8	30.2

Appendix B – Zinc 2nd Rougher Concentrate Regrind Circuit

Regrind Circuit Location
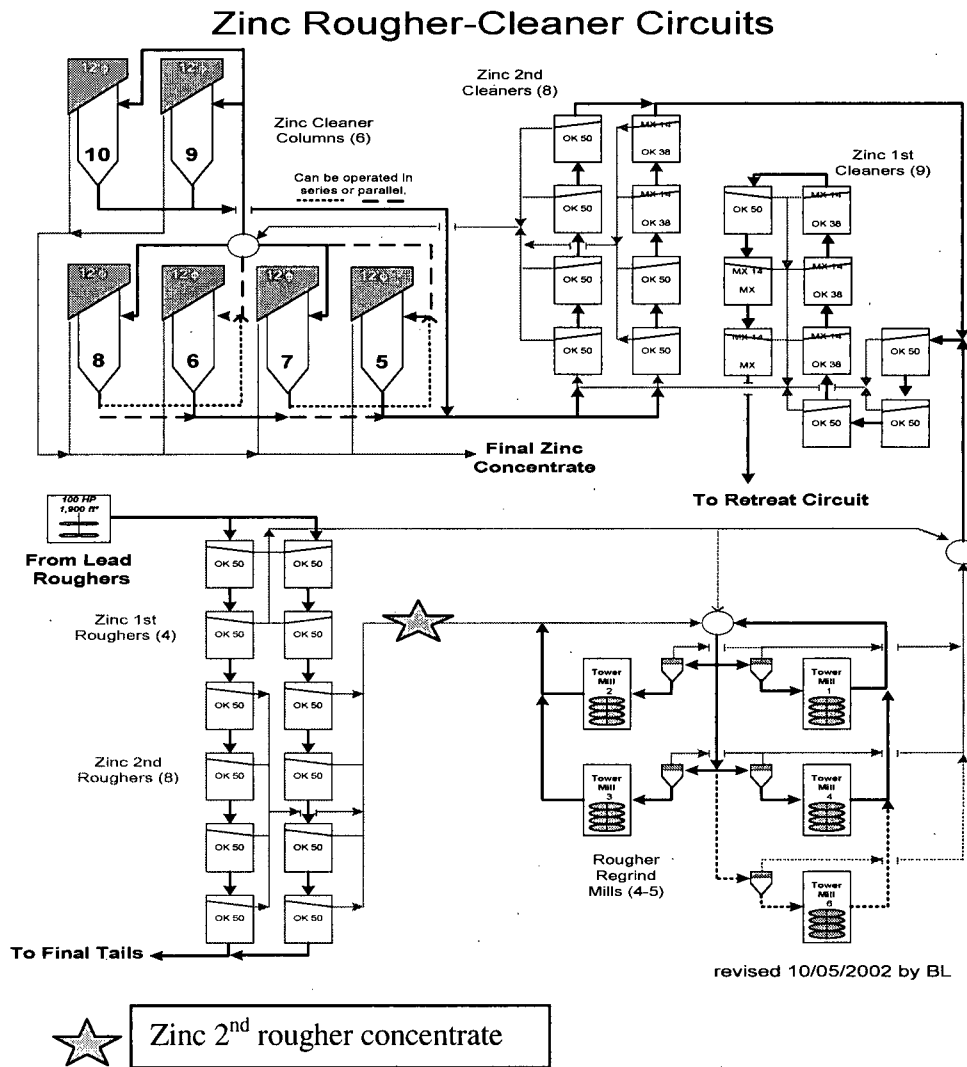
Figure B-I. Zinc rougher-cleaner flotation circuit at the Red Dog Mine

Characterization of Circuit

Table B-I. Mineralogy of zinc 2nd rougher concentrate

Head Assay (%)					Calculated Mineralogy (%)				MLA Modal Mineralogy (%)			
Pb	Zn	Fe	SiO$_2$	Ba	Galena	Sphalerite	Pyrite	NSG	Galena	Sphalerite	Pyrite	Quartz
2.8	38.5	7.8	17.0	2.1	3.3	60.4	12.7	23.6	2.3	64.7	15.6	14.8

Table B-II. Particle size distributions (Zinc 2nd rougher regrind circuit)

Regrind Circuit Sample	P_{80} (µm)	Specific Surface Area	$P_{80}:P_{20}$	Rosin-Rammler Distribution		
				Size Coefficient, a	Width Coefficient, b	Coefficient of Determination, R^2
Zinc 2nd rougher concentrate	48.6	0.92	9.0	26.85	1.25	0.992
Zinc rougher tower mill feed	76.8	0.44	5.9	44.55	1.24	0.989
Zinc rougher tower mill discharge	39.9	0.85	8.0	23.26	1.25	0.995
Zinc 1st cleaner feed (cyclone o/f)	28.2	1.18	6.0	17.41	1.37	0.997

Netzsch Mill Grinding Trials

Table B-III. Energy requirements (Zinc 2nd rougher regrind; Netzsch mill)

Test	Pump (rpm)	Flow (L/min)	% solids	kW	F_{80} (µm)	P_{80} (µm)	Solid Flow (t/hr)	Specific Energy Consumption (kWhr/t)
Empty				0.6				
Run 1	400	2.95	40.72%	1.7	48.6	21.81	0.103	10.6
Run 2	600	4.16	37.03%	1.5	48.6	27.71	0.128	7.1
Run 3	85	0.61	41.03%	2.0	48.6	10.41	0.022	64.5
Run 4	300	2.53	39.98%	1.7	48.6	20.71	0.086	12.8
Run 6	200	1.48	42.44%	1.75	48.6	16.84	0.055	20.8

Table B-IV. Particle size distributions (Zinc 2nd rougher regrind; Netzsch mill products)

Feed Sample (Netzsch)	P_{80} (µm)	Specific Surface Area (m^2/g)	$P_{80}:P_{20}$	Rosin-Rammler Distribution		
				Size Coefficient, a	Width Coefficient, b	Coefficient of Determination, R^2
	21.8	1.56	6.8	15.66	1.34	0.987
	27.7	1.75	7.1	19.04	1.27	0.994
Zinc 2nd rougher concentrate	10.4	2.83	5.3	8.47	1.48	0.980
	20.7	1.89	6.1	15.83	1.39	0.990
	16.8	1.69	6.0	12.78	1.40	0.990

Stirred Media Detritor Grinding Trials

Table B-V. Energy requirements (Zinc 2nd rougher regrind; SMD using screened samples)

LABORATORY STIRRED MEDIA DETRITOR TEST DATA SHEET								
metso minerals								
Project: UBC Fine Grinding			**Application:** Zinc 2nd Rougher Conc			**% Solids:** 40%		
Sampling: Screened			**Media:** Colorado River Sand					

Details				**Sample Number**				
		FEED	1	2	3	4	5	6
Charge								
total volume	ml		1408	1408	1408	1408	1408	1408
media ratio	v/v		50%	50%	50%	50%	50%	50%
slurry volume	ml		704	704	704	704	704	704
media volume	ml		704	704	704	704	704	704
Media								
density	kg/m^3		2650	2650	2650	2650	2650	2650
mass	g		1866	1866	1866	1866	1866	1866
Feed								
dry solids density	kg/m^3	3900	3900	3900	3900	3900	3900	3900
liquid density	kg/m^3	1000	1000	1000	1000	1000	1000	1000
slurry solids content	% m/m	40.0	40.0	40.0	40.0	40.0	40.0	40.0
slurry density	kg/m^3	1423	1423	1423	1423	1423	1423	1423
slurry solids content	%v/v	14.6	14.6	14.6	14.6	14.6	14.6	14.6
slurry mass	g		1002	1002	1002	1002	1002	1002
solids mass - dry	g		401	401	401	401	401	401
powder moisture content	% m/m		3.3	3.3	3.3	3.3	3.3	3.3
solids mass - "wet"	g		415	415	415	415	415	415
water volume	ml		587	587	587	587	587	587
Work Input								
required work input	kWhr/t	0	5	10	20	31	53	70
required power	kWhr		0.0020	0.0040	0.0080	0.0124	0.0210	0.0281
Particle Size								
D80	µm	48.6	33.6	28.4	19.1	12.6	7.4	6.1

Table B-VI. Energy requirements (Zinc 2nd rougher regrind; SMD using syringe samples)

LABORATORY STIRRED MEDIA DETRITOR
TEST DATA SHEET

metso minerals

Project: UBC Fine Grinding **Application:** Zinc 2nd Rougher Conc **% Solids:** 40%
Sampling: Syringe **Media:** Colorado River Sand

Details		FEED	1	2	3	4	5	6
Charge								
total volume	ml		1408	1408	1408	1408	1408	1408
media ratio	v/v		50%	50%	50%	50%	50%	50%
slurry volume	ml		704	704	704	704	704	704
media volume	ml		704	704	704	704	704	704
Media								
density	kg/m^3		2650	2650	2650	2650	2650	2650
mass	g		1866	1866	1866	1866	1866	1866
Feed								
dry solids density	kg/m^3	3900	3900	3900	3900	3900	3900	3900
liquid density	kg/m^3	1000	1000	1000	1000	1000	1000	1000
slurry solids content	% m/m	40.0	40.0	40.0	40.0	40.0	40.0	40.0
slurry density	kg/m^3	1423	1423	1423	1423	1423	1423	1423
slurry solids content	%v/v	14.6	14.6	14.6	14.6	14.6	14.6	14.6
slurry mass	g		1002	1002	1002	1002	1002	1002
solids mass - dry	g		401	401	401	401	401	401
powder moisture content	% m/m		0.0	0.0	0.0	0.0	0.0	0.0
solids mass - "wet"	g		401	401	401	401	401	401
water volume	ml		601	601	601	601	601	601
Work Input								
required work input	kWhr/t	0	5	11	23	32	50	70
required power	kWhr		0.0020	0.0044	0.0092	0.0128	0.0200	0.0281
Particle Size								
D80	µm	48.6	31.4	21.5	12.1	10.0	7.1	5.8

Table B-VII. Particle size distributions (Zinc 2nd rougher regrind; SMD products)

Feed Sample (SMD)	P_{80} (µm)	Specific Surface Area (m^2/g)	$P_{80} \cdot P_{20}$	Rosin-Rammler Distribution		
				Size Coefficient, a	Width Coefficient, b	Coefficient of Determination, R^2
Zinc 2nd rougher concentrate	33.6	1.46	7.3	20.16	1.21	0.994
	28.4	1.5	6.1	17.64	1.20	0.991
	19.1	1.6	4.3	15.40	1.23	0.98
	12.6	3.33	4.3	11.41	1.27	0.976
	7.4	2.71	4.0	5.74	1.63	0.994
	6.1	2.73	3.9	7.24	1.30	0.948

Mineral Liberation Analysis

Table B-VIII. Mineral liberation analysis (Zinc 2nd rougher regrind circuit and mill products)

Sample Number	Sample Name	+38 µm	C1/2	C3	C4	C5	C6	C7	% Zinc Assay	% Zinc MLA	% Lead Assay	% Lead MLA	% Iron Assay	% Iron MLA	% Silica Assay	% Quartz MLA	Zn Sulphide Liberation % Liberated	Zn Sulphide Liberation % Binary	Pb Sulphide Liberation % Liberated	Pb Sulphide Liberation % Binary	Pyrite Liberation % Liberated	Pyrite Liberation % Binary	Quartz Liberation % Liberated	Quartz Liberation % Binary
1357										42.0		1.4		7.9		16.3	65.9	27.2	1.3	44.0	24.9	46.0	25.8	58.2
475									46.0	44.1	2.4	1.1	10.8	12.9	4.5	2.5	83.8	13.8	11.5	60.8	58.0	34.3	15.9	57.8
476	Zinc 2nd Rougher Concentrate	29.9	8.2	14.6	10.6	5.2	18.1	13.4	43.3	41.6	1.6	0.7	8.8	11.1	15.2	11.2	85.7	12.8	6.2	62.6	66.0	27.3	39.6	50.3
477									41.1	40.1	1.3	0.5	9.6	11.7	16.3	16.6	91.1	8.3	14.3	68.1	78.5	17.9	55.2	39.2
478									40.7	38.1	1.2	1.0	9.5	11.7	14.8	12.5	90.1	8.9	14.6	64.7	77.5	19.5	61.2	32.2
479									36.3	33.3	3.5	3.7	8.8	11.1	16.5	18.0	92.6	6.8	73.9	22.4	84.4	14.2	78.9	15.3
495									45.4	42.4	2.8	1.6	12.4	14.3	2.9	1.1	85.7	12.3	34.5	45.1	61.7	32.3	3.2	61.2
496									44.1	40.9	2.5	1.5	11.2	13.6	7.7	5.8	86.0	12.2	30.3	49.9	69.0	25.9	38.3	49.3
497	Zn Rougher Tower Mill Feed	56.7	12.3	11.5	4.6	2.0	6.9	6.0	42.4	41.1	2.6	2.1	9.1	11.5	14.4	9.1	90.5	8.2	45.6	40.7	77.1	19.0	53.1	38.7
500									42.4	38.5	2.6	2.8	9.1	10.5	14.4	12.5	89.5	8.6	43.9	38.9	76.7	18.8	64.9	27.9
501									38.4	35.3	7.4	8.9	7.4	9.0	16.6	9.1	91.8	7.1	73.2	22.4	79.9	16.8	79.4	17.4
502									45.0	42.6	2.2	1.2	12.2	14.2	1.1	1.3	86.2	11.8	25.3	49.2	69.0	26.1	10.8	59.2
503									44.5	42.2	2.0	1.1	9.7	11.9	8.5	7.4	88.2	10.3	36.2	43.5	71.0	23.6	51.4	41.3
504	Zinc Rougher Tower Mill Discharge	21.7	9.3	15.2	12.1	6.6	20.4	14.7	43.1	42.0	2.0	1.3	8.2	10.2	13.5	11.1	91.5	7.5	52.5	34.6	78.1	18.5	67.3	28.1
505									43.6	41.1	2.2	1.5	7.5	9.2	15.4	13.8	90.0	8.1	30.4	42.7	76.3	19.6	70.1	24.6
506									41.9	39.3	4.7	4.9	7.0	9.5	16.9	10.0	93.9	5.3	72.6	22.2	85.7	11.2	92.9	5.8
507									31.3	47.9	1.6	0.7	4.0	9.1	4.6	4.4	85.7	12.0	21.2	42.7	51.6	37.9	15.9	65.7
508									46.2	42.4	1.2	0.7	7.3	9.5	15.2	12.7	87.4	10.7	28.7	40.2	65.0	28.1	49.1	44.4
509	Zinc Rougher Cyclone Overflow	6.3	2.2	14.3	16.2	9.0	32.9	19.1	44.1	41.1	1.3	1.1	8.2	10.4	17.1	12.2	91.2	7.8	28.2	52.2	75.9	20.4	63.4	31.6
510									44.0	38.6	1.7	1.4	8.0	10.4	16.8	14.2	92.3	6.6	35.1	45.2	77.4	18.7	68.5	25.4
511									41.1	36.5	4.1	4.8	7.4	10.0	17.3	11.1	94.2	5.0	68.7	24.6	87.1	10.8	81.1	15.8
1354										37.9		1.6		8.2		21.6	65.2	27.3	3.8	45.2	41.7	32.1	35.3	39.7
1052										45.2		0.8		12.9		2.0	84.8	13.6	18.6	56.1	58.6	35.2	15.1	59.9
1053	Coarse SMD Product (P$_{80}$=28µm)	14.7	4.4	10.6	11.5	6.6	28.3	23.9		42.2		0.7		9.9		12.9	85.9	12.6	24.6	52.2	57.5	35.4	50.4	41.6
1054									42.4	40.4	2.5	2.3	8.7	10.4	13.5	12.0	86.4	11.9	34.6	48.8	65.6	29.5	63.2	31.0
1055									43.0	41.8	1.5	1.6	8.7	9.7	11.4	11.3	88.5	10.4	27.8	56.7	64.9	30.4	67.3	27.4
1056									40.1	39.7	3.7	4.5	8.1	9.6	11.9	6.8	87.1	11.3	53.0	36.6	64.2	28.7	71.5	23.0
1019										36.2		0.5		11.0		20.8	79.1	18.7	19.7	53.2	50.6	41.1	56.2	37.5
1020	Medium SMD Product (P$_{80}$=20µm)	6.3	2.6	6.7	10.6	8.0	38.4	27.4	39.3	39.4	1.7	1.4	9.0	10.8	15.5	14.8	84.9	13.7	35.7	45.6	59.0	36.5	66.5	28.3
1021									42.1	41.8	3.0	3.1	8.3	10.2	11.9	10.2	89.6	9.1	27.7	50.6	67.5	28.4	69.0	26.2
1022									43.6	41.4	3.3	4.2	7.8	9.1	10.5	6.7	88.4	10.2	52.4	36.0	61.6	28.9	75.8	18.9
1057										23.8		0.5		14.0		33.4	78.5	18.9	22.7	48.4	64.2	31.2	69.8	27.0
1058	Fine SMD Product (P$_{80}$=13µm)	3.2	0.7	3.0	6.0	6.1	44.0	37.0		32.0		0.5		13.8		21.1	80.7	17.7	26.1	52.9	56.5	38.6	70.6	25.4
1059										39.4		1.0		10.7		14.9	91.4	7.2	19.7	51.1	62.5	30.3	79.8	17.0
1060									42.9	41.5	3.1	3.9	7.6	9.0	10.8	7.1	87.3	10.7	54.0	32.4	52.0	35.8	76.5	16.5
1356										27.1		0.7		4.5		48.2	67.0	28.1	2.6	49.1	26.5	46.7	49.9	43.1
1028										46.5		0.9		11.5		3.0	83.8	14.1	18.0	51.7	52.9	38.2	20.1	59.5
1029	Coarse Netzsch Product (P$_{80}$=28µm)	5.8	3.9	14.5	15.7	8.2	30.3	21.6	41.9	41.0	1.2	0.8	8.3	9.6	12.6	15.1	76.9	20.0	15.4	54.0	45.3	42.0	43.4	46.8
1030									42.2	42.0	1.3	0.8	8.5	10.2	13.8	12.1	81.9	15.7	16.4	52.6	53.0	39.0	52.5	38.9
1031									43.1	42.3	1.4	1.5	8.5	8.8	12.5	11.7	87.5	10.8	29.4	47.7	59.1	32.5	57.9	33.7
1032									38.9	40.1	4.1	4.8	8.2	9.3	12.2	6.0	90.7	8.2	58.1	32.1	67.7	25.3	81.3	15.0
1013										43.9		1.0		13.3		3.3	85.5	12.6	16.2	51.6	62.6	30.9	29.5	49.6
1014										38.9		0.5		10.1		17.9	79.9	17.9	11.2	60.1	53.8	38.2	52.1	41.3
1015	Medium Netzsch Product (P$_{80}$=21µm)	1.9	1.2	7.3	13.2	9.1	37.1	30.2	41.8	40.1	1.0	0.7	8.7	10.3	15.9	14.9	79.0	18.4	28.0	44.1	47.4	45.0	60.2	33.6
1016									42.5	41.5	1.1	1.2	8.4	9.1	13.6	13.4	90.0	8.6	28.4	41.6	63.8	30.8	67.7	27.9
1017									40.4	40.0	3.5	4.7	7.9	8.9	12.2	7.9	87.6	10.5	50.2	32.7	57.4	32.5	75.3	19.6
1038										33.7		1.1		12.7		18.8	76.7	18.9	32.5	40.8	44.1	45.0	72.7	21.9
1039	Fine Netzsch Product (P$_{80}$=10µm)	0.3	0.5	0.8	2.3	3.2	50.4	42.5		35.4		1.3		12.4		15.5	85.6	11.1	18.4	39.4	41.4	41.2	78.2	16.4
1040									39.3	41.2	2.7	3.3	8.0	9.6	15.5	7.8	86.4	11.5	41.7	37.7	52.5	36.2	83.8	12.8

Appendix C – Zinc 1st Retreat Concentrate Regrind Circuit

Regrind Circuit Location

Zinc Retreat Circuit
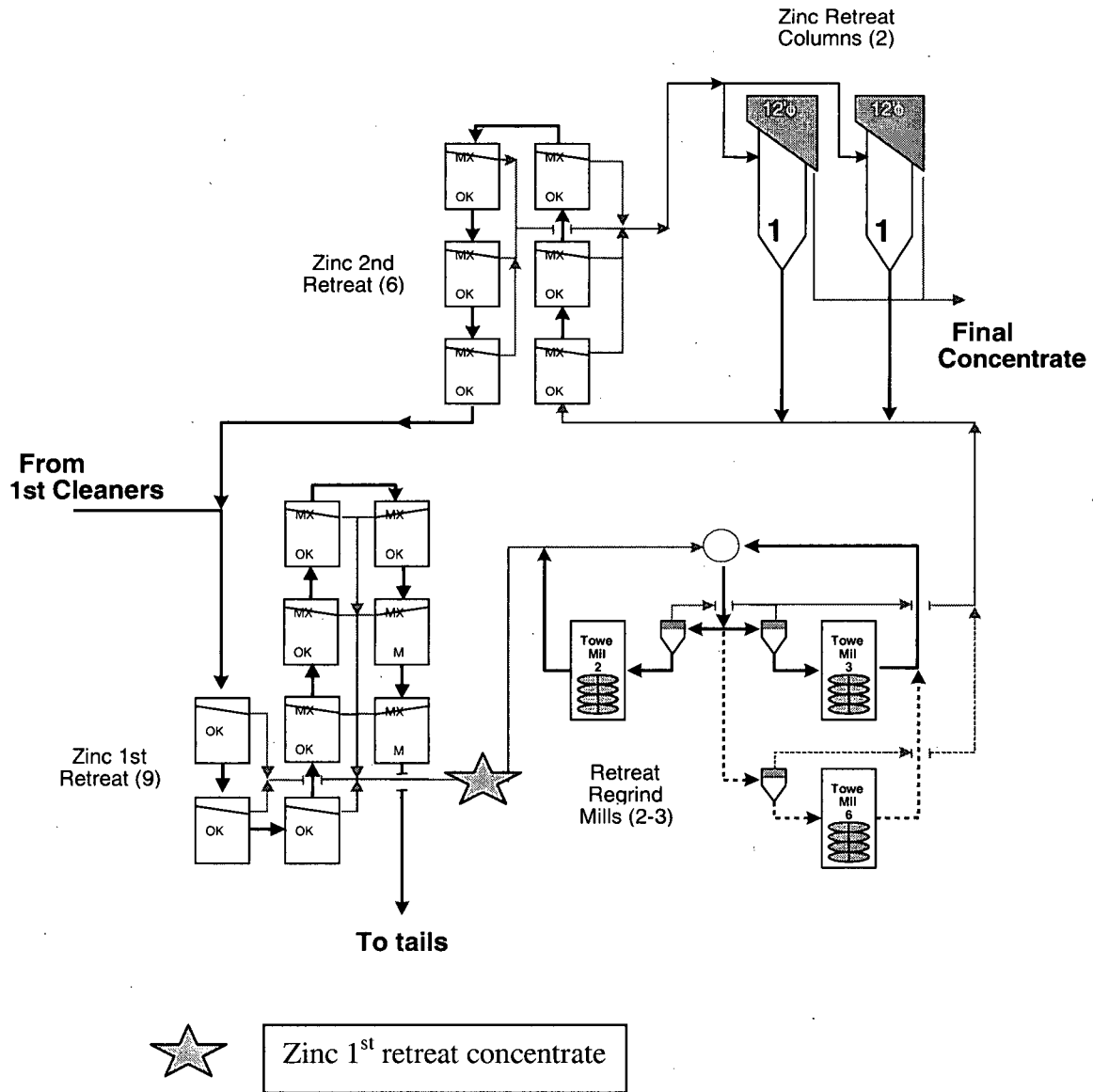
Figure C-I. Zinc retreat flotation circuit at the Red Dog Mine

Characterization of Circuit

Table C-I. Mineralogy of zinc 1st retreat concentrate

Head Assay (%)					Calculated Mineralogy (%)				MLA Modal Mineralogy (%)			
Pb	Zn	Fe	SiO$_2$	Ba	Galena	Sphalerite	Pyrite	NSG	Galena	Sphalerite	Pyrite	Quartz
3.2	41.7	8.3	18.5	1.2	3.7	65.3	13.3	17.7	2.7	65.2	16.7	12.5

Table C-II. Particle size distributions (Zinc 1st retreat regrind circuit)

Regrind Circuit Sample	P_{80} (µm)	Specific Surface Area	$P_{80}:P_{20}$	Rosin-Rammler Distribution		
				Size Coefficient, a	Width Coefficient, b	Coefficient of Determination, R^2
Zinc 1st retreat concentrate	29.4	0.94	5.8	19.80	1.32	0.998
Zinc retreat tower mill feed	37.1	0.72	4.3	17.67	1.21	0.998
Zinc retreat tower mill discharge	29.9	1.06	5.9	25.54	1.33	1.000
Zinc 2nd retreat feed (cyclone o/f)	22.5	1.18	4.2	20.62	1.20	0.999

Netzsch Mill Grinding Trials

Table C-III. Energy requirements (Zinc 1st retreat regrind; Netzsch mill)

Test	Pump (rpm)	Flow (L/min)	% solids	kW	F_{80} (µm)	P_{80} (µm)	Solid Flow (t/hr)	Specific Energy Consumption (kWhr/t)
Empty				0.60				
Run 1	500	2.67	37.7%	1.85	29.5	13.2	0.084	14.8
Run 2	600	3.90	39.3%	1.70	29.5	22.7	0.131	8.4
Run 3	550	3.93	36.3%	1.65	29.5	20.9	0.118	8.9
Run 4	515	3.76	36.3%	1.60	29.5	20.15	0.113	8.9
Run 5	490	3.56	30.5%	1.60	29.5	20.07	0.085	11.8
Run 6	293	2.16	36.6%	1.70	29.5	15.85	0.065	16.8
Run 7	160	1.17	38.5%	1.80	29.5	11.7	0.038	31.6
Run 8	70	0.42	40.3%	1.80	29.5	8.27	0.014	82.8
Run 9	110	0.62	38.5%	1.75	29.5	9.41	0.020	56.9

Table C-IV. Particle size distributions (Zinc 1st retreat regrind; Netzsch mill products)

Feed Sample (Netzsch)	P_{80} (µm)	Specific Surface Area (m^2/g)	P_{80}:P_{20}	Rosin-Rammler Distribution		
				Size Coefficient, a	Width Coefficient, b	Coefficient of Determination, R^2
	13.2	1.79	4.7	9.76	1.60	0.993
	22.7	1.31	5.5	15.49	1.47	0.996
	20.9	1.48	4.4	15.36	1.53	0.996
	20.2	1.37	5.2	13.80	1.51	0.996
Zinc 1st retreat concentrate	20.1	1.45	5.4	14.21	1.52	0.996
	15.9	1.56	4.7	11.36	1.56	0.995
	11.7	1.94	4.2	9.32	1.58	0.991
	8.2	2.59	4.0	7.85	1.51	0.982
	9.4	2.20	3.5	8.25	1.54	0.982

Stirred Media Detritor Grinding Trials

Table C-V. Energy requirements (Zinc 1st retreat regrind; SMD using syringe samples)

metso minerals

LABORATORY STIRRED MEDIA DETRITOR
TEST DATA SHEET

Project: UBC Fine Grinding   Application: Zinc 1st Retreat Conc.   % Solids: 40%
Sampling: Syringe   Media: Colorado River Sand

Details			FEED	1	2	3	4	5	6	7
Charge										
total volume	ml			1408	1408	1408	1408	1408	1408	1408
media ratio	v/v			50%	50%	50%	50%	50%	50%	50%
slurry volume	ml			704	704	704	704	704	704	704
media volume	ml			704	704	704	704	704	704	704
Media										
density	kg/m^3			2650	2650	2650	2650	2650	2650	2650
mass	g			1866	1866	1866	1866	1866	1866	1866
Feed										
dry solids density	kg/m^3	4020		4020	4020	4020	4020	4020	4020	4020
liquid density	kg/m^3	1000		1000	1000	1000	1000	1000	1000	1000
slurry solids content	% m/m	40.0		40.0	40.0	40.0	40.0	40.0	40.0	40.0
slurry density	kg/m^3	1430		1430	1430	1430	1430	1430	1430	1430
slurry solids content	%v/v	14.2		14.2	14.2	14.2	14.2	14.2	14.2	14.2
slurry mass	g			1006	1006	1006	1006	1006	1006	1006
solids mass - dry	g			403	403	403	403	403	403	403
powder moisture content	% m/m			0.0	0.0	0.0	0.0	0.0	0.0	0.0
solids mass - "wet"	g			403	403	403	403	403	403	403
water volume	ml			604	604	604	604	604	604	604
Work Input										
required work input	kWhr/t	0		5	10	21	45	60	80	90
required power	kWhr			0.0020	0.0040	0.0085	0.0181	0.0242	0.0322	0.0362
Particle Size										
D80	µm	29.5		22.6	16.8	14.0	11.6	8.8	7.1	7.0

Table C-VI. Particle size distributions (Zinc 1st retreat regrind; SMD products)

Feed Sample (SMD)	P_{80} (µm)	Specific Surface Area (m^2/g)	P_{80}:P_{20}	Rosin-Rammler Distribution		
				Size Coefficient, a	Width Coefficient, b	Coefficient of Determination, R^2
Zinc 1st retreat concentrate	14.2	1.77	5.5	9.57	1.41	0.997
	20.3	1.44	5.0	14.63	1.45	0.995
	13.4	1.78	4.3	10.10	1.55	0.995
	11.6	2.19	4.5	7.97	1.60	0.998
	7.8	2.76	4.5	5.79	1.60	0.994
	23.1	1.44	5.0	15.15	1.39	0.999
	6.1	3.35	4.1	5.37	1.69	0.982

Mineral Liberation Analysis

Table C-VII. Mineral liberation analysis (Zinc 1st retreat regrind circuit and mill products)

Sample Number	Sample Name	+38 µm	C1/2	C3	C4	C5	C6	C7	% Zinc Assay	% Zinc MLA	% Lead Assay	% Lead MLA	% Iron Assay	% Iron MLA	% Silica Assay	% Quartz MLA	Zn Sulphide % Liberated	Zn Sulphide % Binary	Pb Sulphide % Liberated	Pb Sulphide % Binary	Pyrite % Liberated	Pyrite % Binary	Quartz % Liberated	Quartz % Binary
1358										32.2		2.4		6.0		33.9	45.5	40.7	2.1	35.5	13.9	41.7	28.2	57.8
460										42.2		2.0		12.0		5.5	71.0	24.2	21.1	47.0	43.2	37.8	11.6	50.8
461	Zinc 1st Retreat Concentrate	9.5	2.8	17.0	20.7	11.3	22.9	15.8	41.0	38.6	1.9	1.2	7.6	10.0	23.2	17.1	72.4	23.7	15.5	45.7	52.0	30.4	26.9	50.9
462									43.8	40.2	1.7	0.9	8.4	11.2	18.6	13.3	82.5	15.4	20.0	50.4	65.2	23.8	38.0	43.0
463									45.2	40.8	1.7	1.6	9.3	11.5	12.7	10.3	82.6	15.0	20.1	51.3	63.1	24.9	36.7	42.7
464									44.3	40.8	3.5	3.5	9.4	11.5	9.4	5.9	91.7	7.4	68.0	25.7	78.0	16.1	63.5	25.4
455									49.1	44.5	3.1	1.9	9.2	11.3	5.7	3.1	76.3	19.2	25.6	33.9	48.9	34.1	8.4	54.9
456									46.5	42.6	1.8	1.2	8.6	11.1	12.8	9.0	78.6	17.9	25.0	35.4	56.0	28.3	26.3	45.7
457	Zinc Retreat Tower Mill Feed	18.1	5.8	27.0	18.8	5.5	11.8	13.0	47.0	42.0	1.5	0.8	9.6	12.6	11.7	7.6	85.0	13.4	28.4	44.5	70.3	21.5	39.0	42.0
458									47.0	41.6	1.6	1.4	9.1	11.6	11.7	9.3	84.7	12.9	23.0	40.0	67.3	22.0	43.9	37.2
459									37.0	40.4	3.1	5.9	7.9	10.3	11.2	6.5	90.4	8.2	63.0	30.4	80.1	11.6	68.0	23.9
465										43.8		1.8		11.5		3.0	77.2	18.2	16.8	37.0	49.4	34.6	6.0	51.6
466									45.9	41.9	1.8	1.1	9.1	11.3	10.5	9.3	80.5	16.3	16.4	39.5	60.0	26.4	33.7	44.2
467	Zinc Retreat Tower Mill Discharge	6.3	3.4	19.9	19.8	9.2	24.7	16.6	48.5	41.5	1.5	1.0	9.5	12.1	12.4	8.9	86.1	12.1	34.5	33.5	67.6	23.1	49.3	35.8
468									45.5	40.7	1.6	1.4	8.7	11.0	14.1	11.2	87.3	10.6	21.7	42.8	67.8	21.9	58.5	29.5
469									42.9	41.2	4.5	3.1	7.4	10.3	16.0	8.8	90.7	8.0	52.7	36.8	77.1	15.5	80.5	11.6
485										42.7		1.3		10.0		8.2	72.4	22.4	14.7	36.7	40.7	32.7	19.6	46.9
486									38.7	37.0	1.5	1.0	6.5	8.7	25.7	22.5	74.1	22.1	23.5	34.2	55.7	28.3	35.2	47.9
487	Zinc Retreat Cyclone O/F	3.0	0.9	12.8	21.5	13.9	30.8	17.2	41.5	40.8	1.3	1.0	7.5	10.3	17.9	13.7	84.2	13.7	36.8	34.8	66.8	21.2	40.1	41.9
488									42.8	41.2	1.4	1.4	8.6	10.4	14.7	11.5	84.9	12.5	21.9	40.9	66.1	23.6	43.9	37.9
912									40.9	38.7	4.0	4.9	8.7	10.5	11.7	8.1	84.7	12.1	43.1	36.6	55.7	28.6	54.6	29.8
918									38.5	36.5	0.8	0.4	7.5	9.9	23.1	21.5	74.7	21.9	37.2	35.6	54.1	27.3	39.5	43.6
919									37.7	37.2	0.9	0.6	8.0	9.9	20.5	20.5	78.8	18.2	23.6	42.0	60.6	24.5	43.4	41.4
920	Coarse SMD Product (P80=23µm)	3.2	6.2	16.7	20.5	11.0	28.9	13.5	41.4	40.4	1.3	1.0	8.5	11.0	13.7	12.8	87.1	11.4	32.3	48.0	68.6	20.5	52.5	30.1
921									42.0	39.7	2.8	2.3	8.6	9.8	10.5	13.5	88.7	9.0	22.9	45.5	69.4	18.9	68.2	19.7
922									40.5	39.7	5.1	4.1	8.4	10.6	8.2	8.8	93.1	6.1	81.3	16.4	81.9	11.4	77.5	16.3
913										25.6		0.6		10.8		37.0	78.2	19.1	29.1	45.2	66.6	22.6	57.6	33.7
914									31.7	30.8	0.9	0.5	9.3	12.0	28.4	26.7	83.5	15.0	42.4	40.5	69.0	22.5	62.1	30.5
915	Medium SMD Product (P80=16µm)	0.9	2.0	7.4	16.5	13.2	40.0	20.0	38.7	38.3	1.3	0.8	9.2	11.0	17.8	16.5	91.6	7.8	60.1	27.0	82.8	12.3	74.8	19.9
916									42.0	40.1	1.9	1.9	8.6	9.8	13.6	14.0	90.3	8.6	54.1	33.3	73.4	18.4	66.8	24.7
917									42.2	40.1	3.6	4.1	7.9	9.7	10.6	9.1	88.5	9.8	34.0	52.0	73.4	18.4	63.3	22.8
949										12.5		0.8		16.8		43.9	78.2	16.3	44.7	38.5	85.3	11.2	88.5	8.7
950	Fine SMD Product (P80=8µm)	0.4	0.1	0.4	1.6	3.4	57.1	37.0		21.8		1.8		16.2		29.2	91.7	7.1	47.6	39.5	87.7	9.4	89.2	8.5
951									41.5	39.5	3.0	3.6	7.9	10.1	16.1	11.6	93.2	5.9	58.4	34.9	78.7	16.7	87.1	8.8
923										33.5		0.6		9.8		25.9	73.6	22.4	15.6	38.1	51.3	32.4	43.1	43.2
924									36.0	36.1	1.4	0.9	8.3	10.1	22.5	21.1	77.8	18.0	13.3	35.3	57.2	27.2	45.8	39.2
925	Coarse Netzsch Product (P80=23µm)	0.7	3.1	12.9	20.7	12.5	32.1	18.0	40.1	39.5	1.8	1.6	8.6	10.6	16.2	14.2	83.7	13.2	25.7	38.7	60.7	23.8	56.0	26.3
926									39.7	39.0	2.4	2.1	8.2	9.9	13.8	15.0	88.9	9.3	35.2	36.5	69.5	21.3	61.9	28.3
927									39.8	39.8	4.0	4.6	8.0	9.7	12.8	9.6	86.4	11.0	35.0	39.4	59.7	24.9	65.1	20.0
928										30.3		0.9		9.9		29.8	73.4	22.1	20.8	39.6	55.5	27.3	54.2	34.5
929									33.4	34.6	2.1	1.5	8.8	11.7	22.1	19.1	78.3	16.9	24.0	29.5	60.3	24.3	53.8	33.1
930	Medium Netzsch Product (P80=14µm)	0.1	1.2	7.1	16.5	13.1	39.4	22.6	39.0	38.4	2.1	1.9	8.7	11.3	15.1	14.0	84.7	12.4	21.3	39.9	62.5	23.8	63.3	24.7
931									40.5	40.1	2.3	2.6	8.3	10.4	14.5	11.7	90.0	8.9	57.8	32.8	76.2	17.3	52.8	37.4
932									39.5	38.5	3.3	5.7	7.6	10.1	14.2	9.2	90.1	8.5	61.7	31.6	75.6	19.3	62.5	26.1
1042	Fine Netzsch Product (P80=8µm)	0.0	0.2	0.5	1.8	2.6	59.3	35.6		36.0		2.2		12.8		13.0	76.7	95.0	20.7	42.3	57.7	89.5	62.5	90.5
1043									41.0	41.5	3.1	2.9	8.3	10.7	13.7	7.4	87.6	98.0	40.8	40.1	64.1	94.6	80.7	94.0

Appendix D – Effect of Stress Intensity on Mineral Breakage

Table D-I. P_{80} data by mineral, residence time and impeller speed

Impeller Speed		2000 rpm				1700 rpm				1400 rpm				1200 rpm				1000 rpm			
	Residence Time (sec)	0.0	18.8	43.4	65.7	0.0	19.5	41.9	64.8	0.0	23.8	46.8	66.7	0.0	23.8	50.2	75.6	0.0	25.0	50.6	74.5
	Quartz	53.4	20.5	10.7	7.0	41.1	29.7	17.7	11.3	53.4	41.0	27.6	20.7	46.3	42.7	32.4	25.6	53.4	52.7	40.1	33.1
	Magnetite	52.3	20.9	14.0	11.5	52.3	37.5	26.9	19.8	52.3	41.2	29.9	22.4	52.3	44.8	39.5	34.4	52.3	49.8	44.5	38.1
P_{80} (µm)	Calcite	43.5	11.3	6.9	4.7	43.5	14.4	16.0	9.7	43.5	12.0	9.1	8.2	43.5	18.4	45.3	13.0	43.5	13.8	16.1	17.4

Table D-II. Breakage rates by mineral and impeller speed

	Slopes				
	2000	1700	1400	1200	1000
Calcite	1.71	1.58	1.32	1.05	1.19
Magnetite	1.67	0.76	0.45	0.23	0.19
Quartz	1.75	0.56	0.50	0.29	0.25

Table D-III. Breakage rates by F_{80}, mineral and impeller speed

	Impeller Speed	2000 rpm			1700 rpm			1400 rpm			1200 rpm			1000 rpm		
Quartz	F_{80} (µm)	53.4	20.5	10.7	41.1	29.7	17.7	53.4	41.0	27.6	46.3	42.7	32.4	53.4	52.7	40.1
	Slope between F_{80} and P_{80}	1.8	0.4	0.2	0.6	0.5	0.3	0.5	0.6	0.3	0.2	0.4	0.3	0.0	0.5	0.3
Magnetite	F_{80} (µm)	52.3	20.9	14.0	52.3	37.5	26.9	52.3	41.2	29.9	52.3	44.8	39.5	52.3	49.8	44.5
	Slope between F_{80} and P_{80}	1.7	0.3	0.1	0.7	0.5	0.3	0.5	0.5	0.4	0.3	0.2	0.2	0.1	0.2	0.3
Calcite	F_{80} (µm)	43.5	11.3	6.9	43.5	14.4	16.0	43.5	12.0	9.1	43.5	18.4	45.3	43.5	13.8	16.1
	Slope between F_{80} and P_{80}	1.7	0.2	0.1	1.6		0.3	1.3	0.1	0.0	1.1			1.2		

Table D-IV. Operating conditions and mineral fractions for breakage rate grinding trials

Impeller Speed (rpm)	Pass	Weight %			Power Draw (kW)	Temperature (°C)	Pressure (bar)	Flowrate (L/min)
		Magnetite	Calcite	Quartz				
	1	11.3	13.0	75.6	0.8	21	0.2	2.9
	2	10.2	13.2	76.5	0.8	22	0.2	2.8
1000	3	9.7	13.8	76.6	0.8	22	0.2	3.0
	1	11.3	13.0	75.7	1.1	22	0.2	3.0
	2	9.9	13.5	76.6	1.1	24	0.2	2.7
1200	3	9.8	15.9	74.3	1.1	26	0.2	2.8
	1	10.9	13.1	76.0	1.5	20	0.2	3.0
	2	10.0	13.4	76.6	1.5	23	0.2	3.1
1400	3	9.9	13.7	76.4	1.5	26	0.2	3.6
	1	10.5	15.9	73.6	2.6	28	0.4	3.7
	2	9.7	12.8	77.5	2.6	33	0.4	3.2
1700	3	10.0	13.2	76.8	2.7	37	0.4	3.1
	1	11.4	12.3	76.3	4.0	36	0.4	3.8
	2	10.8	12.9	76.3	4.0	45	0.4	2.9
2000	3	11.2	12.7	76.1	4.0	48	0.4	3.2

Appendix E – MLA Polished Section Index

Table E-I. Polished section index

Sample #	Sample Name	Size Fraction
455	Zn Retreat Tower Mill Feed	C1/2
456	Zn Retreat Tower Mill Feed	C3
457	Zn Retreat Tower Mill Feed	C4
458	Zn Retreat Tower Mill Feed	C5
459	Zn Retreat Tower Mill Feed	C6
460	Zn Retreat Conc	C1/2
461	Zn Retreat Conc	C3
462	Zn Retreat Conc	C4
463	Zn Retreat Conc	C5
464	Zn Retreat Conc	C6
465	Zn Retreat Tower Mill Discharge	C1/2
466	Zn Retreat Tower Mill Discharge	C3
467	Zn Retreat Tower Mill Discharge	C4
468	Zn Retreat Tower Mill Discharge	C5
469	Zn Retreat Tower Mill Discharge	C6
470	Pb Tower Mill Feed	C1/2
471	Pb Tower Mill Feed	C3
472	Pb Tower Mill Feed	C4
473	Pb Tower Mill Feed	C5
475	Zn Rougher Conc	C1/2
476	Zn Rougher Conc	C3
477	Zn Rougher Conc	C4
478	Zn Rougher Conc	C5
479	Zn Rougher Conc	C6
480	Pb Tower Mill Discharge	C1/2
481	Pb Tower Mill Discharge	C3
482	Pb Tower Mill Discharge	C4
483	Pb Tower Mill Discharge	C5
484	Pb Tower Mill Discharge	C6
485	Zn Retreat Cyc O/F	C1/2
486	Zn Retreat Cyc O/F	C3
487	Zn Retreat Cyc O/F	C4
488	Zn Retreat Cyc O/F	C5
490	Pb Column Tails	C1/2
491	Pb Column Tails	C3
492	Pb Column Tails	C4
493	Pb Column Tails	C5
495	Zn Rougher Tower Mill Feed	C1/2
496	Zn Rougher Tower Mill Feed	C3
497	Zn Rougher Tower Mill Feed	C4
500	Zn Rougher Tower Mill Feed	C5

501	Zn Rougher Tower Mill Feed	C6
502	Zn Rougher Tower Mill Discharge	C1/2
503	Zn Rougher Tower Mill Discharge	C3
504	Zn Rougher Tower Mill Discharge	C4
505	Zn Rougher Tower Mill Discharge	C5
506	Zn Rougher Tower Mill Discharge	C6
507	Zn Rougher Cyc O/F	C1/2
508	Zn Rougher Cyc O/F	C3
509	Zn Rougher Cyc O/F	C4
510	Zn Rougher Cyc O/F	C5
511	Zn Rougher Cyc O/F	C6
512	Pb Scav Feed	C1/2
513	Pb Scav Feed	C3
514	Pb Scav Feed	C4
515	Pb Scav Feed	C5
516	Pb Scav Feed	C6
910	Pb Col Tails	C6
911	Pb Tower Mill Feed	C6
912	Zn Retreat Cyc O/F	C6
913	SMD Run 1 (Zn Ret SMD Med)	C1/2
914	SMD Run 1 (Zn Ret SMD Med)	C3
915	SMD Run 1 (Zn Ret SMD Med)	C4
916	SMD Run 1 (Zn Ret SMD Med)	C5
917	SMD Run 1 (Zn Ret SMD Med)	C6
918	SMD Run 6 (Zn Ret SMD Cr)	C1/2
919	SMD Run 6 (Zn Ret SMD Cr)	C3
920	SMD Run 6 (Zn Ret SMD Cr)	C4
921	SMD Run 6 (Zn Ret SMD Cr)	C5
922	SMD Run 6 (Zn Ret SMD Cr)	C6
923	Isa Run 2 (Zn Ret Isa Cr)	C1/2
924	Isa Run 2 (Zn Ret Isa Cr)	C3
925	Isa Run 2 (Zn Ret Isa Cr)	C4
926	Isa Run 2 (Zn Ret Isa Cr)	C5
927	Isa Run 2 (Zn Ret Isa Cr)	C6
928	Isa Run 6 (Zn Ret Isa Med)	C1/2
929	Isa Run 6 (Zn Ret Isa Med)	C3
930	Isa Run 6 (Zn Ret Isa Med)	C4
931	Isa Run 6 (Zn Ret Isa Med)	C5
932	Isa Run 6 (Zn Ret Isa Med)	C6
949	SMD Run 5 (Zn Ret SMD Fine)	C4
950	SMD Run 5 (Zn Ret SMD Fine)	C5
951	SMD Run 5 (Zn Ret SMD Fine)	C6
1010	PCT SMD Fine	C4
1011	PCT SMD Fine	C5
1012	PCT SMD Fine	C6
1013	Zn Ro Isa Med	C1/2
1014	Zn Ro Isa Med	C3
1015	Zn Ro Isa Med	C4

1016	Zn Ro Isa Med	C5
1017	Zn Ro Isa Med	C6
1019	Zn Ro SMD Med	C3
1020	Zn Ro SMD Med	C4
1021	Zn Ro SMD Med	C5
1022	Zn Ro SMD Med	C6
1023	PCT SMD Cr	C1/2
1024	PCT SMD Cr	C3
1025	PCT SMD Cr	C4
1026	PCT SMD Cr	C5
1027	PCT SMD Cr	C6
1028	Zn Ro Isa Cr	C1/2
1029	Zn Ro Isa Cr	C3
1030	Zn Ro Isa Cr	C4
1031	Zn Ro Isa Cr	C5
1032	Zn Ro Isa Cr	C6
1033	PCT Isa Cr	C3
1034	PCT Isa Cr	C4
1035	PCT Isa Cr	C5
1036	PCT Isa Cr	C6
1038	Zn Ro Isa Fine	C4
1039	Zn Ro Isa Fine	C5
1040	Zn Ro Isa Fine	C6
1042	Zn Ret Isa Fine	C5
1043	Zn Ret Isa Fine	C6
1045	PCT Isa Fine	C5
1046	PCT Isa Fine	C6
1049	PCT Isa Med	C4
1050	PCT Isa Med	C5
1051	PCT Isa Med	C6
1052	Zn Ro SMD Cr	C1/2
1053	Zn Ro SMD Cr	C3
1054	Zn Ro SMD Cr	C4
1055	Zn Ro SMD Cr	C5
1056	Zn Ro SMD Cr	C6
1057	Zn Ro SMD Fine	C3
1058	Zn Ro SMD Fine	C4
1059	Zn Ro SMD Fine	C5
1060	Zn Ro SMD Fine	C6
1062	PCT SMD Med	C3
1063	PCT SMD Med	C4
1064	PCT SMD Med	C5
1065	PCT SMD Med	C6
1066	PCT Isa Cr (30% solids)	C3
1067	PCT Isa Cr (30% solids)	C4
1068	PCT Isa Cr (30% solids)	C5
1069	PCT Isa Cr (30% solids)	C6
1108	PCT Isa Fine (check)	C6

1109	PCT Isa Fine (check)	C6
1110	Zn Ro SMD Cr (check)	C3
1111	Zn Ro SMD Cr (check)	C3
1354	Zn Ro SMD Cr	+38µm
1356	Zn Ro Isa Cr	+38µm
1357	Zn Rougher Conc	+38µm
1358	Zn Retreat Conc	+38µm